SINGLE INPUT – SINGLE OUTPUT MODELING OF ENVELOPE TRACKING POWER AMPLIFIERS

BY

Saif Najmeddin

A Thesis Presented to the
DEANSHIP OF GRADUATE STUDIES

KING FAHD UNIVERSITY OF PETROLEUM & MINERALS

DHAHRAN, SAUDI ARABIA

In Partial Fulfillment of the
Requirements for the Degree of

MASTER OF SCIENCE

In

ELECTRICAL ENGINEERING

April 2015

KING FAHD UNIVERSITY OF PETROLEUM & MINERALS

DHAHRAN- 31261, SAUDI ARABIA

DEANSHIP OF GRADUATE STUDIES

This thesis, written by **SAIF NAJMEDDIN** under the direction his thesis advisor and approved by his thesis committee, has been presented and accepted by the Dean of Graduate Studies, in partial fulfillment of the requirements for the degree of **MASTER OF SCIENCE IN ELECTRICAL ENGINEERING.**

Dr. Oualid Hammi
(Advisor)

Dr. Ali Ahmad Al-Shaikhi
Department Chairman

Dr. Azzedine Zerguine
(Member)

Dr. Salam A. Zummo
Dean of Graduate Studies

Dr. Mohammad S. Sharawi
(Member)

12/5/15

Date

Dedicated to

My Mother Saeda,

Father Sameer, Brother Samer,

Spirit of My grandfather, Omaya Tahboub.

All Palestinian have the spirit of resistance against occupation

ACKNOWLEDGEMENTS

All praise is to Allah, الحمد لله رب العالمين, the Almighty who gave me the opportunity to pursue the MS degree course at King Fahd University of Petroleum and Minerals, and guided me in every facet of this work to help accomplish it successfully. May the peace and blessings of Allah be upon his prophet, Muhammad (S.A.W).

Acknowledgement is due to the King Fahd University of Petroleum and Minerals for providing the financial support and world class facilities in academic and extra-curricular activities.

I would like to express my appreciation to many people whose help, directly or indirectly, made this thesis work possible. With deep and indebted sense of gratitude, I would like to express my sincere thanks to my thesis advisor, Dr. Oualid Hammi for his invaluable support, guidance, continuous encouragement and every possible cooperation throughout the period of my research and preparation of thesis documentation. Working with him was a wonderful and learning experience. A special note of acknowledgement to the iRadio Laboratory, University of Calgary for their support and assistance in providing the measurement data used in this work.

My sincere thanks and appreciation is due to the thesis committee members Dr. Azzedine Zerguine and Dr. Mohammad Sharawi for investing their time and their support, critical reviews and suggestions which helped improve this work.

I am grateful to all the faculty and staffs of the Electrical Engineering department, who have in one way or other enriched my academic and research experience at KFUPM. I owe a deep sense of gratefulness to my numerous friends and

colleagues whose presence and moral support made my entire stay at KFUPM enjoyable and fruitful. I would like to sincerely thank them all, especially Amjad, Fadi, Ali, Ahmad, Emad, Hanzala, Mohammad and Osman.

Finally, I would like to express my profound gratitude to my parents, my brother and all family members for their constant inspiration, incessant prayers, love, support and encouragement that motivated me to complete this work.

TABLE OF CONTENTS

LIST OF TABLES

LIST OF FIGURES

LIST OF ABBREVIATIONS

LTE	Long Term Evolution
WiMAX	Wireless Interoperability for Microwave Access
DPD	Digital Predistortion
DUT	Device Under Test
PA	Power Amplifier
PAPR	Peak to Average Power Ratio
LDMOS	Laterally Diffused Metal Oxide Semiconductor
MP	Memory Polynomial
GMP	Generalized Memory Polynomial
EMP	Envelope Memory Polynomial
TNTB	Twin Nonlinear Two-Box
HMEM	Hybrid Memory Polynomial - Envelope Memory Polynomial
NMSE	Normalized Mean Square Error

ABSTRACT

Full Name : Saif Najmeddin

Thesis Title : Single Input – Single Output Modeling of Envelope Tracking Power Amplifiers.

Major Field : Electrical Engineering

Date of Degree : April 2015

In new generation wireless systems, where capacity and speed have been increased considerably, wide bandwidth and high peak to average power ratio (PAPR) signals are used. In these conditions, the power amplifier becomes an important and challenging component. Any power amplifier is expected to provide an appropriate output power with high gain and suitable trade-off between efficiency and linearity. Envelope tracking power amplifiers have recently attracted the power amplifier designers. They have the ability to deal with high PAPR of the modern signals by allowing the amplifier drain bias to track the magnitude of the input signal envelope.

In this work, behavioral modelling using conventional models has been done for an envelope tracking power amplifier employing different shaping functions. Memory polynomial, generalized memory polynomial and forward twin-nonlinear two-box models were used as conventional models.

Two new models have been proposed to deal with envelope tracking power amplifiers. These models are labelled polar memory polynomial model and polar generalized memory polynomial model. The polar memory polynomial model is consists of two parallel functions; one memory polynomial and one memoryless

polynomial, whereas the second model, the polar generalized memory polynomial model contains a generalized memory polynomial function for the amplitude part and a memoryless polynomial function for the phase part.

The performances of the two proposed models were compared with conventional models especially the memory polynomial model and the generalized memory polynomial model using experimental data. The results showed the superiority of the proposed models for various test signals and drain voltage shaping functions.

ABSTRACT (ARABIC)

ملخص الرسالة

الاسم الكامل: سيف سمير عبد السلام نجم الدين

عنوان الرسالة:النمذجة السلوكية لمكبر الطاقة المتتبع للغلاف احادي المدخل احادي المخرج.

التخصص: الهندسة الكهربائية

تاريخ الدرجة العلمية: أبريل 2015

تتميز الأجيال الجديدة من انظمة الإتصالات اللاسلكية بانها قادرة على التعامل مع سعة أكبر وبسرعة أكبر من الاجيال السابقة. في هذه الأجيال يتم الإعتماد على الاشارات ذات النطاق العريض التي تحمل نسبة طاقة كبيرة مقارنة مع معدل الطاقة التي تحتويها (PAPR). مع هذه الظروف بات مكبر الطاقة (PA) عنصرا مهما وأساسيا وأصبح يشكل تحديا للمصممين والمختصين. يفترض بأي مكبر طاقة أن يعطي طاقة مخرجة مناسبة بزيادة تتناسب مع تصميمه وان يكون هناك تناسب بين صفتي كفاءة الطاقة و خطية العملية.

مكبر الطاقة المتتبع للغلاف (ET PA) جذب المصممين والمهتمين بمكبرات الطاقة بشكل كبير في الأعوام الأخيرة. حيث ان هذا النوع من مكبرات الطاقة يعمل بشكل كفؤ مع الإشارات اللاسلكية لأنظة الإتصالات الحديثة وذلك من خلال السماح لمزرود الجهد بالتغير بناء على تتبع قيمة الغلاف للإشارة المدخلة.

النمذجة السلوكية لمكبر الطاقة لفتت نظر الباحثين وحازت على إهتمامهم في الفترة الاخيرة وأثبتت انها قادرة على ان تكون مفيدة بالنسبة لدائرة تقليل التشويه الرقمية التي تحسن الاداء وتحافظ على خطية العلاقة. في هذا العمل؛ تم إنجاز النمذجة السلوكية لمكبرات الطاقة المتتبعة للغلاف باستخدام النماذج التقليدية مع اقترانات متنوعة. النماذج التي اعتمدت كنماذج تقليدية في هذا الهمل هي : النموذج متعدد الاوجه ذو الذاكرة (MP) و النموذج متعدد الاوجه ذو الذاكرة العام (GMP) والنموذج الامامي للتوأم الغير خطي ثنائي المربع العادي (FTNTB). تم إقتراح نموذجين جديدين للتعامل مع مكبرات الطاقة المتتبعة للغلاف. هذا النموذجان هما : النموذج القطبي متعدد الاوجه ذو الذاكرة (Polar MP) و النموذج القطبي متعدد الاوجه ذو الذاكرة العام (Polar GMP).

يتكون النموذج القطبي متعدد الاوجه ذو الذاكرة من اقترانين متوازيين هما : النموذج متعدد الاوجه ذو الذاكرة والثاني النموذج متعدد الاوجه بدون ذاكرة، بينما يتكون النموذج القطبي متعدد الاوجه ذو الذاكرة العام من اقترانين ايضا وهما : النموذج متعدد الاوجه ذو الذاكرة العام لنمذجة القيمة والثاني النموذج متعدد الاوجه بدون ذاكرة لنمذجة الاتجاه.

تم مقارنة أداء النموذجين المقترحين مع النماذج التقليدية وخاصة النموذج متعدد الاوجه ذو النموذج متعدد الاوجه ذو الذاكرة العام وذلك باستخدام بيانات التجربة على مكبر الطاقة. وقد أظهرت النتائج أفضلية للنموذجين المقترحين على اختلاف الاشارات والاقترانات المستخدمة، حيث ان النموذجين المقترحين يصلان الى نفس كفاءة النماذج التقليدية بعدد أقل من العوامل وتصل نسبة تقليل العوامل التي تعبر عن صعوبة النموذج الى حوالي 55% في بعض الحالات.

CHAPTER 1

INTRODUCTION

Wireless communication systems and technologies have advanced rapidly in the past couple of decades and are overwhelming nowadays life and markets. Nevertheless, the telecommunication industry is still facing a lot of challenges while trying to present its ultimate services to customers. One of the most critical challenges is located on the base station part especially in cellular networks. Designers try to cope with the evolution in cellular networks for emerging technologies such as Long Term Evolution (LTE) and Wireless Interoperability for Microwave Access (WiMAX). These evolutions in standards necessitate some technical changes and even new ways of thinking to be able to achieve the desired goals such as higher data throughput and "greener" communication systems. The demand on increasing radio frequency (RF) power amplifier (PA) performance is still among the top requirements. Performance of power amplifiers is affected by the increase in the peak-to-average power ratio (PAPR) of the communication signals. This results in low power efficiency which is against the green communication concept taking into account that base stations are responsible for about 80% of the energy consumed by a cellular network [1], and that the power amplifier is responsible for most of this consumption. This situation opens a track to the concept of envelope tracking (ET) power amplifiers which is perceived as the next generation technology of power amplifiers.

In envelope tracking systems, the PA is continuously operating almost at peak efficiency as the signal envelope varies. In this chapter, many power amplifiers types and

technologies are described; the concept of behavioral modelling of power amplifiers is analyzed, the features of envelope tracking power amplifiers and their mode of operations are introduced.

1.1 RF Power Amplifiers

The main function of power amplifiers is to increase or amplify the power level of the input signal. For any power amplifier, the goal is to provide an appropriate output power with high gain and suitable trade-off between efficiency and linearity.

For reliable transmission, the output power should be sufficient. High gain of the PA will decrease the size and the manufacturing cost of the components and it will minimize the number of stages needed to get the desired output power. The high efficiency improves thermal management, battery life and operational cost. Very high linearity is essential for bandwidth efficient modulations. It is impossible to achieve all of these criteria together; there are a lot of conflicting issues, so the solution will require a certain level of compromise between these criteria. Accordingly, these considerations led to various classes of power amplifiers such as class A, class B, class AB, class C.

Class A is the most linear but most inefficient of all power amplifier classes having theoretically about 50% peak efficiency. Class B amplifiers create large amount of distortions but have a maximum theoretical efficiency of 78.5%. Class AB is less efficient than class B but achieves better linearity. Class C amplifiers are nonlinear amplifiers but high efficiencies (up to 90%) are achievable.

RF PA can be designed using different semiconductor technologies. Si BJT, Si LDMOS FET, SiGe HBT and GaN are some of these technologies [2]. The widely

adopted technology for RF power amplifiers employed in wireless communication base stations is the Laterally Diffused Metal Oxide Semiconductor (LDMOS) [2].

1.2 Behavioral Modeling and Digital Predistortion

As it is clear that there is a need for a trade-off between efficiency and linearity in RF power amplifiers, a lot of techniques were developed to get better linearity and efficiency. These techniques will be discussed more in the literature review reported in chapter 2.

All power amplifiers including ET PAs need techniques to enhance their linearity property. There are many linearization techniques but the most important and commonly used technique that is used in order to solve the nonlinearity problem exhibited by the base station power amplifier is digital predistortion (DPD). The digital predistortion can be described simply as the inverse of a PA; it will be connected before the power amplifier, so the complete cascaded system will have a linear behaviour. Behavioral modelling is important when DPD is considered. The objective of behavioral modeling is to give accurate mathematical formula that describes the input and output signals relation without performing any physical analysis of the system and it is thus a valuable process for assessment of the transmitter performance and design of the digital predistorter [3].

It is very necessary to have the input and output signals of the device under test (DUT) to give an accurate mathematical description that will give a vision of interactions that occur between the signals. Figure 1.1 describes the concept of behavioral modeling.

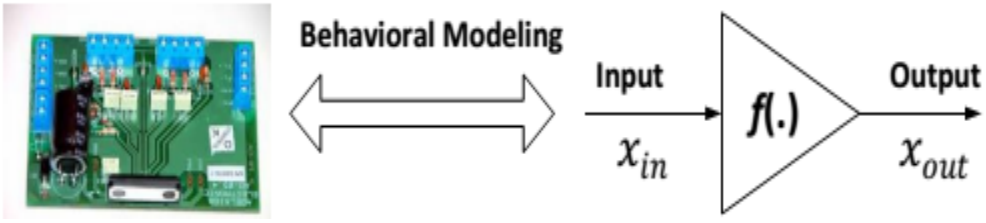

Figure 1.1 Concept of black box based behavioral modeling [3]

1.3 Static Nonlinearity and Memory Effects

There are two types of distortions in power amplifiers: static nonlinearity and dynamic nonlinearity. Dynamic distortions also known as memory effects are caused by the thermal and electrical memory effects in power amplifiers. When a high PAPR signal is being transmitted via power amplifier, which is the case in the signals of modern systems. The transistor temperature increases very fast when the peak occurs. Thus for a couple of microsecond the temperature of the transistor rises up [3].

Another type of distortions is the static nonlinearity or memoryless nonlinearity. This factor corresponds to the DUT distortion without the existence of memory effect. As a result, the characteristics of the signal will determine the nonlinearity of the power amplifier. This includes the signal bandwidth, the peak to average power ratio (PAPR) of the signal, and its complementary cumulative distribution function (CCDF) [3].

1.4 Envelope Tracking Power Amplifier (ET PA)

A high peak-to-average power ratio is a basic and unavoidable feature in modern modulated signals. Conventional power amplifiers that use a fixed bias, must be operated at relatively high output power back off, to avoid great distortion in the signal when its envelope excursion is near the amplifier's peak power. Since the amplifier is efficient only when operating in compression, it spends more time operating far below its maximum efficiency which results in poor average efficiency [4].

Envelope tracking is a way of overcoming this problem by allowing the amplifier's drain bias to track the magnitude of the input signal envelope. At low level of the input signal envelope, the drain bias can be lowered so the amplifier operates closer to its optimal efficiency point for low and high input power levels.

ET systems improve the efficiency but often result in poor linearity performance since the bias of the amplifier is varying. Both, the linearity and the efficiency performances of the envelope tracking power amplification system depend on several factors such as the efficiency of the supply modulator, the efficiency of the power amplifier, and the mapping function used to map the signal's envelope into a variable drain supply voltage [4]. The purpose of this work is to investigate the effects of the signal's envelope mapping function on the linearity and efficiency performances of the envelope tracking power amplifier.

1.5 Problem Statement

Modern mobile communication networks make use of LTE signals which are of wide bandwidth and high PAPR. These signal characteristics stimulate the static nonlinearity and the memory effects of the power amplifier wherein the power amplifier output is influenced by the present input sample and also previous input samples.

A power amplifier uses a considerable portion of the total energy consumed by the entire telecommunication network. For the signal not to be distorted when its envelope excursion is near its peak, constant drain PAs are usually operated in deep back-off. Since the amplifier is efficient only when operating in compression but spends more time operating far below its maximum efficiency, poor average efficiency is obtained. ET is a method to solve this low efficiency issue; since it allows the drain bias of the PA to track the magnitude of the envelope of the input signal. According to that, the design and modeling of ET PA received a huge attention from researchers.

The objective of behavioral modeling is to develop a model that will be able to describe the nonlinear operation of the power amplifier while maintaining accuracy. In this regard, different behavioral models have been proposed in literature. One of the most important aspects that need to be considered while selecting a model is its complexity. Dimensions of the model determine its size and complexity.

This thesis work attempts to achieve new single input single output (SISO) models that describe ET PA accurately and have good performance with low complexity and benchmark them against conventional models.

1.6 Thesis Objectives

The objectives of this thesis are the following:

1. Assess the performance of the conventional Single Input Single Output (SISO) power amplifier models for ET PA with different shaping functions.
2. Develop a new SISO model suitable for envelope tracking power amplifiers.
3. Evaluate the performance of the new model with different shaping functions of ET PA.
4. Validate the performance of the new model with different signals.

1.7 Thesis Organization

The thesis is divided into five chapters. The first chapter introduces the area of the work and defines the problem addressed in this thesis. It includes overview of RF power amplifiers, the principle of behavioral modeling and digital predistortion, the concept of static nonlinearity and memory effects, the basic idea of envelope tracking power amplifier, problem description and thesis objectives.

Literature review of envelope tracking power amplifier concept, different behavioral models, including their mathematical formulations and block diagrams are presented in Chapter 2. These models include memory polynomial based models, the two-box model structures, and the conventional Volterra structure.

In Chapter 3, the characteristics of the device under test, the measurement set-up, and the different shaping functions used are described. The number of coefficients of each model and its complexity are also reported.

In Chapter 4, the proposed polar memory polynomial and polar generalized memory polynomial models are introduced and validated using LTE signals of 5MHz and 20MHz bandwidths. The proposed models performance has been compared with that of the conventional SISO models. Conclusions and future work are stated in Chapter 5.

CHAPTER 2

Literature Review: Envelope Tracking Power Amplifier and PA Behavioral Models

In this chapter, the principles of ET PA and the different behavioral models will be introduced. Envelope tracking technique has emerged since 1980s to improve power-added efficiency (PAE) of FET amplifiers[4][5]. This technique has attracted the designers of power amplifier recently according to its capability to deal with high peak to average power ratio of modern signals. It is noticeable that there is increasing in the PAPR in new generation of the wireless systems, Table 2.1 describes this increase according to wireless generation.

Table 2.1 PAPR of different communication standards

Standard	Launched	Typ. carrier BW (MHz)	Approx. PAPR (dB)
2G cellular (GSM)	1991	0.2	0.0
2.75G cellular (GSM+EDGE)	2003	0.2	3.5
3G cellular (WCDMA FDD)	2001	5	7.0
Wi-Fi (IEEE 802.11 a/g)	2003	20	9.0
WiMAX (IEEE 802.16d)	2004	20	8.5
Wi-Fi (IEEE 802.11 n)	2007	20	9.0
3.5G cellular (HSDPA)	2007	5	8.0
3.9G cellular (LTE)	2009	20	10.0

The idea of ET PA is based on using an RF power amplifier, in which the supply voltage tracks the signal envelope. Thus, the efficiency of the RF PA increases significantly. Then, one can use any of linearization technique to restore the linearity of the power amplifier.

ET PA system has two main paths: the RF path and the envelope path. There are a lot of challenges and design difficulties in these two paths. A detailed description of the two paths, the schematic of ET PA, the main challenges and comparisons between different behavioral models used for this type of power amplifiers are presented in this chapter.

2.1 ET PA Fundamentals

Envelope tracking technique is considered as an efficient way to enhance the efficiency of power amplifier by using the concept of dynamic supply voltage. Figure 2.1 shows the basic configuration of ET PA; mainly it consists of two main paths.

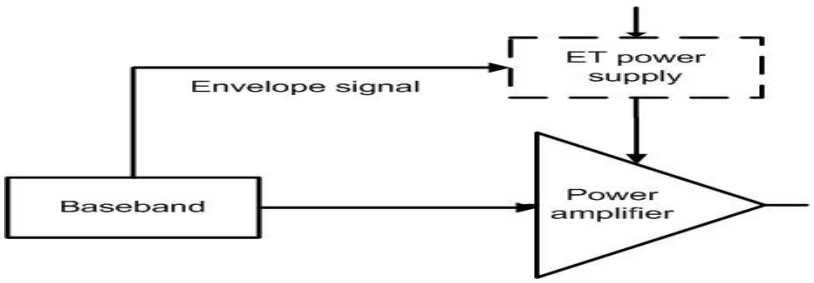

Figure 2.1 The basic configuration of ET PA

The input signal is divided into two paths; the envelope path and the RF path. On the envelope path, the envelope of the input signal is shaped by the shaping function, where the output of the ET power supply gives the supply voltages that track the signal envelope of the input RF signal. This accurate tracking is the core mechanism of the

efficiency enhancement in the ET system. In the RF path, the input RF signal is input into the RFPA.

Figure 2.2 describes this difference between conventional and envelope tracking power amplifier and shows the amount of power dissipation reduction. It is clear that in ET PA, the efficiency improvement will achieve compared with fixed supply voltage where the supply voltage is constant all the time regardless of the input signal variations.

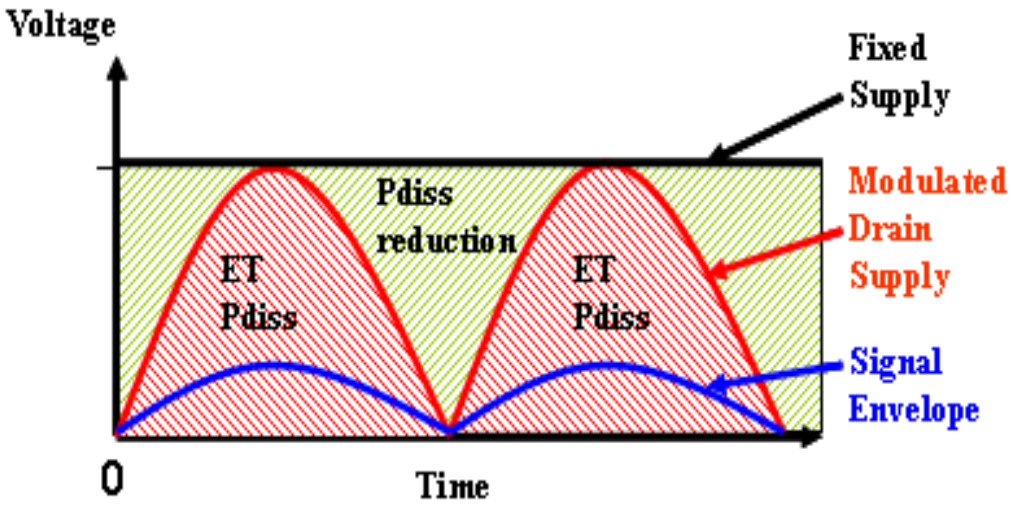

Figure 2.2 Power dissipation reductions in ET PA [6]

It is obvious that the main difference between ET PA and the conventional one is represented in the envelope path of ET PA. Envelope path in ET PA decides the supply voltage according to the instantaneous power levels whereas in conventional PA, the supply voltage is fixed for different levels. This is clear in Figure 2.3 with the schematic for both. In a fixed supply voltage, there is a significant amount of excess power over the desired output waveform and this will become a heat and ultimately affect the process. By tracking the RF signal envelope with close amount of supply voltage allows for a much lower excess voltage. This will lead to decreasing the excess power as it is

illustrated in Figure 2.3 . The supply voltage is changed by a power modulator device, which replaces the normal DC-DC converter delivering power to the RF PA transistor.

The main implementation challenge for an envelope tracking modulator is the needed bandwidth to accurately track the signal amplitude without increasing distortion. It is required a power supply with bandwidth of 1.5 to 3.0x the channel bandwidth, i.e. if one have a 20MHz wide signal, it needs 30 to 60MHz bandwidth in the power modulator to track the signal envelope accurately.

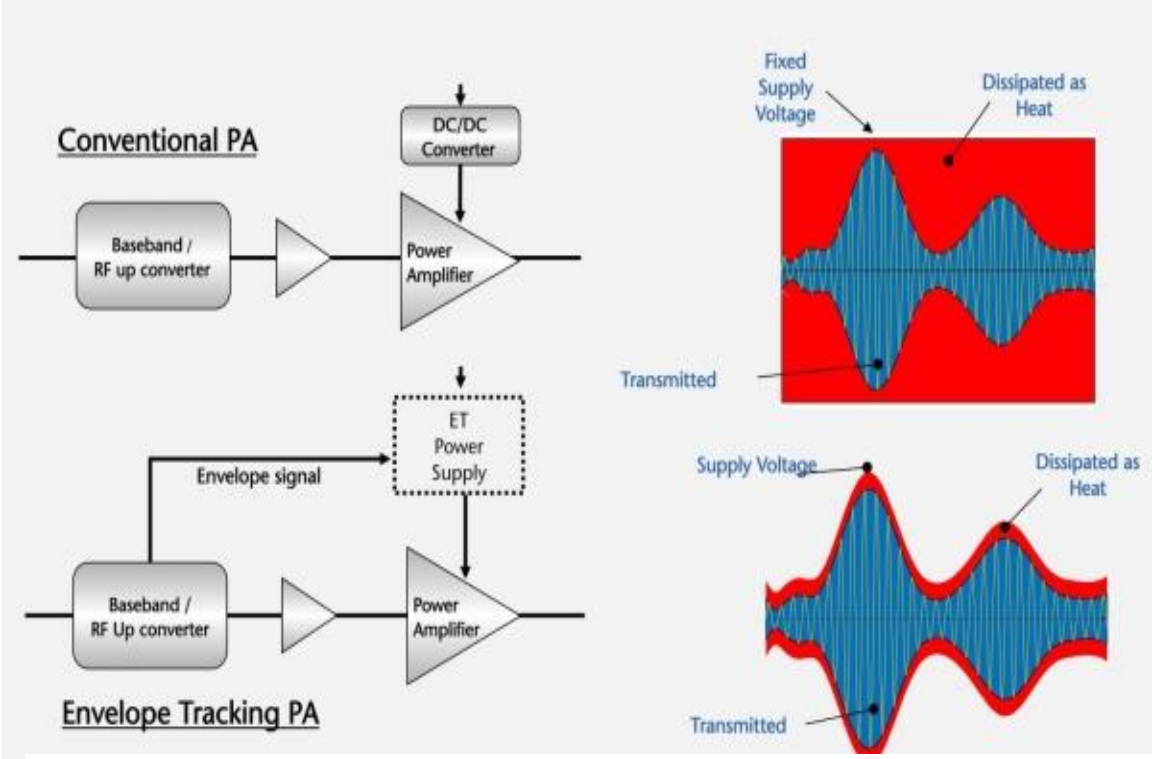

Figure 2.3 Constant supply PA vs ET PA [8]

The power supply modulator has to deliver several watts of power, with extremely low noise and very high slew rates, while achieving energy conversion efficiency around 80%. The most important benefit of using envelope tracking technique is reducing heat dissipation caused by the excess supply level while maintaining the

linearity, which in turn improves the DC to RF conversion efficiency extending the battery lifetime in portable devices and relaxing cooling conditions in higher power applications such as base stations.

There is a main similarity between ET PA technique and envelope elimination and restoration (EER) technique. In these two techniques, the dynamic biasing to the RF PA is adopted. ET involves a supply modulator and a PA with a modulated RF input signal, but EER requires a supply modulator and a switching PA with a constant-envelope RF signal containing only the phase information. Figure 2.4 shows the Block diagrams of envelope tracking PA, and EER. It is observed that the ET PA and EER are very similar, but there are two main differences between these two systems; firstly, the EER RFPA needs to be highly efficient and it is not essential to be linear while ET RFPA needs to work in a linear mode. Secondly, the ET RFPA input signal has both amplitude and phase variations while that of the EER RFPA will only have the phase modulation [7].

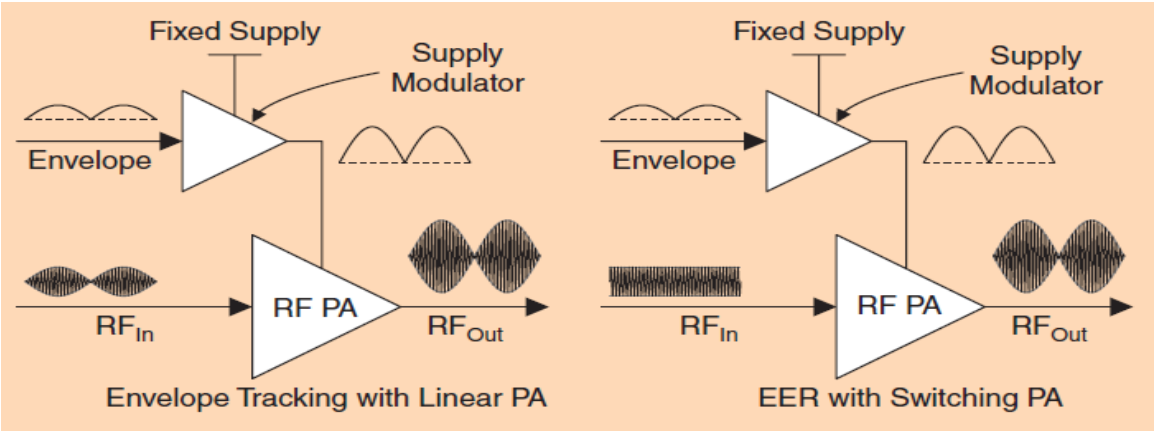

Figure 2.4 Block diagrams of envelope tracking PA, and EER [7].

2.2 ET PA Shaping Functions

The mapping of the envelope signal into a variable drain voltage is called shaping function of ET PA. The shaping functions are applied in the envelope path of ET PA to supply appropriate voltage to the power amplifier. Choosing the shaping function to use in the generation of shaping table is considered as a key aspect in the envelope tracking power amplifier. There are several envelope shaping methods that were proposed to get better efficiency and linearity of the ET PA.

In [9], a discussion of the impact of envelope shaping functions on system linearity and efficiency performance for a given signal statistic was presented. In [10], the description of an optimized envelope shaping function for the envelope tracking power amplifier and its implementation were presented. A new shaping function was presented to improve the efficiency and output power of the power amplifier, as well as its linearity which depends on crest factor reduction with sweet spot tracking. The fabricated ET PA delivers higher efficiency and better linearity than traditional PA for the WCDMA and LTE signals.

The PA is usually modeled as a constant resistor. In [10] the authors proposed an different shaping function and presented its characteristics of current and voltage envelopes and link that connected PA and supply modulator and output capacitance.

It is important to optimize the shaping function in order to reach an acceptable trade-off in terms of power efficiency and linearity of the envelope tracking power amplification system.

It is important to notice that if the supply voltage is lower than the knee voltage, the nonlinearity will be clear in the AM/AM and AM/PM characteristics[11][12].

Multiple types of shaping functions are used to generate appropriate supply voltages to the main path (PA path) as in [13]-[17], the main differences between the shaping functions are determined according to the efficiency, linearity, envelope bandwidth, and complexity. Shaping functions can be categorized in four main types as it is clear from Figure 2.5.

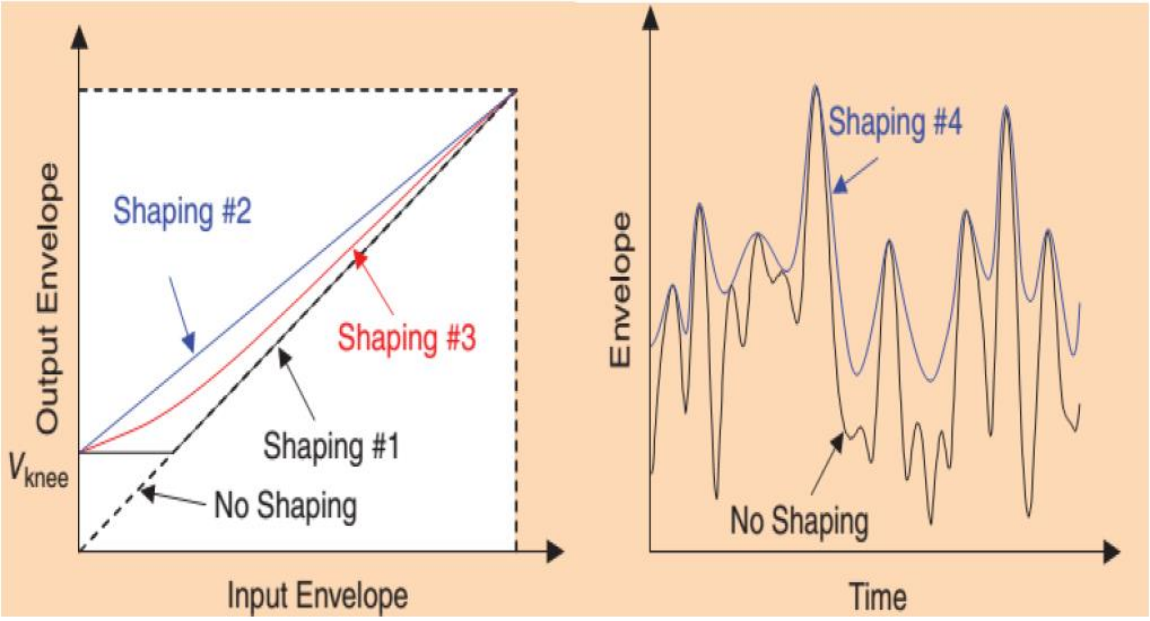

Figure 2.5 Shaping function types [18]

In shaping function #1, the main idea is to avoid voltages lower than the knee voltage. According to this sharp curve, the bandwidth of the envelope signal will be expanded, and then the AM/AM characteristics will be worse.

An offset voltage is added to the original envelope signal in the shaping function #2; by this no change will happen to the envelope signal bandwidth. Compared to shaping function #1, shaping function #2 shows slightly lower efficiency but much better linearity.

Variations in the knee voltage were taken into consideration in the shaping function #3; this type gives intermediate characteristics between shaping functions #1 and shaping functions #2.

In shaping functions #4, the reduction of the envelope signal bandwidth will happen for supply modulators with lower bandwidth specifications [18]. This will reduce the efficiency and gives worse linearity than shaping function #2 and #3. Table 2.2 reports the main differences between these four types.

Table 2.2 Shaping functions comparison

	No Shaping	Shaping #1	Shaping #2	Shaping #3	Shaping #4
Efficiency	Very high	Very high	High	Very high	Good
Linearity	Bad	Not Bad	Very good	Good	Normal
Envelope's BW	No Change	Wider BW	No Change	Wider BW	Reduced BW
Complexity	Very simple	Very simple	Very simple	Complex	Very complex

2.3 Power amplifier behavioral models

Different models were developed to deal with the nonlinear behavior of power amplifiers driven by wide bandwidth signals. Volterra model is considered as the most complex and generalized model that describes the behavioral of power amplifiers.

Different variations and modifications applied on this model are described in [19]-[22]. Another main model that has a lot of variants and widely that is used is the memory polynomial (MP) model. In [23], this model was presented whereas in [24]-[27] different modifications of it were presented. [28] introduced twin-nonlinear two-box (TNTB) models. Details of these models will be presented in the coming sub-sections.

2.3.1 Voltera Model

The Voltera series gives a general way to model nonlinear system with memory, and it is used frequently to describe the relationship between input and output signals of an amplifier [29]-[34]. This model is considered the main of the most different models. At the same time, it is the most sophisticated and unwanted model due to its complexity especially with high nonlinearity order and memory depth. The formulation of the Voltera model is represented as

$$Y_{Voltera}(n) = \sum_{p=1}^{N} \sum_{i_l}^{M} \dots \sum_{i_p}^{M} h_p(i_l, \dots, i_p) \prod_{j=1}^{p} x(n - i_j) \qquad (2.1)$$

where x (n) and $y_{voltera}$(n) represent the input and the output signals, respectively. $h_p(i_l, \dots, i_p)$ is called the p^{th} order Volterra kernel. M is the memory depth and N is the nonlinearity order of the model.

It is clear that by increasing the model dimensions, the number of parameters increases drastically. Taking the fact that all parameters are treated at the same time, the complexity of the model will rise too much making it an unpractical model. Figure 2.6 shows the block diagram of the Voltera model. General Volterra series based models have been successfully applied for radio frequency power amplifier behavioral modeling,

but their high complexity tends to limit their application. According to that, different efforts were consumed to decrease [35],[36]. New simplified Voltera series based model was proposed in [34], by employing a near-diagonality pruning algorithm to remove the coefficients which are very small, or else not impacting the output error.

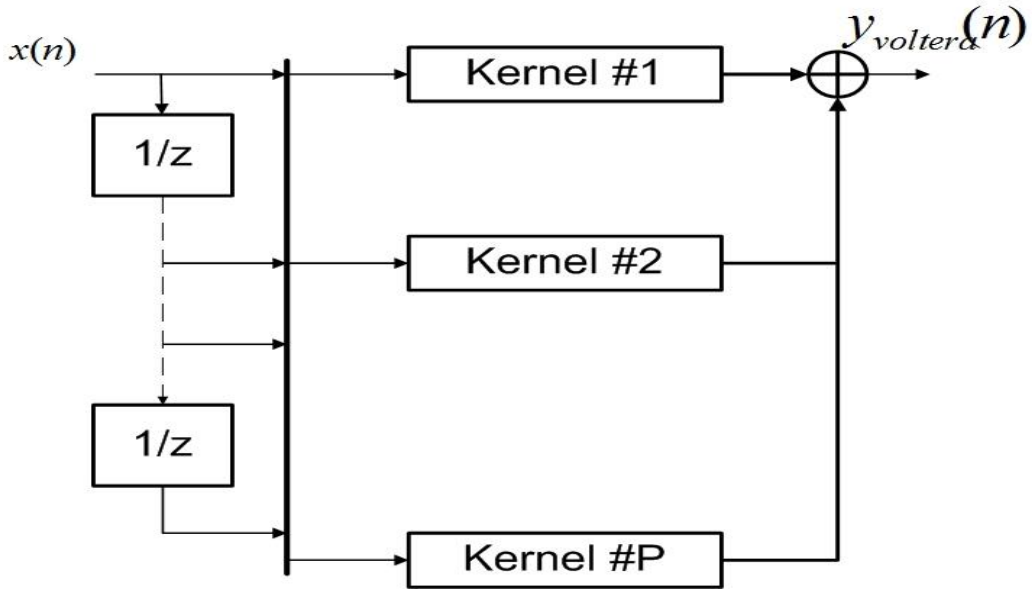

Figure 2.6 Block diagram of the Volterra model

2.3.2 Memory Polynomial Model

This model can be considered as a sub-model of the Voltera series with significantly lower complexity. Memory polynomial model is widely used in the behavioral modeling and predistortion of power amplifiers that exhibit memory effects due to its simplicity and accuracy.

The memory polynomial model is given by:

$$y_{MPM}(n) = \sum_{j=1}^{M} \sum_{i=1}^{N} a_{ij}.x(n+1-j).|x(n+1-j)|^{i-1} \qquad (2.2)$$

where x(n) is the complex input signal, N is the nonlinearity order and M represents the memory depth of the model. a_{ij} are the coefficients of the model, and $y_{mp}(n)$ is the output of the memory polynomial model. In Figure 2.7, the block diagram of the memory polynomial model is depicted.

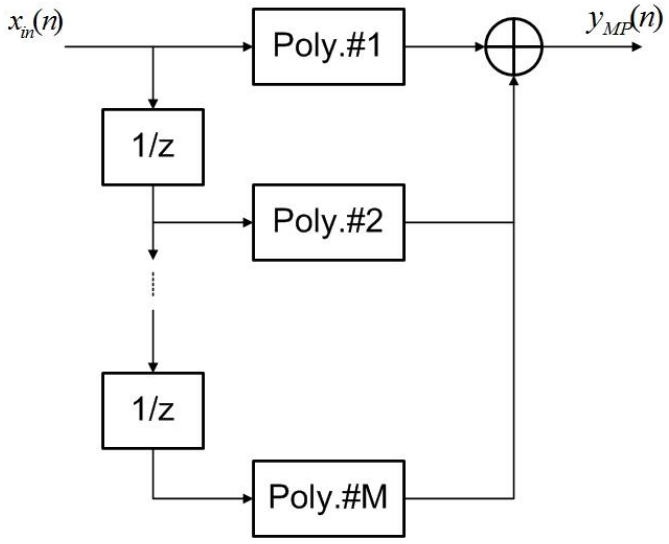

Figure 2.7 Block diagram of the memory polynomial model.

2.3.3 Envelope Memory Polynomial Model

In this model, which is based on the memory polynomial model, the output will be given as follows:

$$y_{EMPM}(n) = x(n)\sum_{j=1}^{M}\sum_{i=1}^{N} a_{ij}.|x(n+1-j)|^{i-1} \qquad (2.3)$$

where x(n) is the input signal, a_{ij} are the model coefficients, M and N are the memory depth and nonlinearity order respectively; and y(n) is the model output.

Figure 2.8 shows the block diagram of the envelope memory polynomial model. It is obvious that the model output depends on the absolute value of the previous baseband complex samples and the actual one also. This model is implemented in complex gain

based architecture and takes advantage of the dependency of PA nonlinearity on the magnitude of the input signal. Contrary to conventional memory polynomials, the proposed model can be used in radio frequency digital predistorters, as well as in baseband [24].

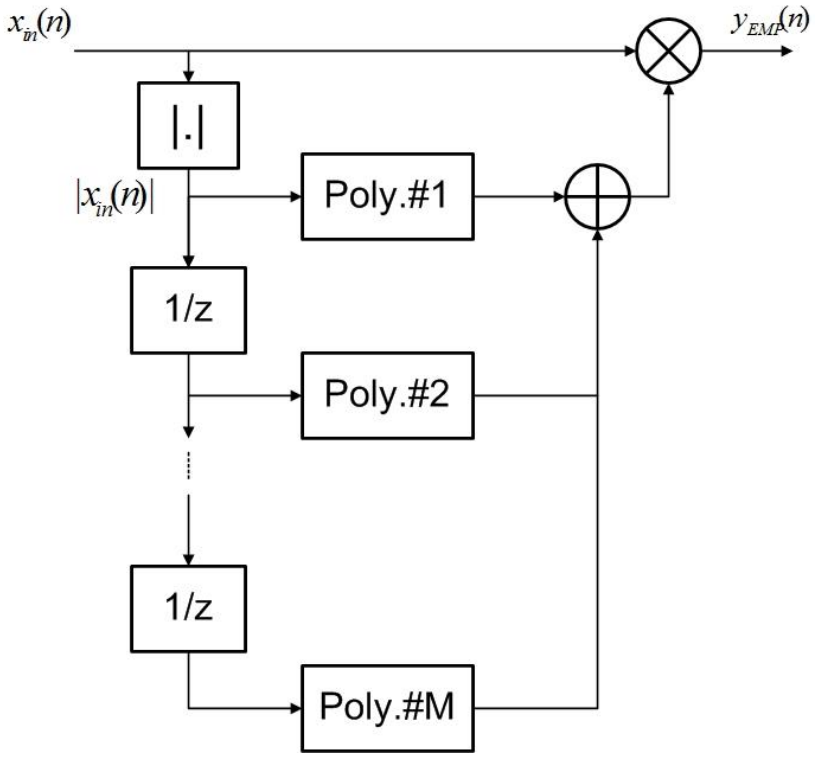

Figure 2.8 Block diagram of envelope memory polynomial model.

2.3.4 Hybrid MP-EMP (HMEM) Model

This model is a parallel combination between memory polynomial model and envelope memory polynomial model. The aim of this model is to gain the advantages of the two compromising models especially in frequency domain [25].

The input signal is applied to both functions and then their outputs are added to yield the overall output signal for the model as it is illustrated in Figure 2.9.

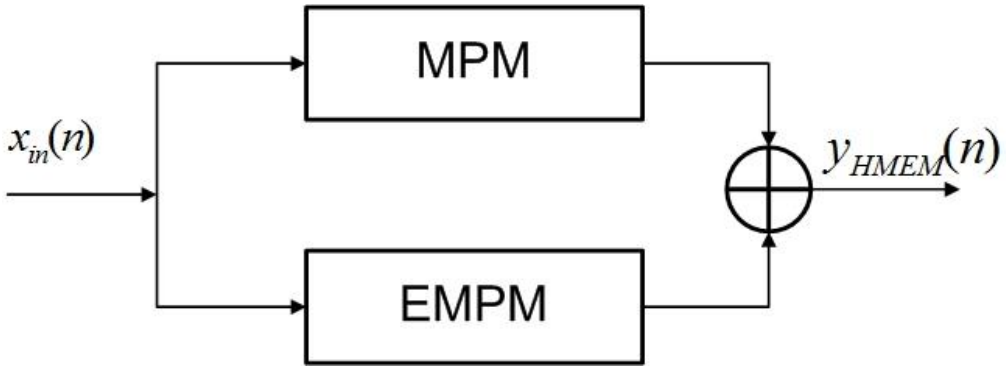

Figure 2.9 Block diagram of Hybrid MP-EMP model

The output of this model can be calculated according to the following formula:

$$y_{HMEM}(n) = \sum_{j=1}^{M_{MP}} \sum_{i=1}^{N_{MP}} a_{ij}.x(n+1-j).|x(n+1-j)|^{i-1} + \sum_{k=1}^{M_{EMP}} \sum_{l=1}^{N_{EMP}} b_{kl}.x(n).|x(n+1-k)|^{l-1} \quad (2.4)$$

where M_{MP}, N_{MP} are the memory depth and nonlinearity order of the memory polynomial model, respectively. M_{EMP}, N_{EMP} are the memory depth and nonlinearity order of the envelope memory polynomial model, respectively. a_{ij} and b_{kl} are the coefficients of the MP and EMP models, respectively.

2.3.5 Twin Nonlinear Two-Box Models

The twin nonlinear two-box (TNTB) models are made of two sub-models: a look-up table model and a memory polynomial model. The look-up table (LUT) is an easily to implement model, and doesn't include memory effects. The block diagram of LUT model is shown in the Figure 2.10.

The LUT output can be calculated through the following equation:

$$y_{LUT}(n) = G(|x_{in}(n)|).x_{in}(n) \quad (2.5)$$

where $G(|x_{in}(n)|)$ represents the instantaneous memoryless gain of the DUT.

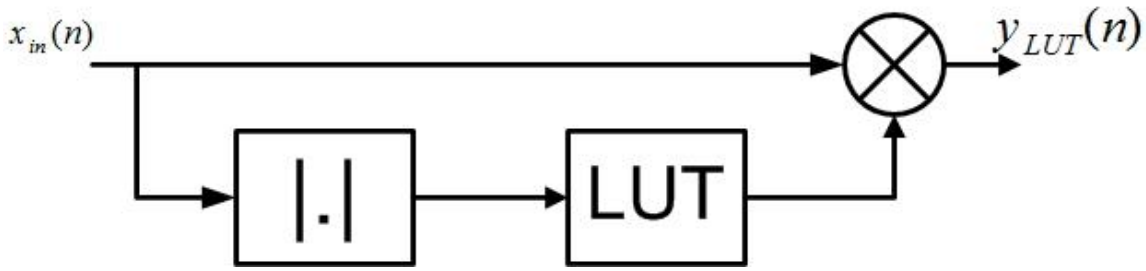

Figure 2.10 block diagram of LUT.

TNTB model, come in different combinations; forward, reverse and parallel as it is shown in the Figure 2.11, Figure 2.12, and Figure 2.13, respectively.

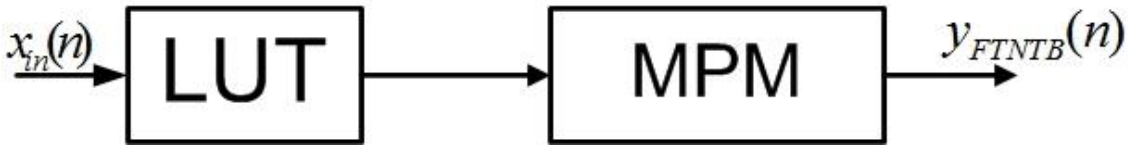

Figure 2.11 Block diagram of the forward TNTB model.

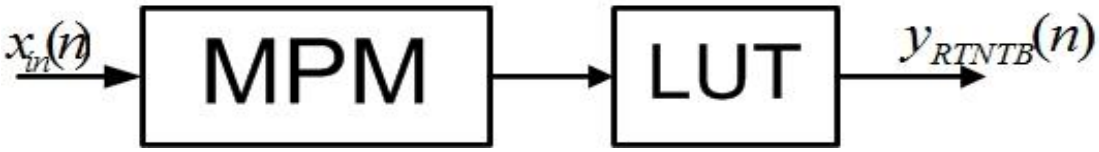

Figure 2.12 Block diagram of the reverse TNTB model.

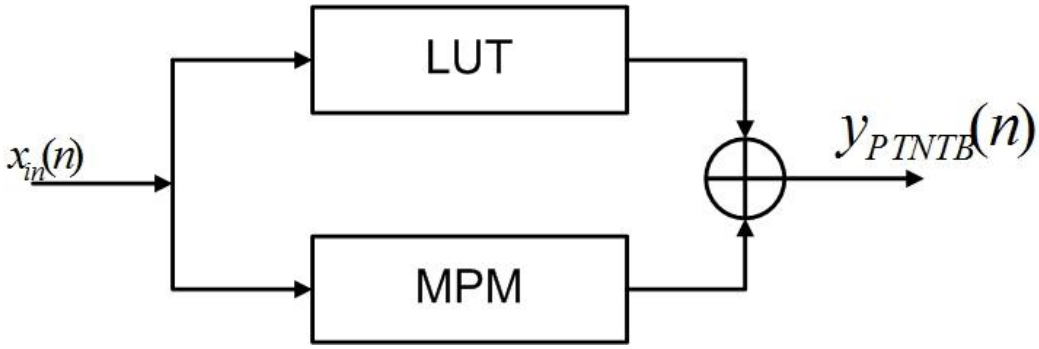

Figure 2.13 Block diagram of the parallel TNTB model.

2.3.6 Generalized Memory Polynomial Model (GMPM)

This model is a version of the memory polynomial with cross terms between the signal and its leading and lagging versions. The output of this model is described in the following equation:

$$y(n) = \sum_{k=0}^{N_a-1} \sum_{m=0}^{M_a-1} a_{km}.x(n-m).|x(n-m)|^k + \sum_{k=1}^{N_b} \sum_{m=0}^{M_b-1} \sum_{l=1}^{L_b} b_{kml}x(n-m).|x(n-m-l)|^k + \sum_{k=1}^{N_c} \sum_{m=0}^{M_c-1} \sum_{l=1}^{L_c} c_{kml}x(n-m).|x(n-m+l)|^k \quad (2.6)$$

here, x(n) and $y_{gmp}(n)$ are the input and the output of the GMP model. a_{km} , b_{kml} and c_{kml} are the coefficients of the time aligned, leading, and lagging branches respectively. M_a and N_a are the memory depth and the nonlinear order of the time-aligned MP part. M_b, N_b and M_c, N_c are memory depths and nonlinearity orders of the lagging and leading branches, respectively. L_b and L_c are the lagging and leading tap lengths, respectively.

2.4 Model Complexity

The complexity of any model can be determined through the number of coefficients needed to deploy this model. It is clear that the number of coefficients can be calculated according the model parameters with different formulas depending on the structure of each model.

This complexity computation will assess in the selection of the behavioral model, as it is preferable to use the lower complexity model if it gives satisfactory performance. Complexity is an important criterion for comparing the behavioral models.

In Table 2.3, summary of the models that was described in this chapter and their complexity computations is shown.

Table 2.3 Summary of models with its complexity

Model	Equation	Number of coefficients
Memory Polynomial	$y_{MPM}(n) = \sum_{j=1}^{M}\sum_{i=1}^{N} a_{ij}.x(n+1-j).\|x(n+1-j)\|^{i-1}$	NM
Envelope Memory Polynomial	$y_{EMPM}(n) = x(n)\sum_{j=1}^{M}\sum_{i=1}^{N} a_{ij}.\|x(n+1-j)\|^{i-1}$	NM
Hybrid MP-EMP	$y_{HMEM}(n) = \sum_{j=1}^{M_{MP}}\sum_{i=1}^{N_{MP}} a_{ji}\cdot x(n+1-j)\cdot\|x(n+1-j)\|^{i-1} + \sum_{k=1}^{M_{EMPM}}\sum_{l=1}^{N_{EMPM}} b_{kl}\cdot x(n).\|x(n+1-k)\|^{l-1}$	$N_{MPM}M_{MPM} + N_{EMPM}N_{EMPM}$
TNTB	$y_{TNTB}(n) = \sum_{j=1}^{M}\sum_{i=1}^{N} a_{ij}.x(n+1-j).\|x(n+1-j)\|^{i-1}$	N_{LUT} + NM
GMPM	$y_{GMP}(n) = \sum_{j=1}^{M_a}\sum_{i=1}^{N_a} a_{ji}\cdot x(n+1-j)\|x(n+1-j)\|^{i-1} + \sum_{j=1}^{M_b}\sum_{i=1}^{N_b}\sum_{l=1}^{L_b} b_{jil}\cdot x(n+1-j)\|x(n+1-j-l)\|^{i-1} + \sum_{j=1}^{M_c}\sum_{i=1}^{N_c}\sum_{l=1}^{L_c} c_{jil}\cdot x(n+1-j)\|x(n+1-j+l)\|^{i-1}$	$N_aM_a + N_bM_bL_b + N_cM_cL_c$

From Table 2.3, one can notice that the memory polynomial has the simplest structure and the lowest number of parameters, where the complexity and number of parameters increase as going from top to bottom reaching to the most complex structure and highest number of parameters of the GMP model.

2.5 Model Evaluation

The most important issue after choosing a certain behavioral model is to examine how well it works. There are a lot of metrics to check the efficiency of the model, one of the most used metrics in the evaluation the performance of the model is the Normalized Mean Square Error (NMSE). Its formula is given as the following [37][38]:

$$NMSE = \frac{\sum_{n=1}^{N} |y_{meas}(n) - y_{mod}(n)|^2}{\sum_{n=1}^{N} |y_{meas}(n)|^2} \qquad 2.6$$

where N is the number of samples in the input and output waveforms that used in the modelling, $y_{meas}(n)$ and $y_{mod}(n)$ are, respectively, the measured output and the model output. The NMSE is mainly affected by the in-band error, and it is easy to calculate. In Figure 2.14 is shown the idea of error calculation between the measured and the modeled signals.

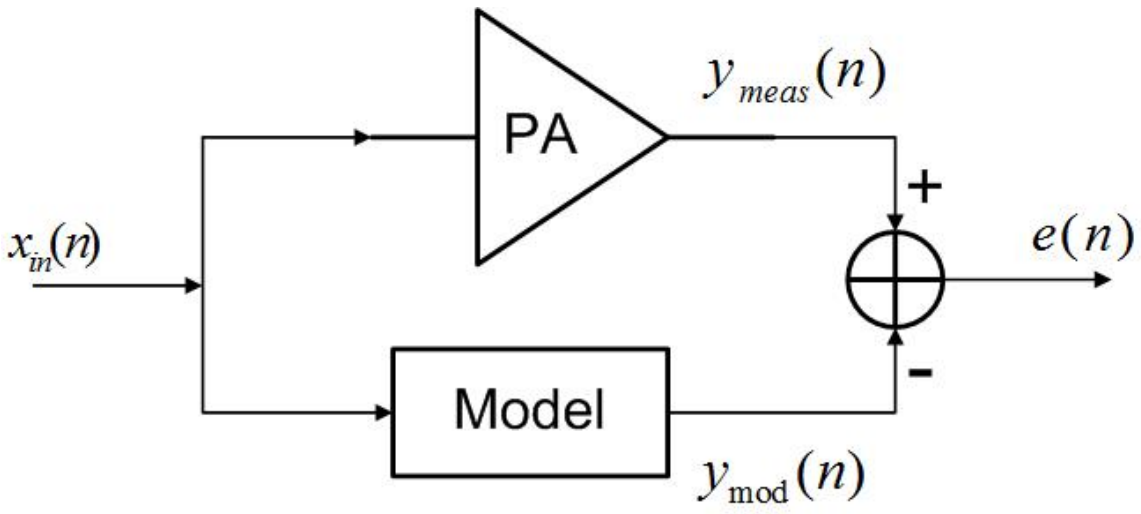

Figure 2.14 Measured and estimated outputs comparison.

2.6 Conclusion

In this chapter, literature review of envelope tracking power amplifier principles, structures, shaping functions and comparison with conventional power amplifier have been presented. Multiples behavioral models and their block diagrams, formulas, and complexity have been analyzed.

In chapter three, the use of memory polynomial, generalized memory polynomial, and forward twin nonlinear box models to mimic the output of an ET PA with four different shaping functions will be discussed.

CHAPTER 3

ET PA Modelling Using Conventional SISO Models

In this chapter, the experiment set-up used for the measurements of conventional and envelope tracking power amplifiers will be presented. The characteristics of the device under test (DUT) will be reported, analyzed, and compared. After that, three main models will be applied to these measurements. The comparisons between the various modeling results are discussed.

3.1 DUT and Experimental Set-up

In this section, details of DUT used in this work and its characteristics will be shown. Also, the block diagram and components of experimental set-up will be introduced in 3.1.2, along with pre-modeling processes that have been done on the input and output data.

3.1.1 DUT Description

The device under test used in this work was a class AB based on Cree's 10 W packaged GaN device (CGH400010), where the frequency of operation is 2.14 GHz. The envelope tracking path was built using four different cases: constant supply voltage and three different dynamic voltages.

The two signals that were used in this work are LTE signals. The first one has 5 MHz bandwidth and 10.24 dB PAPR. The second signal is 20 MHz wide and has a PAPR of 10.68 dB. The sampling frequency was set to 245.76 MHz for both cases due to hardware constraints.

3.1.2 Experimental Set-up

The experimental set-up consists of an arbitrary waveform generator, the device under test (DUT), a vector signal analyzer and a computer that monitors measurements using software as shown in Figure 3.1.

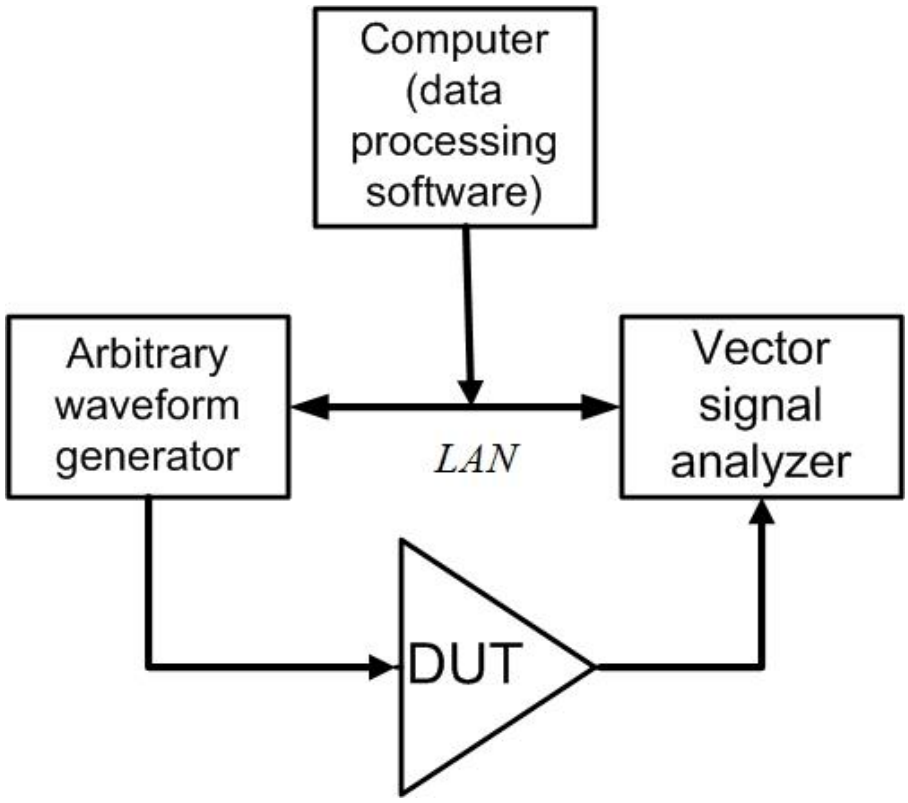

Figure 3.1 Block Diagram of Measurement set-up for DUT

From the computer, the waveform of the signal is downloaded to the arbitrary waveform generator, which will feed the RF signal to the DUT. The output from DUT is obtained through vector signal analyzer that will perform signal down conversion and digitization.

A propagation delay will be produced during the process of obtaining the DUT output which will lead to mismatch between the input and output data samples.

Before identifying the behavioral model, time alignment between input and output signals must be performed. This process was done by amplifiers and predistortion (AMPS) software. An AMP was also used for power adjustment of the data samples.

3.1.3 DUT Characteristics

In this thesis, two main cases are studied; conventional or fixed supply case where a constant supply voltage is used to feed the power amplifier, and the dynamic supply voltage type. Three main cases are involved under the dynamic voltage type: linear, Nujira n6, and Nujira Wilson. These three cases have the same structure; the main difference between them is the shaping function that is used to generate the modulated supply voltages.

All of ET cases are based on the envelope of the input signal. In the linear case, the supply voltage is determined according to the input power of the signal, as it increases the power supply will increase linearly.

In the other two cases, Nujira n6 and Nujira Wilson, the supply voltages are determined according to the following equations [39], respectively,

$$\boldsymbol{V_{n6}(t) = \left[V_{min}^{6} + V_{e}^{6}(t)\right]^{1/6}} \qquad (\mathbf{3.1})$$

$$\boldsymbol{V_{w}(t) = V_{min}\left(\frac{\pi}{\pi-2}\right)\left[1 - \left(\frac{\pi}{2}\right)\cos\left(V_{e}(t)\frac{(\pi-2)}{2V_{min}}\right)\right]} \qquad (\mathbf{3.2})$$

where $V_{min}$the minimum supply voltage of the PA, and V_e is the unshaped input envelope voltage.

The measured DUT input and output waveforms for these four cases for each of the two different LTE signals are the core of this thesis, where they are used in identifying the models and in attempting to come up with new model suitable for envelope tracking power amplifiers.

The AM/AM characteristics for the fixed, linear, n6 and Wilson with 5 MHz wide signal are shown in Figure 3.2. For ET cases, three different shaping functions have nearly the same AM/AM shape with almost same values. The differences between constant voltage and dynamic voltages supply are clearly noticable from the characteristics depicted in Figure 3.2. In dynamic voltage cases, the curvature is very obvious whereas in the fixed case there is a more linear behaviour in the AM/AM characteristic. This is of course expected to affect the performance of the different PA models.

In the AM/PM characteristic which are shown in Figure 3.3, the differnce is only in the value of small signal phase shift but not in the shape of curve. This observation will simplify the enhancement of the conventional models.

The AM/PM charactersitics of ET cases have the same behaviour with different small-signals values. In linear, the phase difference almost cocentrates around zero, whereas in n6 case its around 50, and around 240 degrees for wilson case.

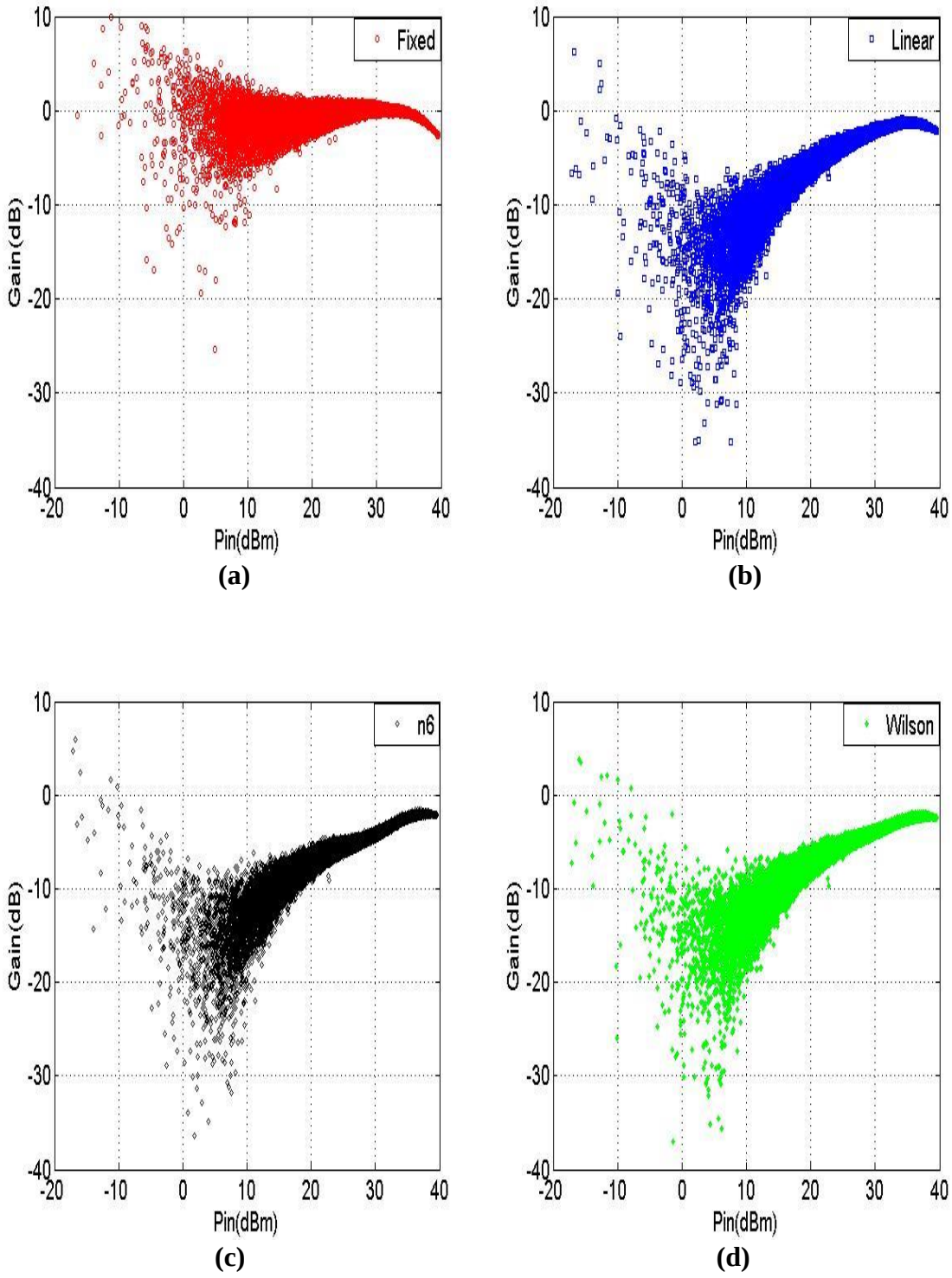

Figure 3.2 AM/AM characteristics of (a) Fixed (b) Linear (c) N6 (d) Wilson for the 5 MHz Signal

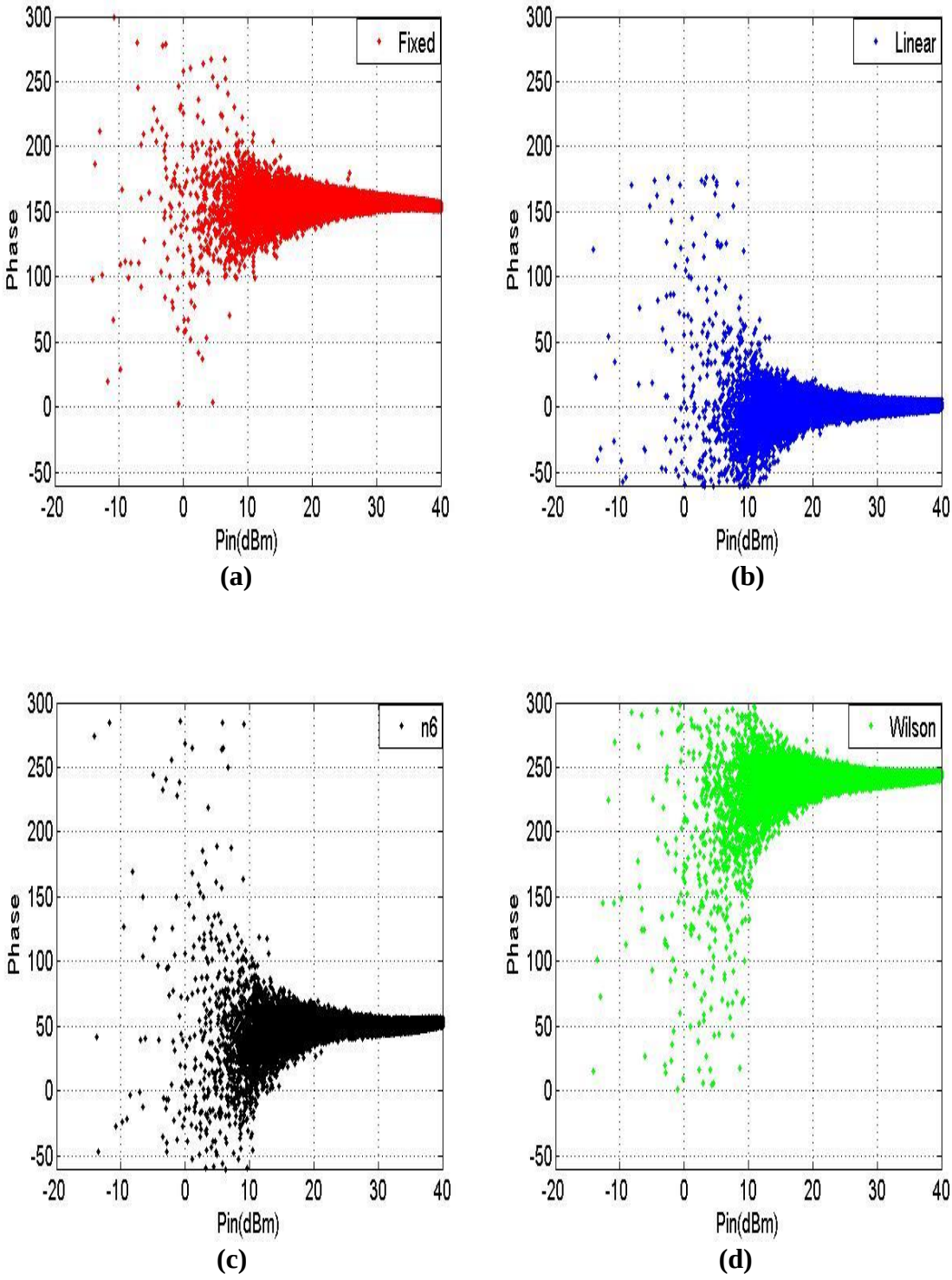

Figure 3.3 AM/PM characteristics of (a) Fixed (b) Linear (c) N6 (d) Wilson for the 5 MHz Signal

For the 20 MHz LTE signal, the AM/AM characteristics for the fixed, linear, n6 and Wilson cases are shown in Figure 3.4. for the dynamic supply voltages, the curvature is very obvious whereas in the fixed case there is a more linear behaviour. For ET cases, linear and n6 cases have nearly the same trend with almost same values. Wilson case has a slight difference from linear and n6 and this is clear for high input power.

In the AM/PM characteristics which are shown in Figure 3.5, the differences is only in the value of angles but not in the trend, which is the same as in the 5 MHz signal.

From AM/AM and AM/PM characteristics of different cases of the 20 MHz test signal, it is noticeable that there is a similarity between the behaviour observed with the 5 MHz signal and that of the 20 MHz signal, but with more spreading which means more memory effects. It is also clear that the shape of the curve for the ET cases have slightly more nonlinear behaviour.

These facts gave us indication that the same way of dealing with one case can be generalized of the envelope tracking power amplifiers driven by the two LTE signals.

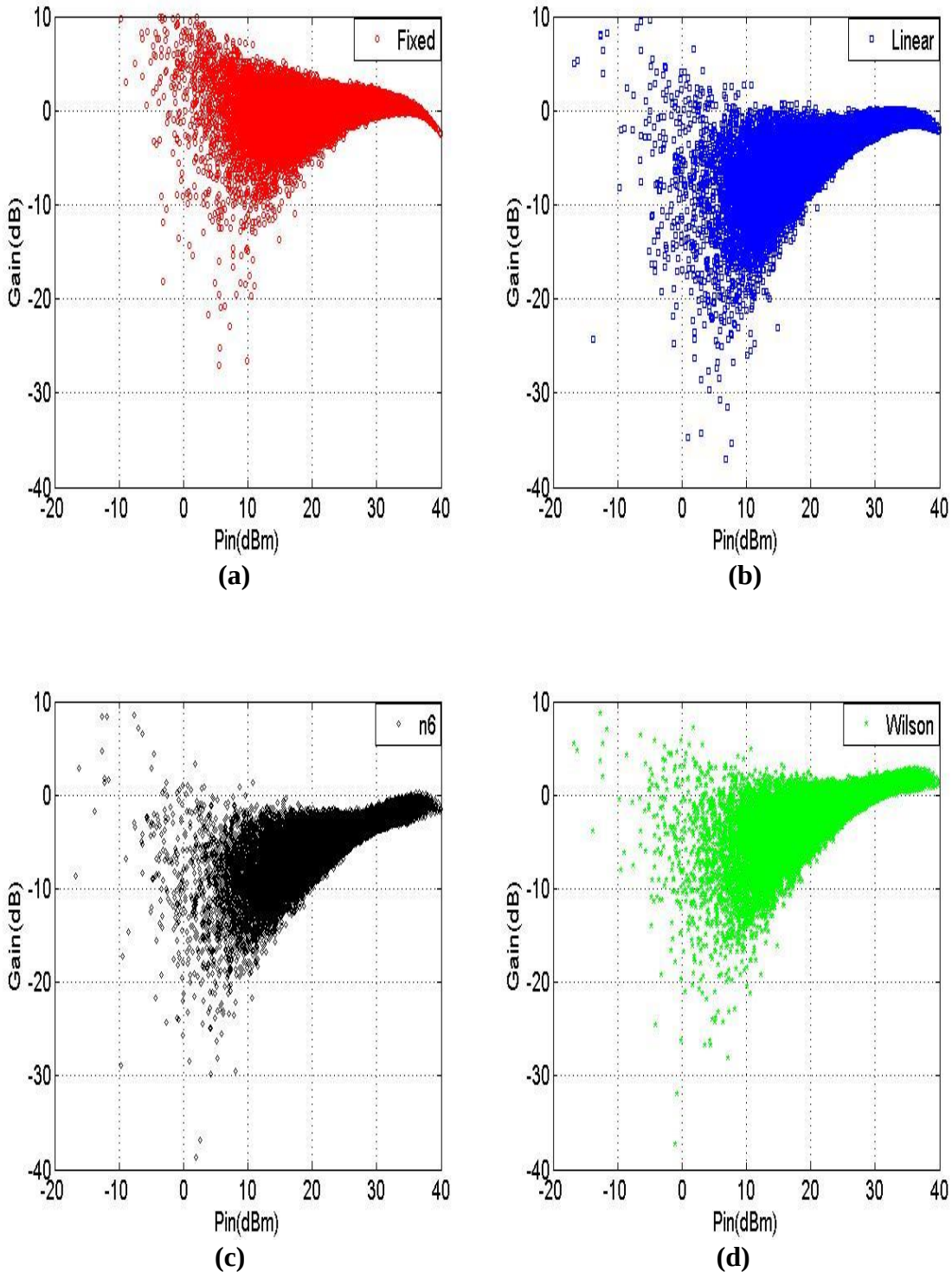

Figure 3.4 AM/AM characteristics of (a) Fixed (b) Linear (c) N6 (d) Wilson for the 20 MHz Signal

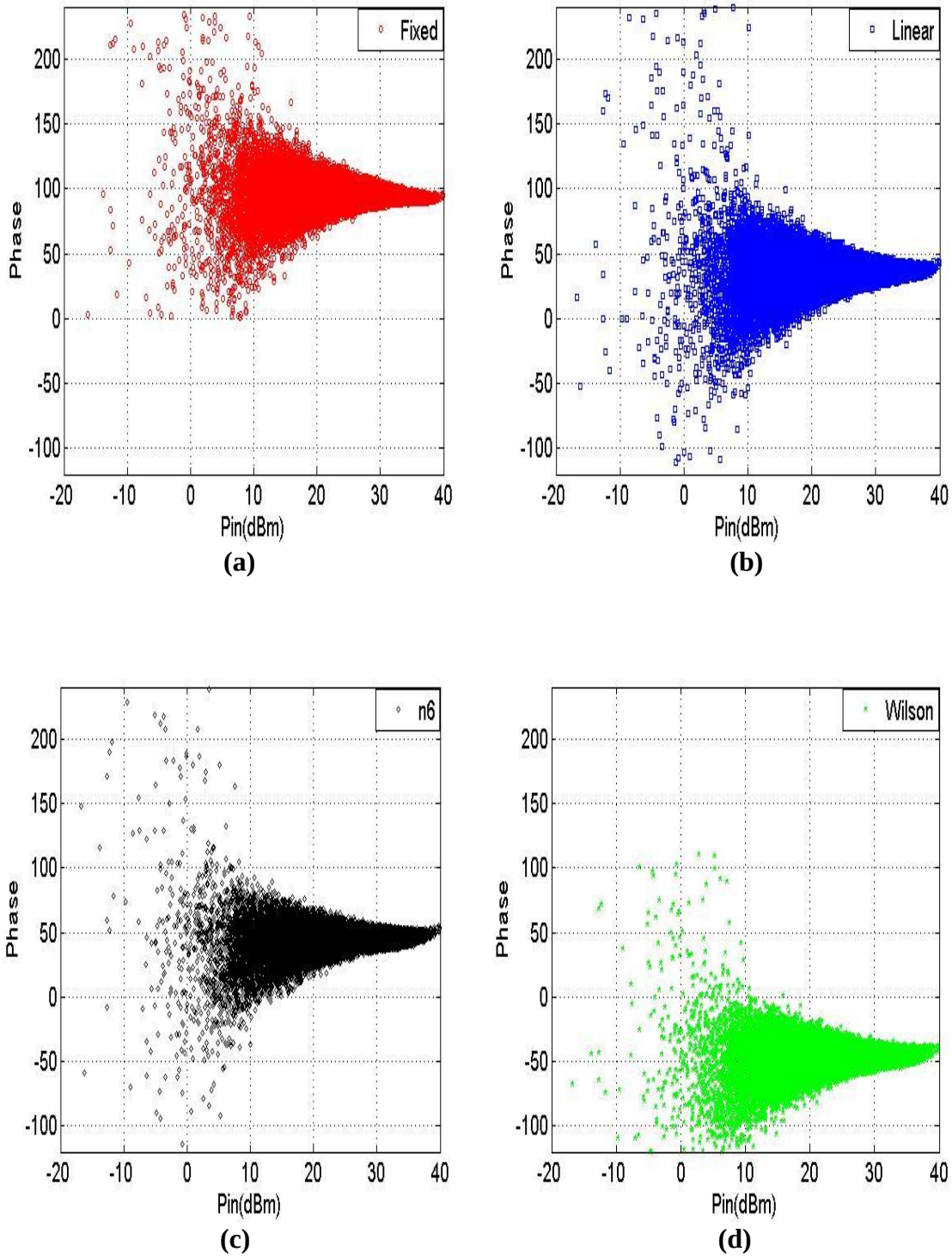

Figure 3.5 AM/PM characteristics of (a) Fixed (b) Linear (c) N6 (d) Wilson for the 20 MHz Signal

3.2 ET PA Modelling Using Memory Polynomial Model

In this section, the performance of the MP model for the four cases will be discussed. The MP model was applied for the four cases by sweeping the memory depth (M) and nonlinearity order (N) from 1 to 10 for each of these parameters (M=1:10, N=1:10). This was done for the two test signals (5 MHz and 20 MHz). In the following sub-sections, the results for each signal will be discussed.

3.2.1 MP Model Performance with 5 MHz LTE Test Signal

In this sub-section, the performance of the MP model for different cases with the 5 MHz LTE signal is discussed. According to the sweep of the parameters, the lowest total number of coefficients is 1 (M=1, N=1), whereas the highest is 100 (M=10, N=10).

The resulting NMSE for various numbers of coefficients for different cases are shown in Figure 3.6. It is clear from first look that constant supply voltage (fixed) has the best performance, and its NMSE is stabilized after 12 coefficients around -36 dB. For envelope tracking cases, they almost stabilize at the same number of coefficients as for the fixed supply case but with lower performance (-31 dB for linear and Wilson, while it is around -30 dB for n6 shaping function).

To assess the performance of the MP model, the lowest value of NMSE for each number of coefficients is considered. In Figure 3.7, the best NMSE is reported as a function of number of coefficients for the four cases. The fixed case shows the best performance, after that the linear and the Wilson have almost the same performance and then the n6 with comparable performance as observed in Figure 3.6.

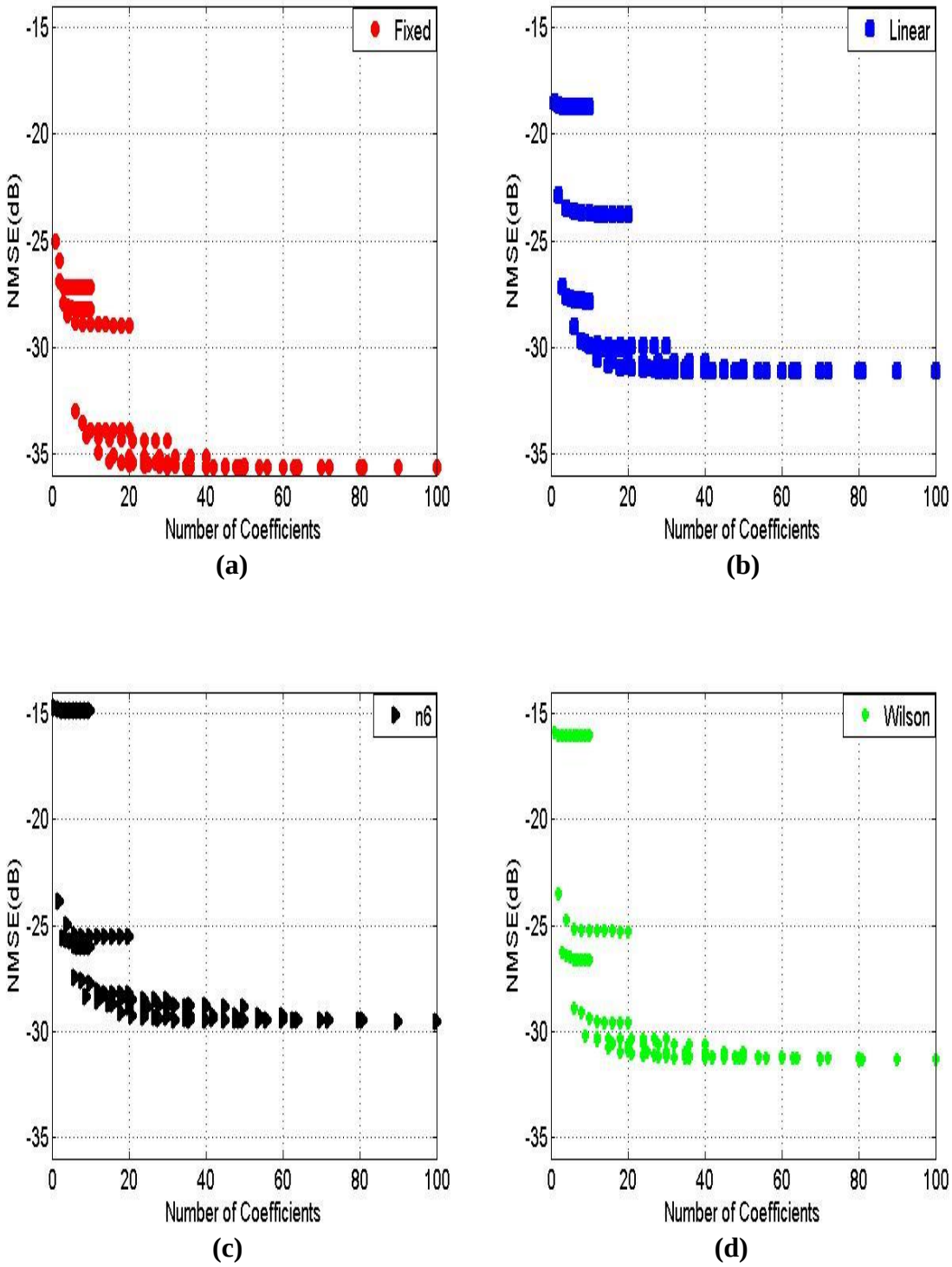

Figure 3.6 NMSE of the MP model vs number of coefficients for (a) Fixed (b) Linear (c) N6 (d) Wilson for the 5 MHz signal

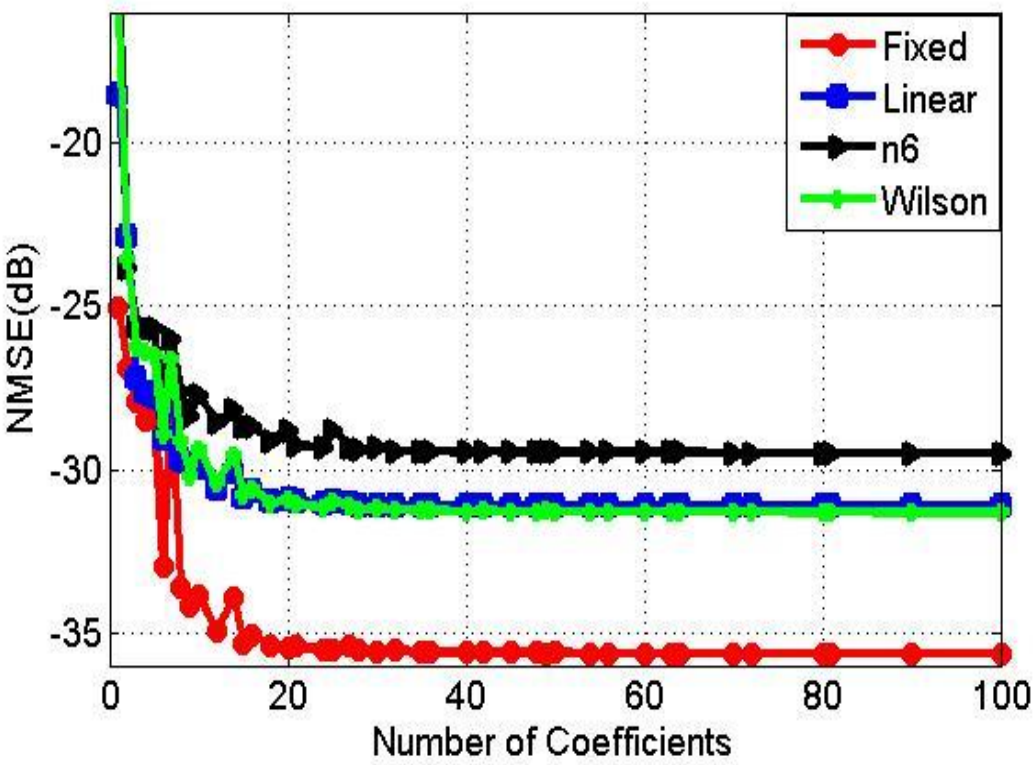

Figure 3.7 Best NMSE of the MP model vs number of coefficients for the 5 MHz signal

3.2.2 MP Model Performance with 20 MHz LTE Test Signal

The procedure for parameters sweep described in 3.2.1 was also used for 20 MHz LTE signal using the MP model for different cases. Thus, the lowest total number of coefficient was 1 (M=1, N=1), while the highest was 100 (M=10, N=10).

In Figure 3.8, the NMSE for different number of coefficients for different cases are reported. From this figure, one can notice some differences between using the MP model with 5 MHz signal and using it with 20 MHz LTE signal. It is obvious that fixed case has the best performance but lower than what was obtained for the 5MHz signal as it stabilizes around -31 dB. For different cases of ET shaping functions, the NMSE is also worse than that of the 5MHz but not too much like in fixed case.

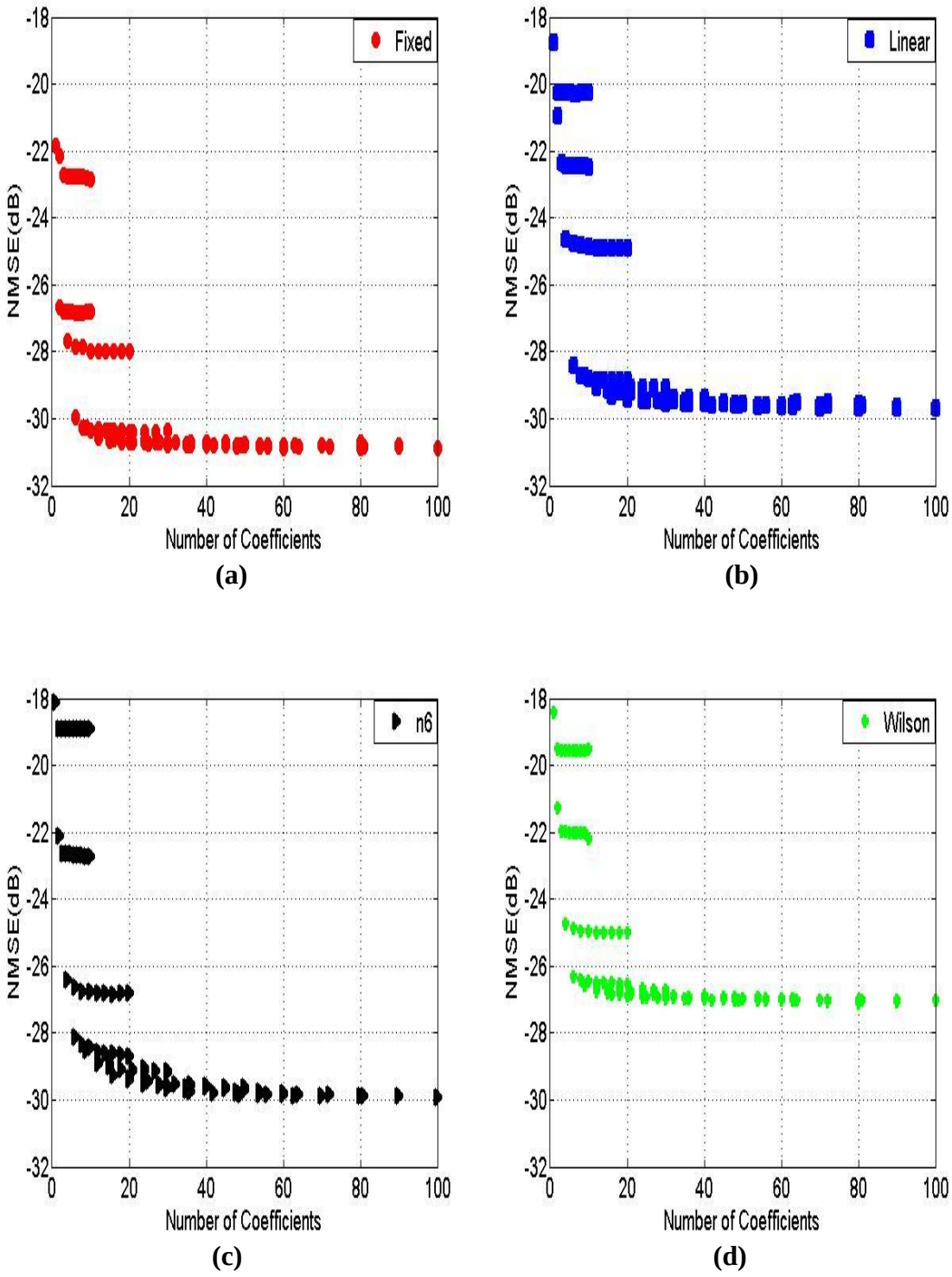

Figure 3.8 NMSE of the MP model vs number of coefficients for (a) Fixed (b) Linear (c) N6 (d) Wilson for the 20 MHz signal

For more clarity, the lowest value of NMSE for the each number of coefficients is obtained. This result is reported in Figure 3.9. It is clear that there is no significant difference between the performance of constant supply voltage case and that of linear and n6 cases.

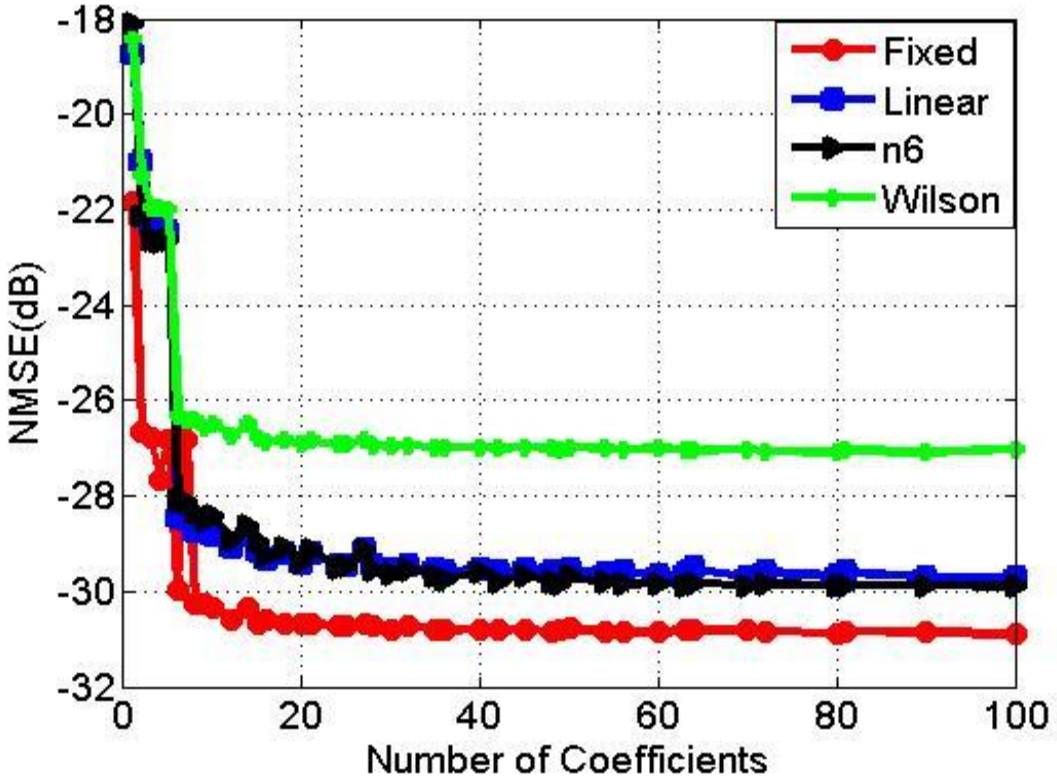

Figure 3.9 Best NMSE of the MP model vs number of coefficients for the 20 MHz signal

It is also obvious that the MP model for Wilson case driven by the 20 MHz LTE signal has the lowest performance. Also, compared with MPM for Wilson in the 5 MHz case, using MP model for Wilson in the 20 MHz case has lower performance by around 3 dB.

3.3 ET PA Modelling Using Generalized Memory Polynomial Model

The GMP model was applied for the four cases considered in the previous section. the model parameters were swept from 1 to 10 for M_a, from 1 to 10 for N_a ,whereas $M_b, N_b, M_c,$ and N_c were swept from 1 to 5. The leading and lagging cross-terms orders (L_b and L_c) were set to 1. Modeling performance of GMP model for the 5 MHz and the 20 MHz LTE signals are reported in sections 3.3.1, 3.3.2 respectively.

3.3.1 GMP Model Performance with 5 MHz LTE Test Signal

Referring the parameters sweep, the lowest number of coefficients of the GMP model is 3 ($M_a = 1,\ N_a = 1,\ M_b = 1, N_b = 1,\ L_b$=1, $M_c = 1, N_c = 1, L_c = 1$), while the highest number of coefficients is 150 ($M_a = 10,\ N_a = 10,\ M_b = 5, N_b = 5,$ L_b=1, $M_c = 5, N_c = 5, L_c = 1$). The modeling results of GMP model for fixed, linear, n6 and Wilson cases with the 5 MHz LTE signal are shown in Figure 3.10.

The results of the GMP model for the four cases with the 5 MHz LTE signal is summarized in Figure 3.11 which shows the best NMSE performance for each number of coefficients. This figure shows the same trend as in MP model with some difference in values of stabilization point for different cases. Fixed voltage has the best performance, then linear and Wilson cases have almost the same performance, and at the end n6 comes with almost -30 dB.

From the same figure, one can see 3 to 4 dB difference between fixed case in one hand and linear and Wilson in the other hand, and this difference increases to almost 6 dB when the fixed case is compared to the n6 case.

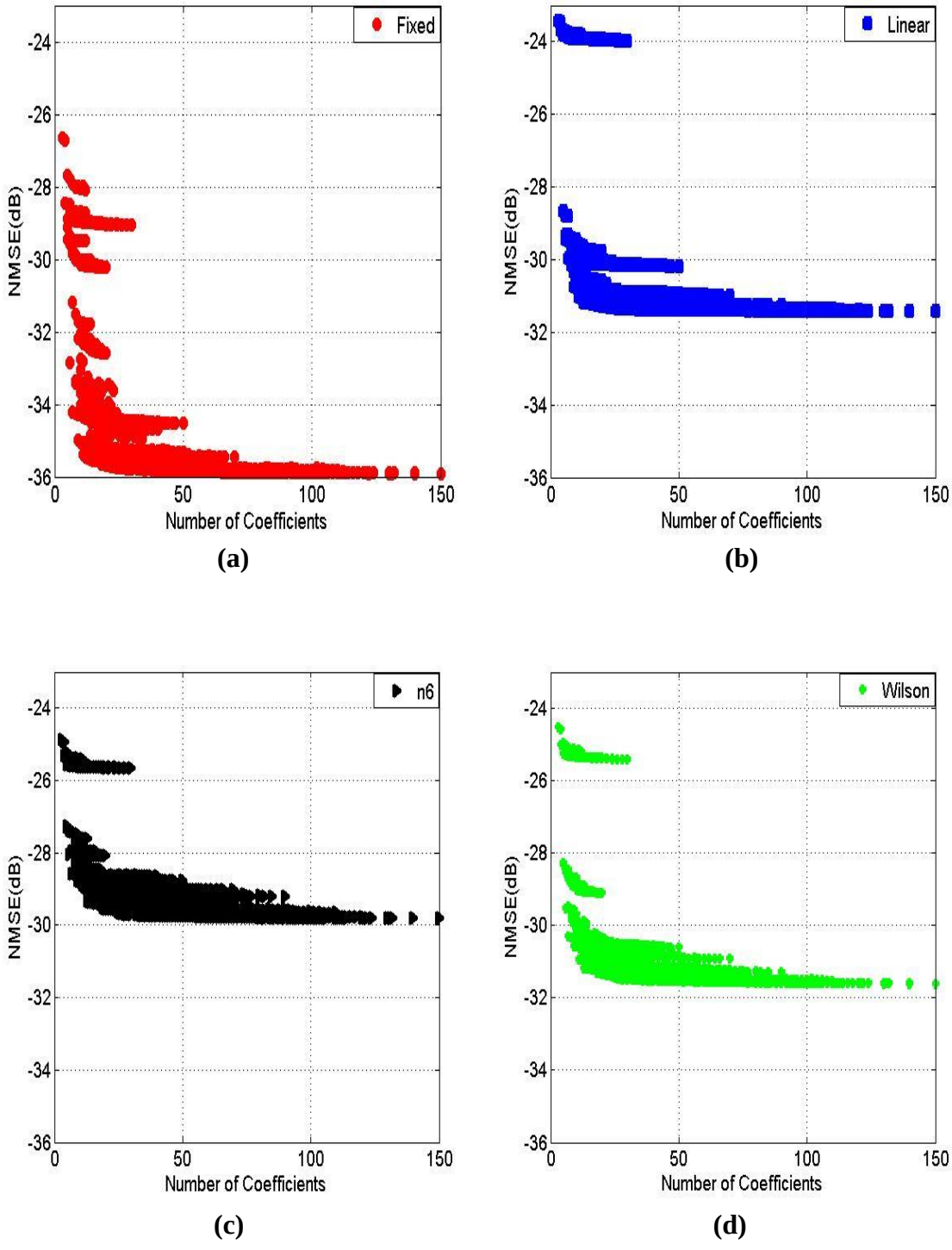

Figure 3.10 NMSE of the GMP model vs number of coefficients for (a) Fixed (b) Linear (c) n6 (d) Wilson for the 5 MHz signal

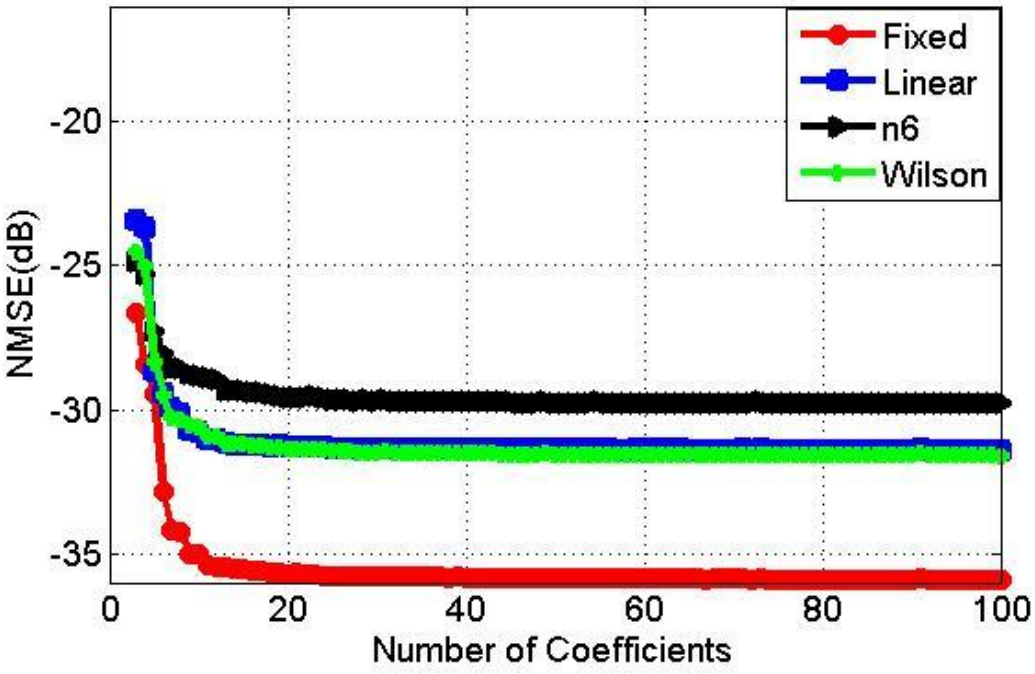

Figure 3.11 Best NMSE of the GMP model vs number of coefficients for the 5 MHz signal

3.3.2 GMP Model Performance with 20 MHz LTE Test Signal

The GMP model was then applied to the 20 MHz LTE signal. The same parameters sweep used for the 5 MHz was applied. Thus, the lowest number of coefficients is 3 ($M_a = 1,\ N_a = 1,\ M_b = 1, N_b = 1,\ L_b$=1, $M_c = 1, N_c = 1, L_c = 1$), whereas the highest number of coefficients is 150 ($M_a = 10,\ N_a = 10,\ M_b = 5, N_b = 5,$ L_b=1, $M_c = 5, N_c = 5, L_c = 1$). In Figure 3.12, the results of the GMP model with the 20 MHz signal are reported for different cases. In Figure 3.13, the best NMSE for each case is shown. The model performance as a function of the shaping function is different from what was observed with the 5 MHz test signal. Fixed supply voltage still has the best NMSE but n6 and linear shaping functions come after that, whereas Wilson has the worst NMSE which is the same as what was obtained with the MP model for the same test signal.

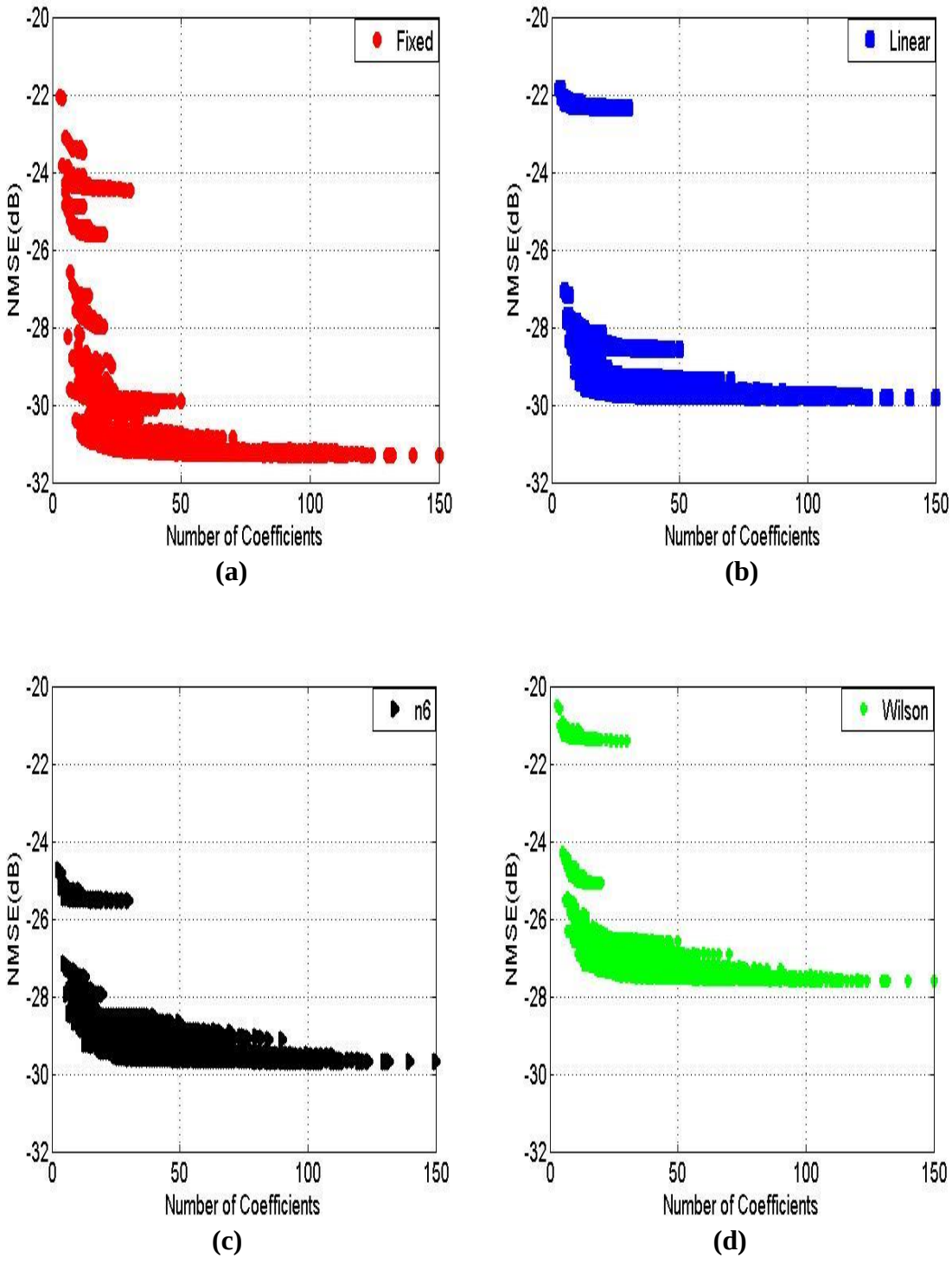

Figure 3.12 NMSE of the GMP model vs number of coefficients for (a) Fixed (b) Linear (c) N6 (d) Wilson for the 20 MHz signal

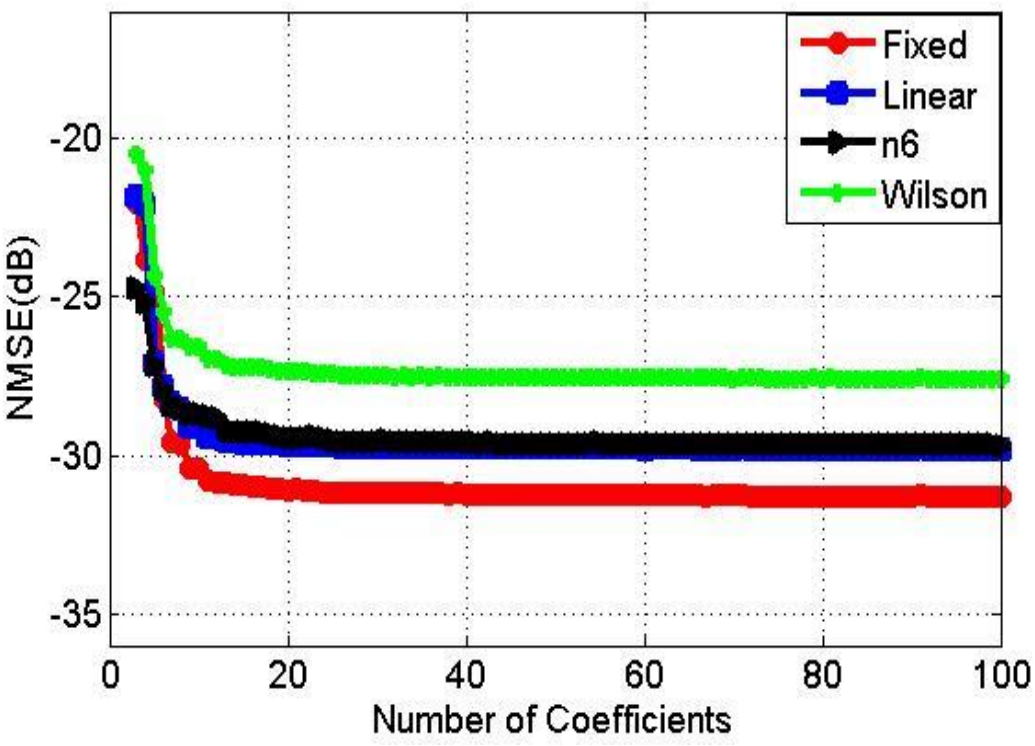

Figure 3.13 Best NMSE of the GMP model vs number of coefficients for the 20 MHz signal

Comparing between using GMP model with the 5 MHz and the 20 MHz LTE signals, one can depict multiple differences. Firstly, the ordering of cases was different. Secondly, for the 20 MHz signal, the difference between the performance of the fixed supply voltage and dynamic supply voltages is low. Thirdly, the performances of using GMP model with 20 MHz are worse than in 5 MHz. Another point related to the Wilson case, there are around 3 dB difference in NMSE between the performance of the GMP model for the 5 MHz signal and that of the 20 MHz signal.

3.4 ET PA Modelling Using FTNTB Model

The identification of FTNTB model is done in two separate steps. Firstly, the LUT is identified, then, in the second step, the MP model coefficients are identified. The FTNTB was applied for the four cases. For each case, the FTNTB model parameters of the second box (MP model) were swept. The memory depth and nonlinearity order were varied from 1 to 10 for each (M=1:10, N=1:10) while the LUT size for the first step was kept unchanged (N_{LUT} =10).

3.4.1 FTNTB Model Performance with the 5 MHz LTE Test Signal

In this sub-section, the performance of the FTNTB model with the 5 MHz LTE signal is reported for the different cases. According to the parameters sweep, the lowest number of coefficients is 11 (N_{LUT}=10, M=1, N=1), while the highest number of coefficients is 110 (N_{LUT}=10, M=10, N=10). In this model, the starting point is at 11 coefficients which is too much compared with 1 in the MP model or 3 in the GMP model.

The results of using FTNTB with the 5 MHz LTE signal are described in Figure 3.14 for fixed, linear, n6, and Wilson. After that, the lowest value of NMSE for each number of coefficients is reported for each case in Figure 3.15. The best performance in the FTNTB model is obtained for fixed case which is the same as the MP model and the GMP model. For dynamic cases, the best performance is obtained for Wilson then linear and n6 with almost same performance. There is at least 3 dB difference between constant supply voltage case and dynamic supply voltage cases. In fixed case, the NMSE stabilizes around -35 dB. For Wilson, the best NMSE is around -32 dB, whereas for n6 and linear it is almost at -31 dB.

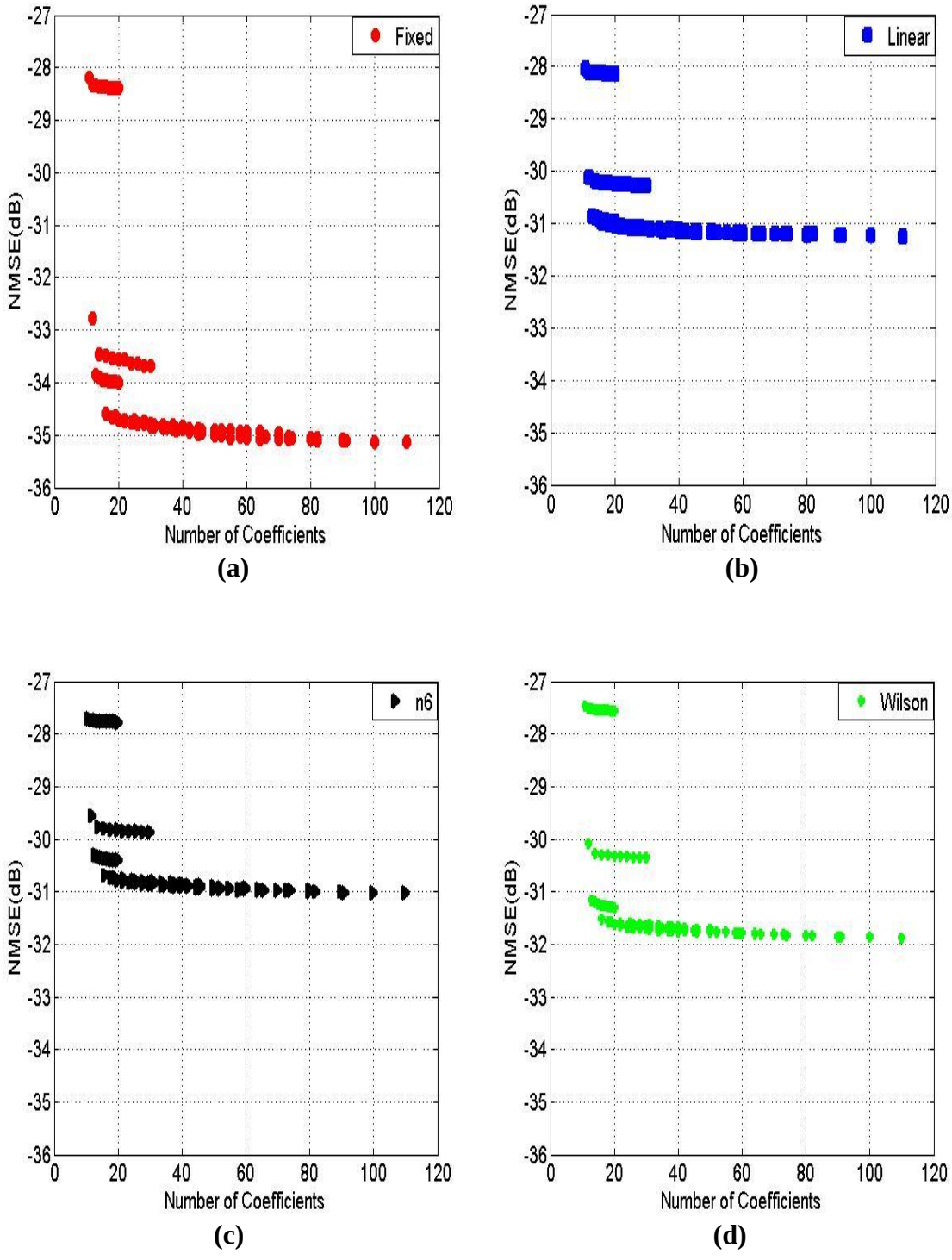

Figure 3.14 NMSE of the FTNTB model vs number of coefficients for (a) Fixed (b) Linear (c) N6 (d) Wilson for the 5 MHz signal

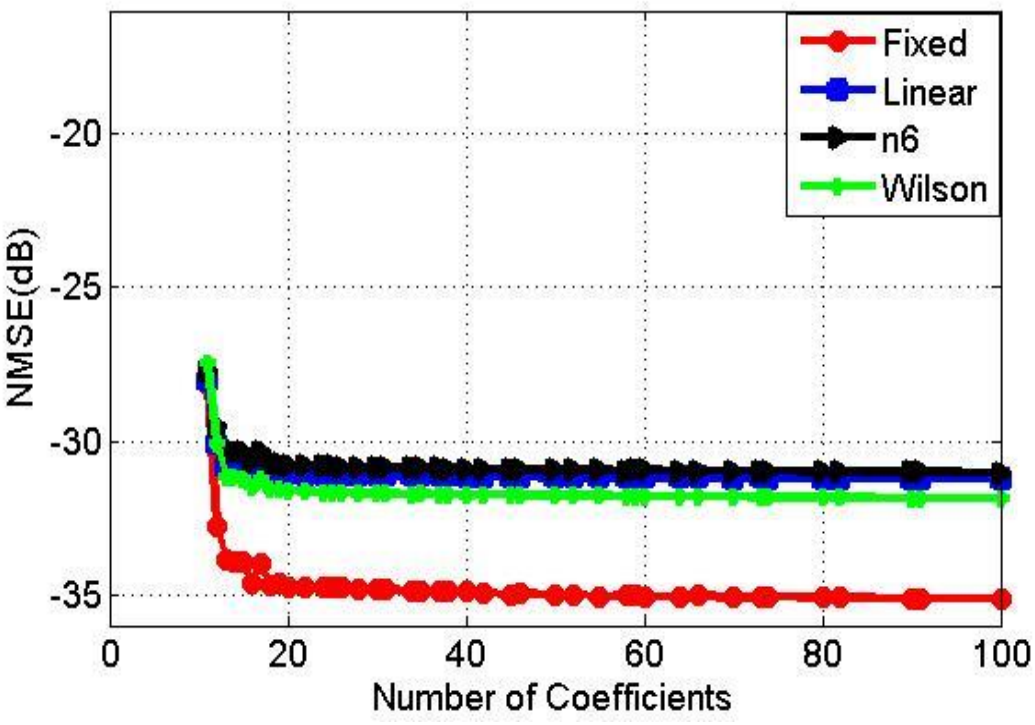

Figure 3.15 Best NMSE of the FTNTB model vs number of coefficients for the 5 MHz signal

3.4.2 FTNTB Model Performance with the 20 MHz LTE Test Signal

As in the previous sections, the same parameters sweep used with the 5 MHz LTE signal is also repeated with the 20 MHz signal. So, for the FTNTB model with the 20 MHz LTE signal, the lowest number of coefficients is 11, whereas the highest is 110. The performance of FTNTB model with the 20 MHz LTE signal is shown in Figure 3.16 for the different shaping functions. The performances of all cases are low, comparing with the performance of the same model with the 5 MHz LTE signal. In Figure 3.17, the best NMSE for each case is shown as a function of the model's number of coefficients.

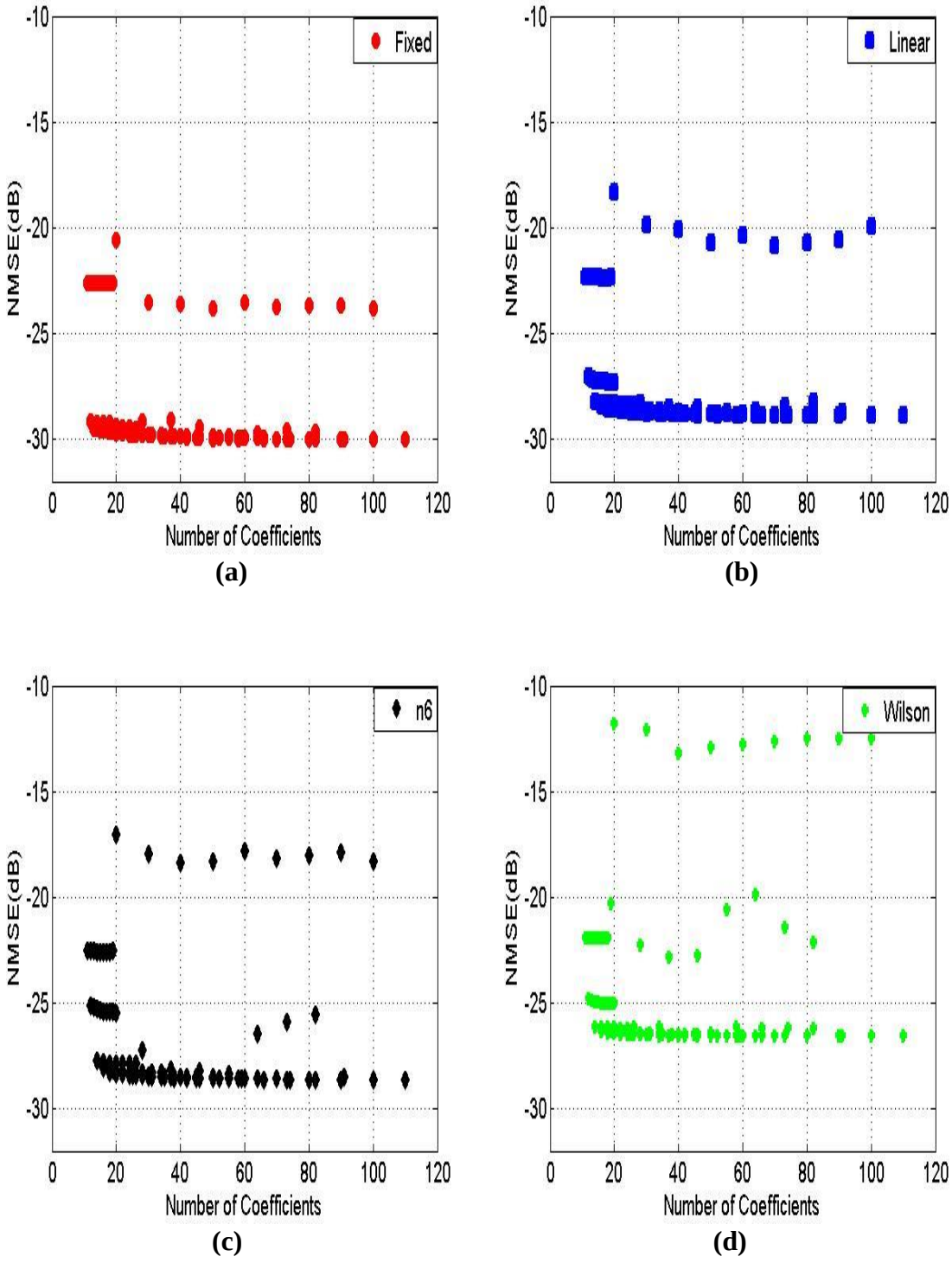

Figure 3.16 NMSE of the FTNTB model vs number of coefficients for (a) Fixed (b) Linear (c) N6 (d) Wilson for the 20 MHz signal

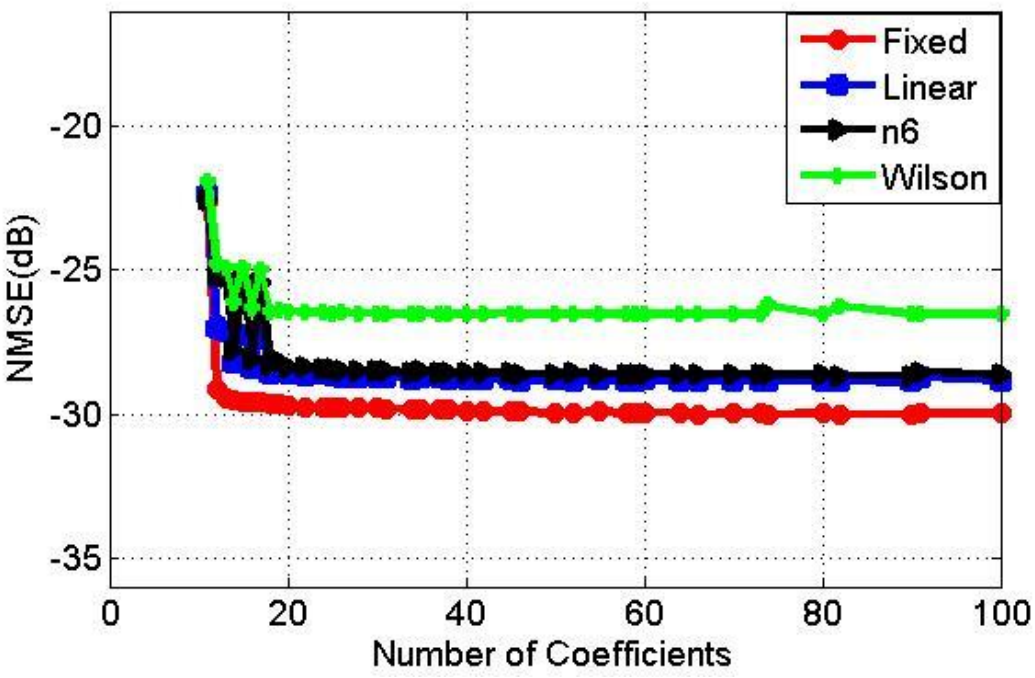

Figure 3.17 Best NMSE of the FTNTB model vs number of coefficients for the 20 MHz signal

After applying the FTNTB model for the 5 MHz and 20 MHz LTE signals, one can consider the results from many aspects. Regarding to the relative performance for the different shaping functions, fixed supply has the best performance with both test signals. ET cases have small variance with the 5 MHz test signal, but with the 20 MHz signal Wilson shaping function has the lowest performance with 2 to 3 dB degradation in the NMSE when compared to the linear and n6 cases.

For Wilson case, at least there are 5 dB difference between the FTNTB model with the 5 MHz and the 20 MHz LTE signals. This behavior is also the same for the MP model and the GMP model.

3.5 Models Performance Benchmarking

After depicting the performances of three state of the art models and seeing the comparison between the four cases for each model, the performance of the different models for each case will be discussed in the coming sub-sections for the two LTE signals.

3.5.1 Models Performance Benchmarking for the 5 MHz LTE Signal

The results of the different models for fixed, linear, n6, and Wilson cases are shown in Figure 3.18 to Figure 3.21. It is obvious that in fixed case for the same number of coefficients, the GMP model has the best performance, then MP model and at the end the FTNTB model. There is no noticeable difference between MP and GMP models but the difference is more apparent with FTNTB model.

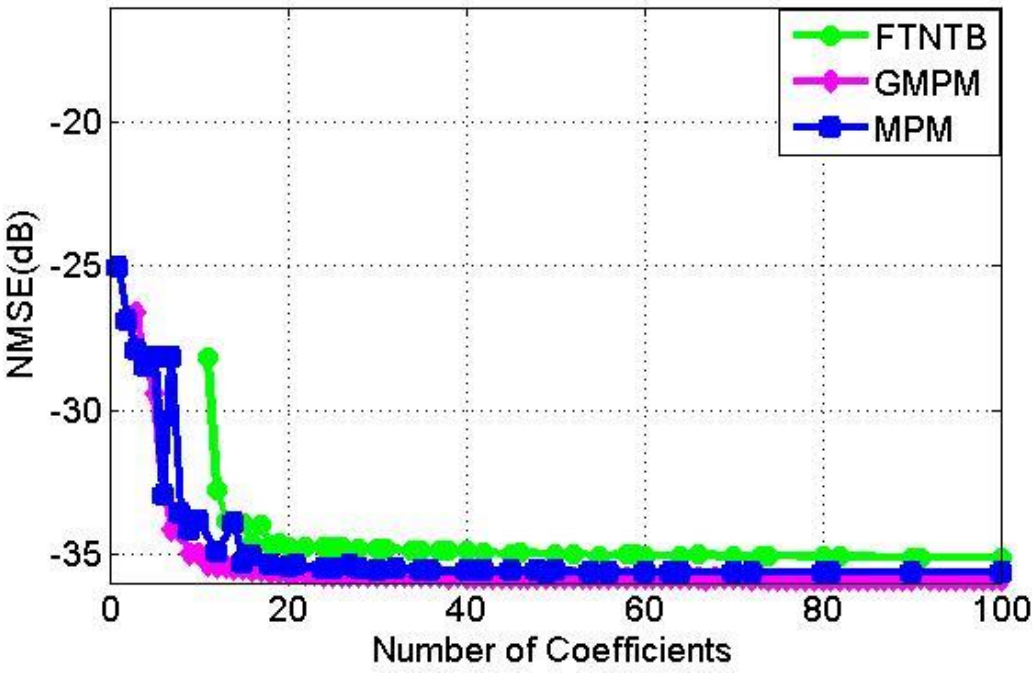

Figure 3.18 NMSE of the different models vs number of coefficients for fixed case for the 5 MHz signal

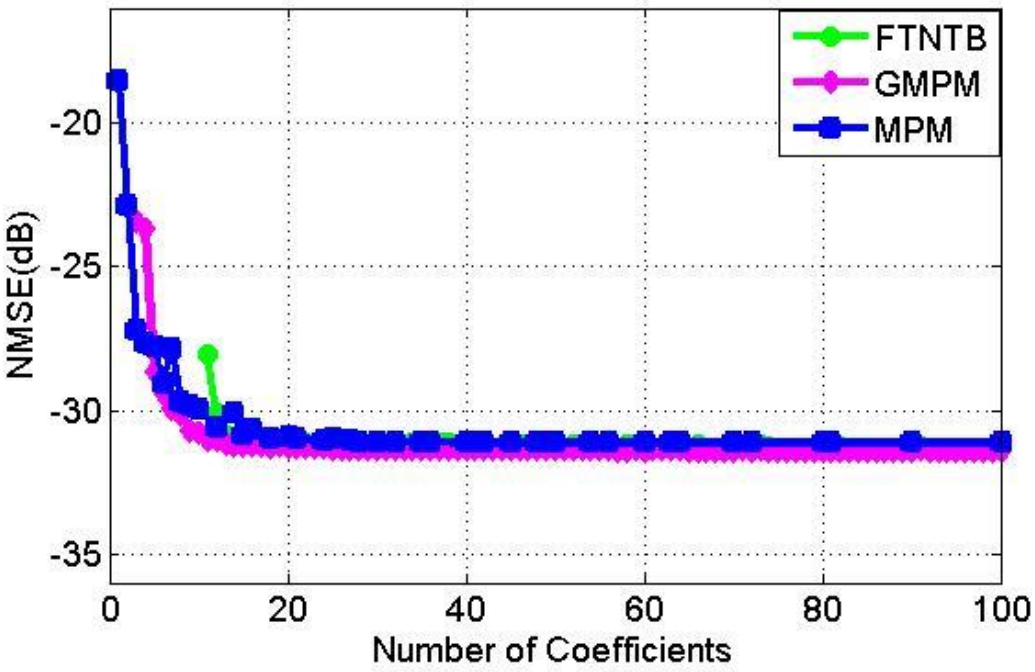

Figure 3.19 NMSE of the different models vs number of coefficients for linear case for the 5 MHz signal

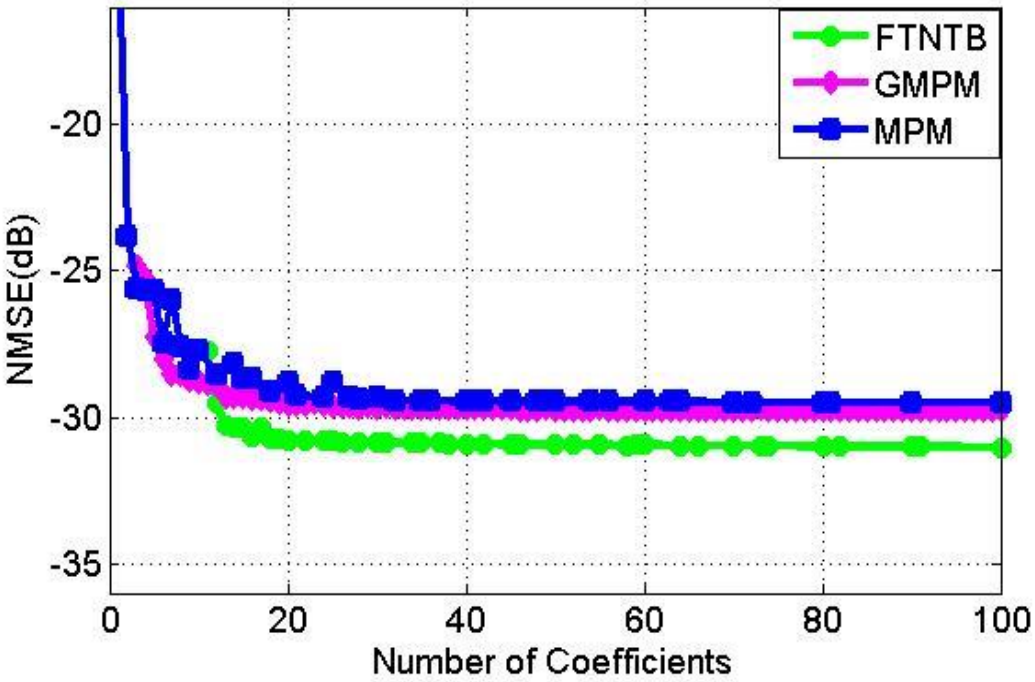

Figure 3.20 NMSE of the different models vs number of coefficients for n6 case for the 5 MHz signal

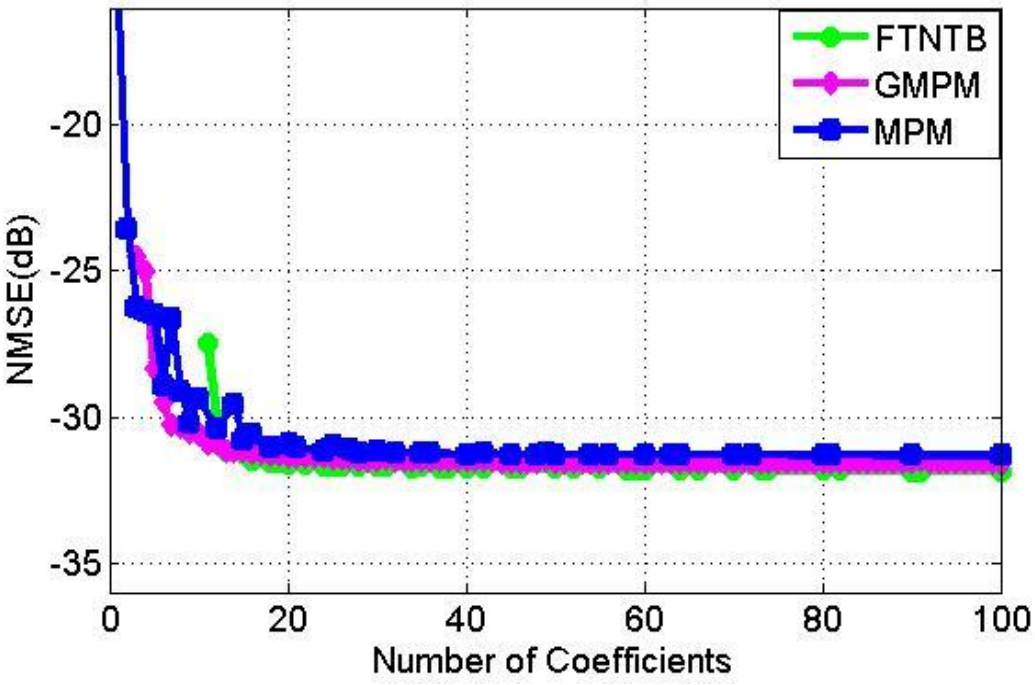

Figure 3.21 NMSE of the different models vs number of coefficients for Wilson case for the 5 MHz signal

For linear case, all models have almost the same performance as seen in Figure 3.19. For n6 case, the FTNTB model has the best performance with 1 dB better performance than MP and GMP models. In Wilson case, the results are shown in Figure 3.21, all models have near performances after stabilization, where all of them have NMSE around -32 dB.

From models benchmarking with 5 MHz signal, one can see that there is no significant difference between all models for all cases. Also, number of coefficients needed to reach stabilization of the NMSE is almost the same in all models is around 20 coefficients for all cases.

3.5.2 Models Performance Benchmarking for the 20 MHz LTE Signal

The use of different models for each shaping function with the 20 MHz LTE signal is the core of this sub-section. Figure 3.22 to Figure 3.25 show the results of using the three standard models for fixed, linear, n6, and Wilson cases, respectively. In fixed case, GMP model has the best performance then the MP model with slight variance and the FTNTB model at the end with almost 1 dB difference. For ET cases, the same trend as for the fixed case is repeated, where the best performance is for the GMP model then the MP model and after that the FTNTB model.

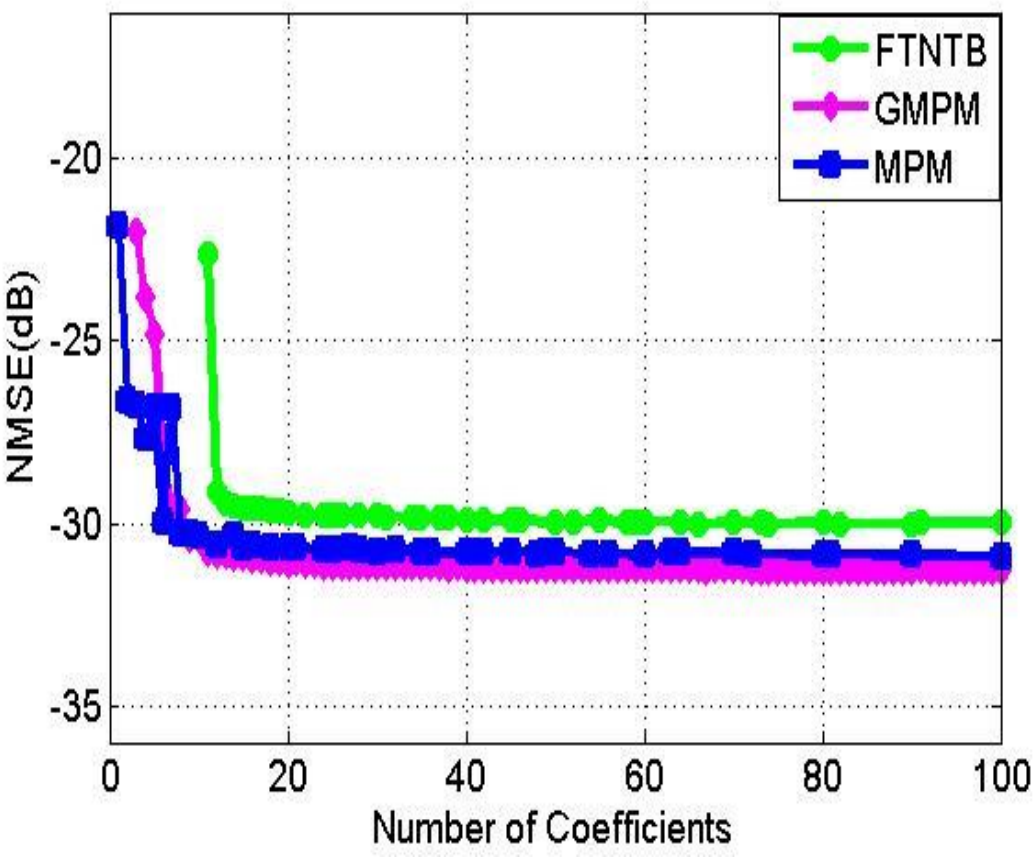

Figure 3.22 NMSE of the different models vs number of coefficients for fixed case for the 20 MHz signal

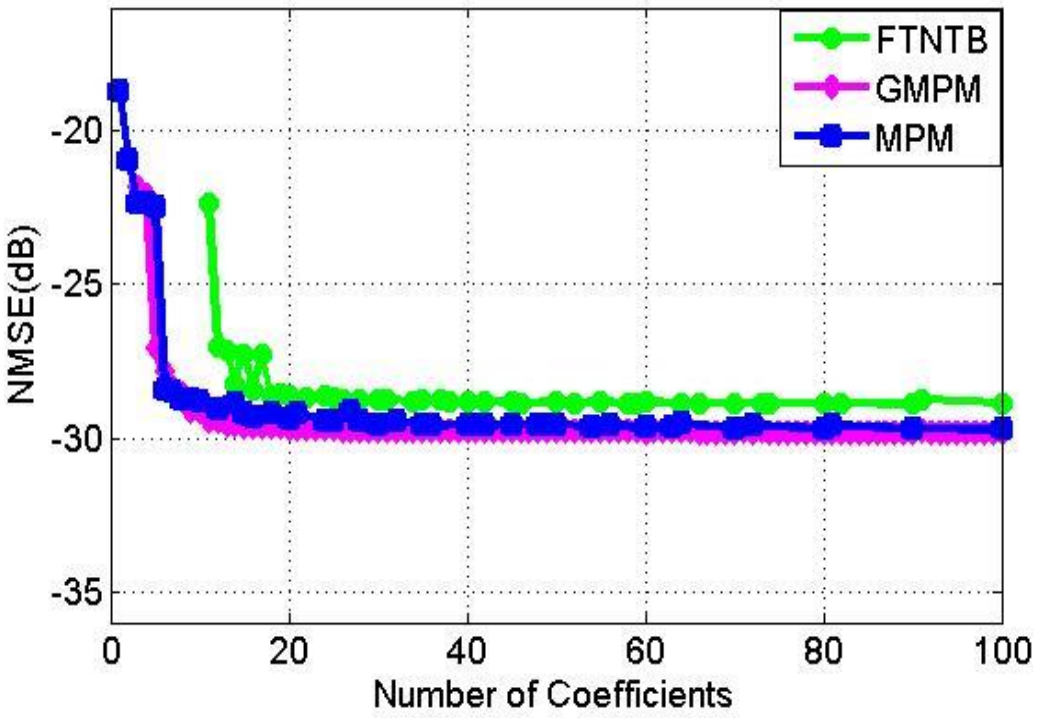

Figure 3.23 NMSE of the different models vs number of coefficients for linear case for the 20 MHz signal

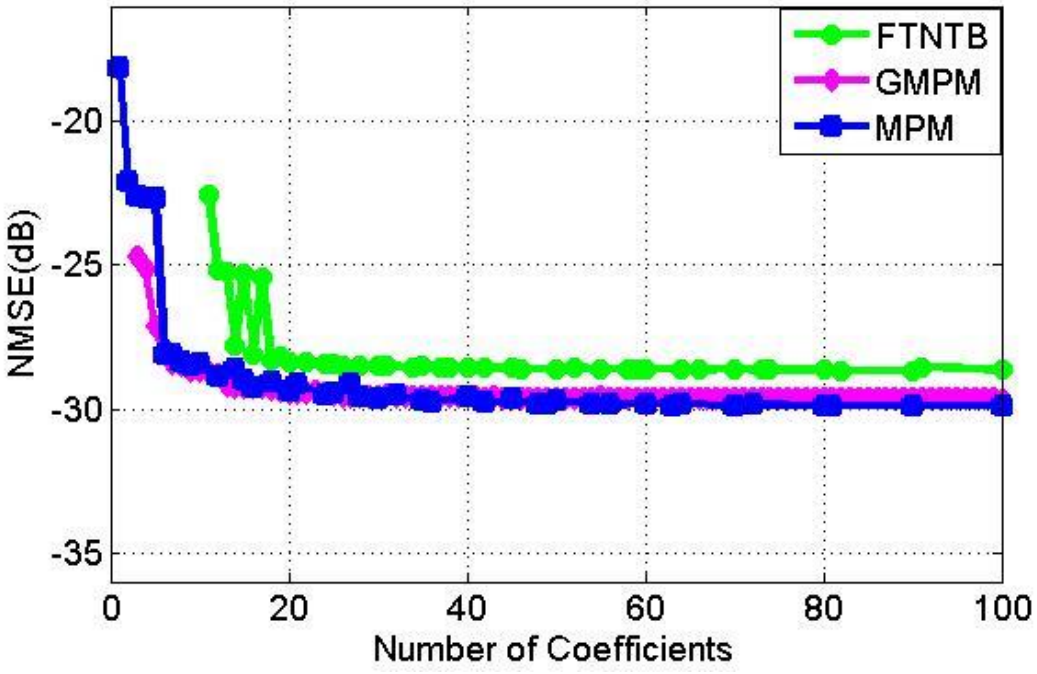

Figure 3.24 NMSE of the different models vs number of coefficients for n6 case for the 20 MHz signal

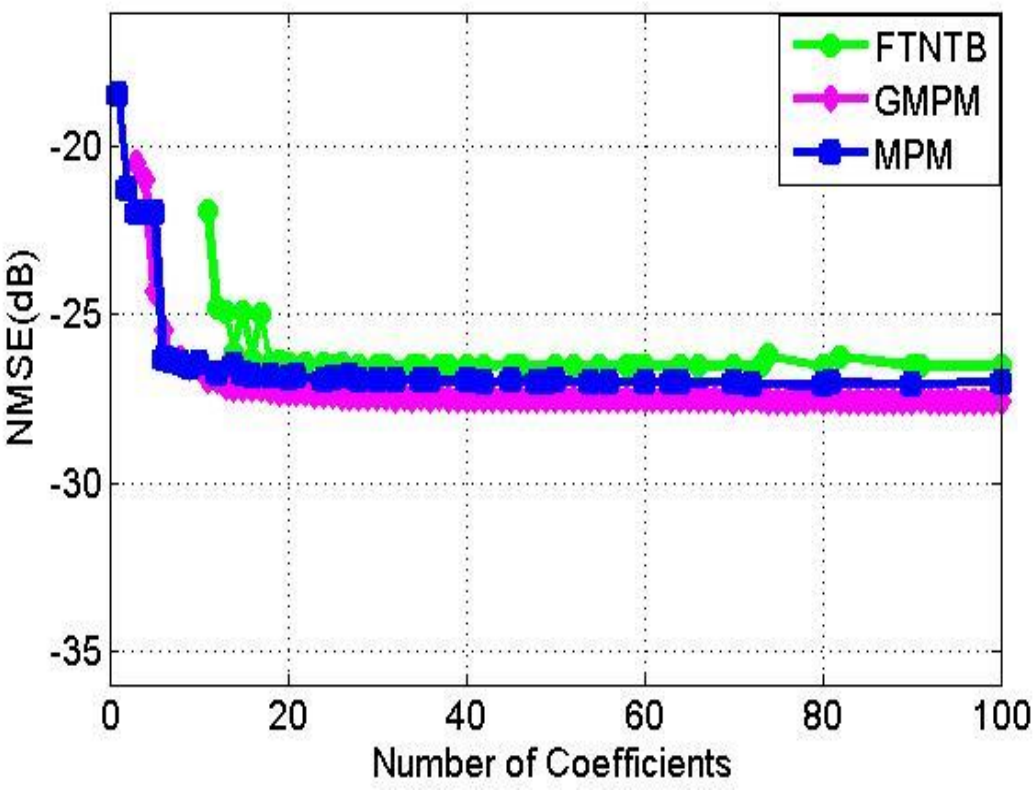

Figure 3.25 NMSE of the different models vs number of coefficients for Wilson case for the 20 MHz signal

In linear and n6 cases, GMP and MP models have almost the same performances; around -30 dB, whereas the FTNTB model an NMSE has -28.5 dB. For Wilson shaping function, GMP model has the best performance with 0.5 dB better than the MP model, whereas the FTNTB model NMSE is almost -26.5 dB.

3.6 Conclusion

In this chapter, the device under test and the experimental set-up used in this work were described. The DUT characteristics were derived using two LTE test signals for the four shaping functions that were considered. The results of using three different state of the art behavioral models with comparisons between them for the different cases were reported. The results that were described in this chapter demonstrate the need for a new behavioral model to describe envelope tracking power amplifiers having various shaping functions.

CHAPTER 4

Novel SISO Models for Envelope Tracking Power Amplifiers

In the previous chapter, the use of different models for several shaping functions was described. From there, and also depending on the characteristics of the different cases, one can see that there is a problem in using the conventional models with envelope tracking power amplifiers as they need a large number of coefficients to get suitable performance. Accordingly, new models are proposed to deal with the modelling of envelope tracking power amplifiers. These models are based on splitting the input and output signals to their magnitude and phase components and then modeling each part independently by suitable models.

Two novel models are proposed in this work: polar memory polynomial model and polar generalized memory polynomial model. The performance of each model and its block diagram are reported in sections 4.1 and 4.2, respectively. Then, a comprehensive comparison between proposed models and conventional models for different cases and different signals are shown clearly. This comparison was done based on the NMSE regarding to the real number of coefficients of each model,

4.1 Polar Memory Polynomial Model

In this model, and based on splitting input and output signals to their magnitude and phase components, a MP model is used for modelling the magnitude part and a memoryless polynomial model is applied for modelling the phase part. Finally, the outputs of both sub-models are combined together to get the final complex signal. Then,

this complex-valued output signal is compared with measured one to evaluate the model performance.

4.1.1 Model Description

At the output of each sub-model, the desired data will be real and of course the coefficients of each model will be real. Also, the magnitude of the output signal will be obtained from the upper model, and its phase will be constructed from the lower model. Then, the magnitude and the phase of the model's output will be combined together to form the complex signal as it is depicted in Figure 4.1.

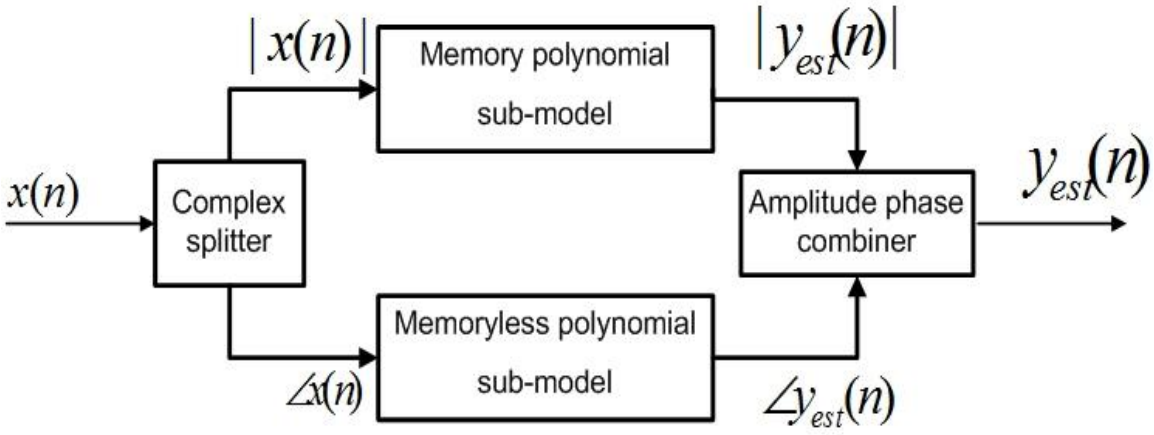

Figure 4.1 Block diagram of the polar memory polynomial model

The estimated magnitude from the MPM model can be constructed as following:

$$|\boldsymbol{y_{est}(n)}| = \sum_{\boldsymbol{j=1}}^{\boldsymbol{M}} \sum_{\boldsymbol{i=1}}^{\boldsymbol{N}} \boldsymbol{a_{ij}}.|\boldsymbol{x(n+1-j)}|^{\boldsymbol{i}} \qquad (\mathbf{4.1})$$

where x(n) is the complex input signal, N is the nonlinearity order and M represents the memory depth of the MP model, a_{ij} are the coefficients of MP model, and $|\boldsymbol{y_{est}(n)}|$ is the magnitude of the model's output signal.

For the memoryless polynomial model, the following equation is used to obtain the output phase:

$$\angle \boldsymbol{y_{est}(n)} = \sum_{\boldsymbol{i=1}}^{\boldsymbol{Q}} \boldsymbol{b_i}.\angle \boldsymbol{x(n)}.|\angle \boldsymbol{x(n)}|^{\boldsymbol{i-1}} \qquad (\mathbf{4.2})$$

where Q is the nonlinearity order of memoryless sub-model, b_i are the coefficients of memoryless polynomial sub-model, and $\angle \boldsymbol{y_{est}(n)}$ is the output of the memoryless polynomial sub-model. The estimated magnitude and phase of the output signal are combined together to form the estimated output complex signal as in the following equation:

$$\boldsymbol{y_{est}(n)} = (\sum_{\boldsymbol{j=1}}^{\boldsymbol{M}} \sum_{\boldsymbol{i=1}}^{\boldsymbol{N}} \boldsymbol{a_{ij}}.|\boldsymbol{x(n+1-j)}|^{\boldsymbol{i}})\, \boldsymbol{e}^{\boldsymbol{j}\sum_{\boldsymbol{i=1}}^{\boldsymbol{Q}} \boldsymbol{b_i}.\angle \boldsymbol{x(n)}.|\angle \boldsymbol{x(n)}|^{\boldsymbol{i-1}}} \qquad (\mathbf{4.3})$$

where $\boldsymbol{y_{est}(n)}$ is the estimated complex output signal of the polar memory polynomial model after combining its magnitude and phase from the two sub-models according to equations (4.1) and (4.2).

The number of coefficients of this model, which is as indication of its complexity, can be calculated by the following:

$$\boldsymbol{Number\ of\ Coefficients} = \boldsymbol{N} * \boldsymbol{M} + \boldsymbol{Q} \qquad (\mathbf{4.4})$$

where N and M are the parameters of the MP model of the magnitude part as shown in equation (4.1), and Q is the order of the memoryless model of the phase part as formulated in equation (4.2).

4.1.2 Model Performance with the 5MHz LTE Test Signal

In this sub-section, the performance of the polar MP model for different cases with the 5 MHz LTE signal is reported. The MP model is applied for the amplitude part for the three ETPA shaping functions. The memory depth and nonlinearity order of the model were swept from 1 to 10 for each (M=1:1:10, N=1:1:10). According to the sweep of the parameters, the lowest number of coefficient is 1, while the highest number of coefficients is 100 for this upper sub-model. For lower sub-model used to model the phase part, the sweep of the memoryless polynomial parameter was done from 1 to 10.

Results of the MP model performance for estimating the amplitude part for linear, n6, and Wilson cases with the 5 MHz LTE signal are shown in Figure 4.2 (a), (b), and (c), respectively. From this figure, one can notice that the three cases stabilize starting from a fairly low number of coefficients with very good performance in the range of -35 dB. The best NMSE performance as a function of the three cases is shown in Figure 4.3. It is clear that there is no significant difference between three cases and they have almost the same performance. For the phase part, the results are shown in Figure 4.4 for the three cases. This figure shows that all cases have the same trend and they stabilize after only four coefficients. Wilson shaping function has the best NMSE performance with around -40 dB, then the linear with -36 dB, and the n6 with around 3.5 dB difference from the Wilson case and almost 0.5 dB from the linear case. After modelling the amplitude and phase components of the output signal with their models independently, the output from each model size of MP model for the amplitude are combined with output of different model sizes of memoryless polynomial of the phase, and then the estimated complex output signal is compared with the measured one.

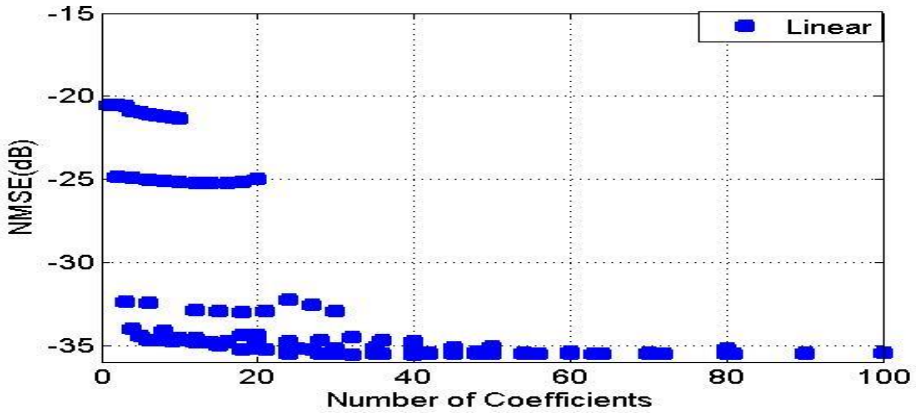

(a)

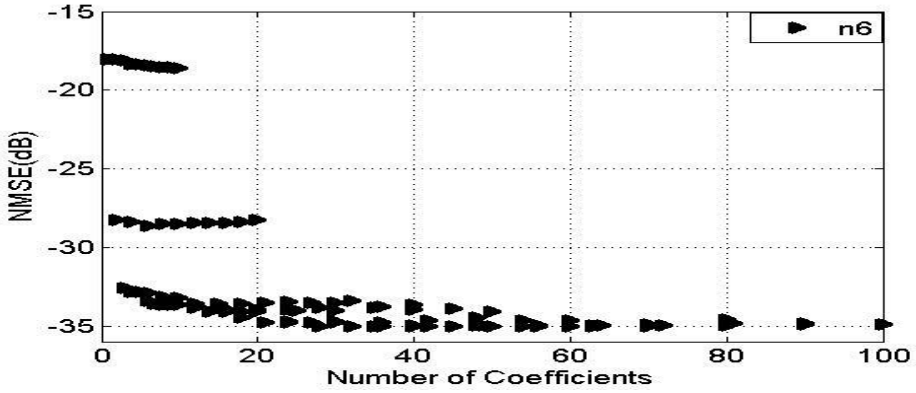

(b)

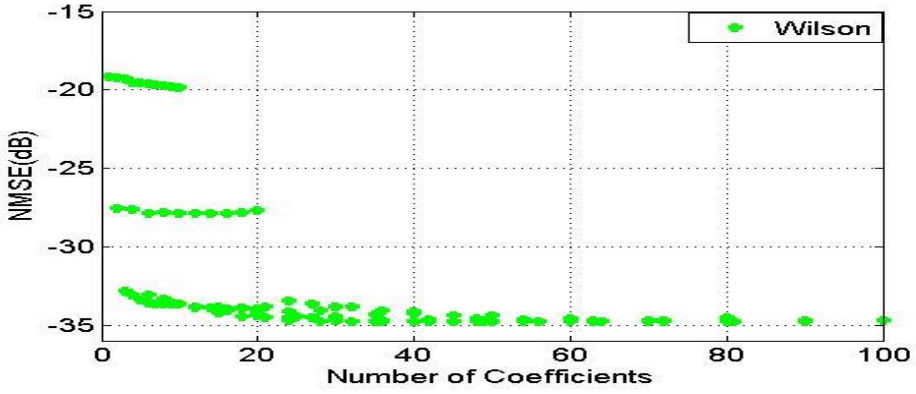

(c)

Figure 4.2 NMSE of the MP model for amplitude vs number of coefficients for (a) Linear (b) n6 (c) Wilson for the 5 MHz signal

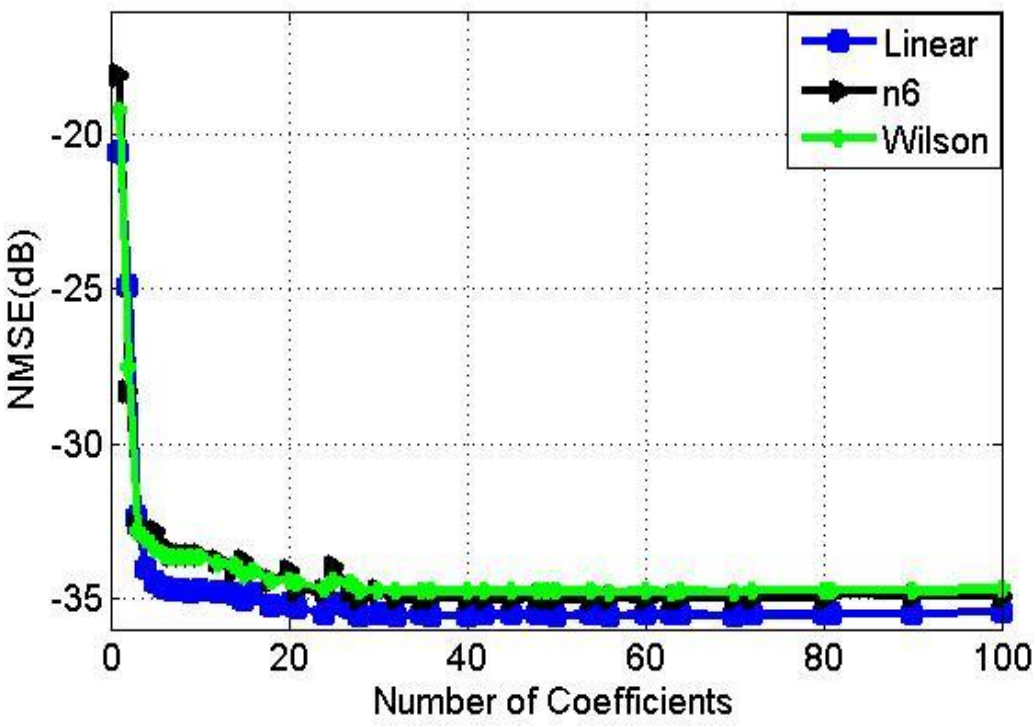

Figure 4.3 Best NMSE of the MP sub-model for amplitude of polar MP model vs number of coefficients for the 5 MHz signal

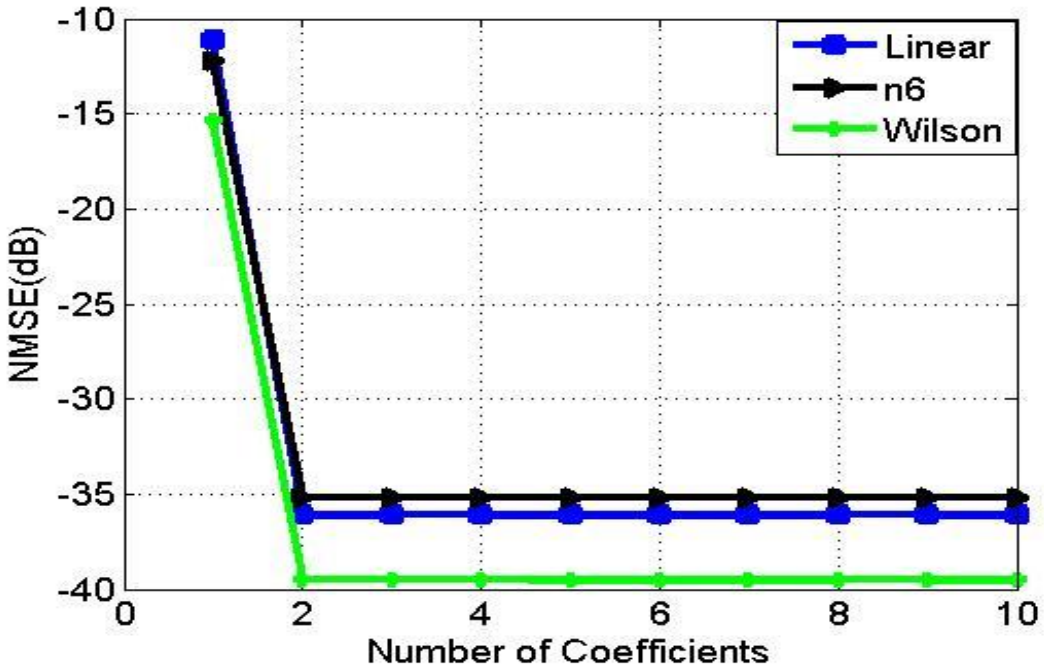

Figure 4.4 NMSE of the memoryless polynomial sub-model for phase of polar MP model vs number of coefficients for the 5 MHz signal

The best performance of the polar MP model for the three shaping functions and the 5 MHz test signal. This figure shows that Wilson and linear cases have almost the same performance and then the n6 case with slightly lower performance around 0.5 dB degradation.

Another important notice one can get from Figure 4.5 is that the proposed model performance converges after a low number of coefficients which is around 8 coefficients in Wilson and linear, and slightly more (approximatly 20 coefficients) for the n6 shaping function.

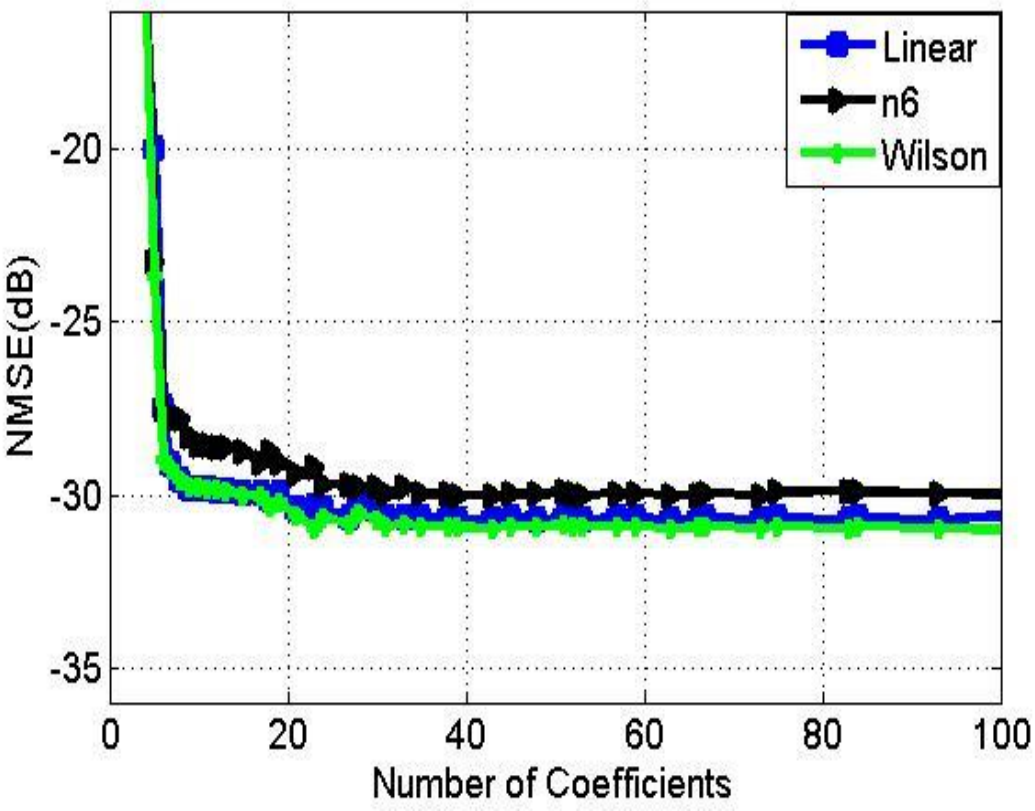

Figure 4.5 Best NMSE of the polar MP model vs number of coefficients for the 5 MHz signal

4.1.3 Model Performance with the 20MHz LTE Test Signal

In this sub-section, the performance of the polar MP model for different shaping functions with 20 MHz LTE signal is reported. The MP model was applied for the amplitude part for the three ETPA shaping functions with a sweep in the memory depth and nonlinearity order from 1 to 10 for each (M=1:1:10, N=1:1:10). According to this sweep, the lowest number of coefficient is 1, whereas the highest number of coefficients is 100 for the upper sub-model. For the lower sub-model used to model the phase part, the parameter sweep of memoryless polynomial was from 1 to 10 (Q=1:1:10) which is the same method as the one used with the 5 MHz signal. In Figure 4.6, NMSE versus number of coefficients of the MP model of the amplitude part for linear, n6, and Wilson for the 20 MHz LTE signal are reported. According to these results, one can see that the three cases stabilize after a low number of coefficients with a NMSE performance in the range of -32 dB. The best NMSE performance as a function of the number of coefficients of the three cases is shown in Figure 4.7. It is clear from this figure that there is no significant difference between the three cases. Also one can notice 3 dB difference when comparing these results with that of the 5 MHz test signal. For the phase part, the results are shown in Figure 4.8 for the three cases. All cases have the same trend and they stabilize after a four coefficients. The best performance is around -35 dB for n6 shaping function, then linear and Wilson with -32.5 dB. After modeling the amplitude and phase with their models independently, the outputs from each model size of MP function for the amplitude are combined with the output of different model sizes of memoryless polynomial function of the phase. Then, the estimated complex output signal is compared with the measured one for 20 MHz signal.

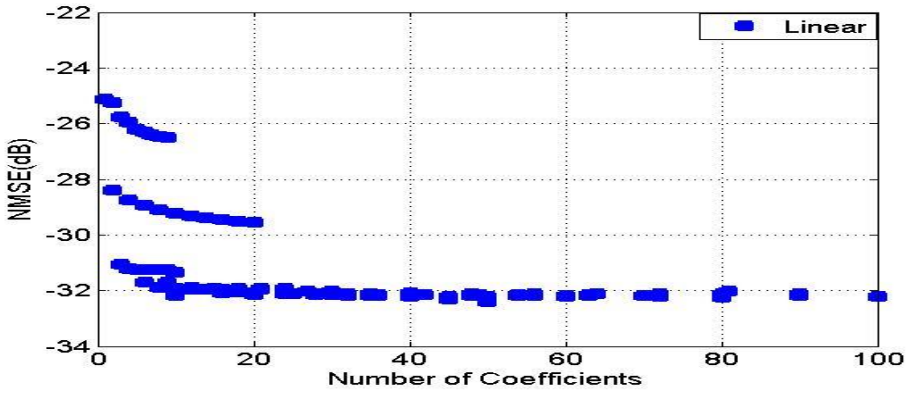

(a)

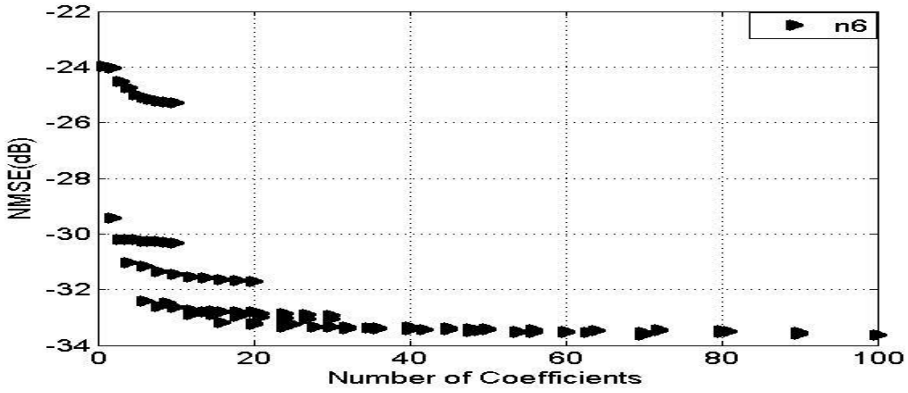

(b)

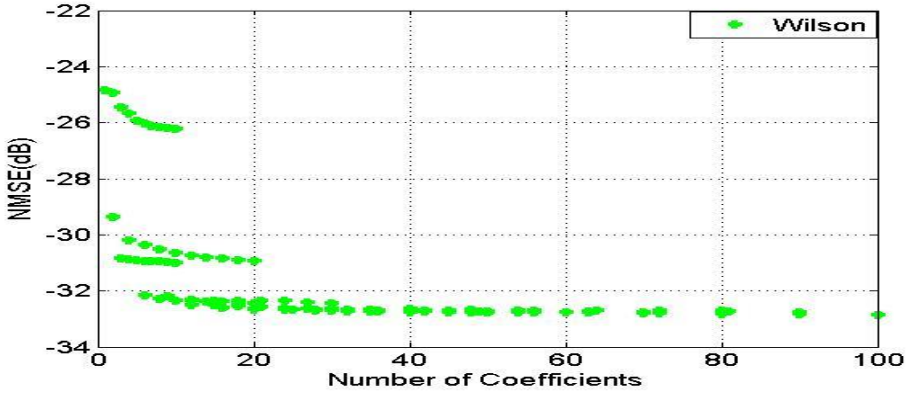

(c)

Figure 4.6 NMSE of the MP sub-model for amplitude vs number of coefficients for (a) Linear (b) n6 (c) Wilson for the 20 MHz signal

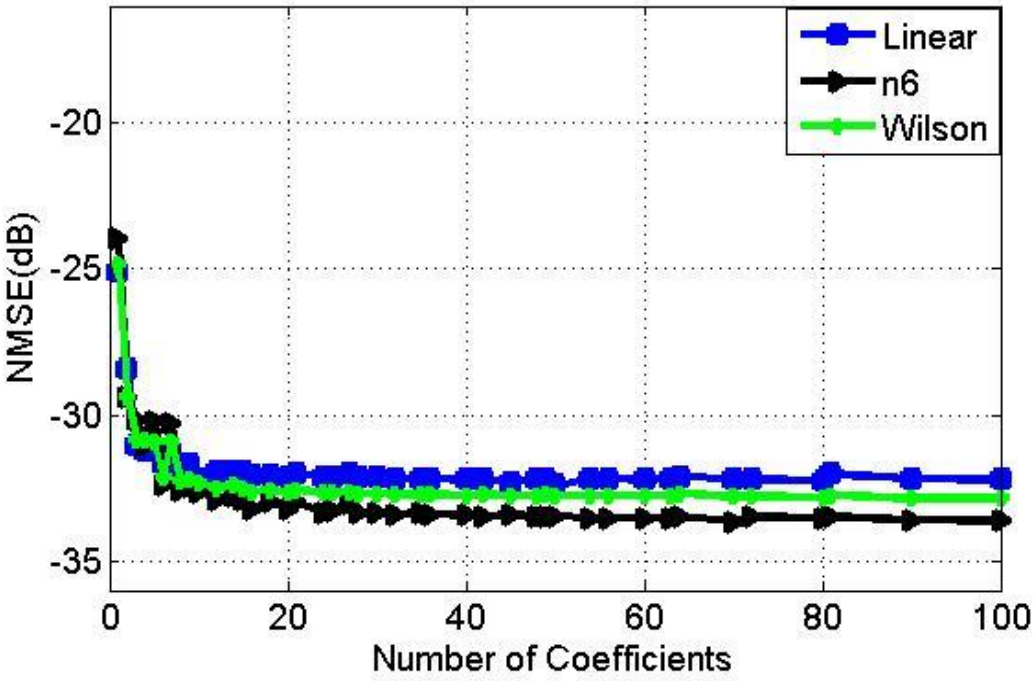

Figure 4.7 Best NMSE of the MP sub-model for amplitude of the polar MP model vs number of coefficients for the 20 MHz signal

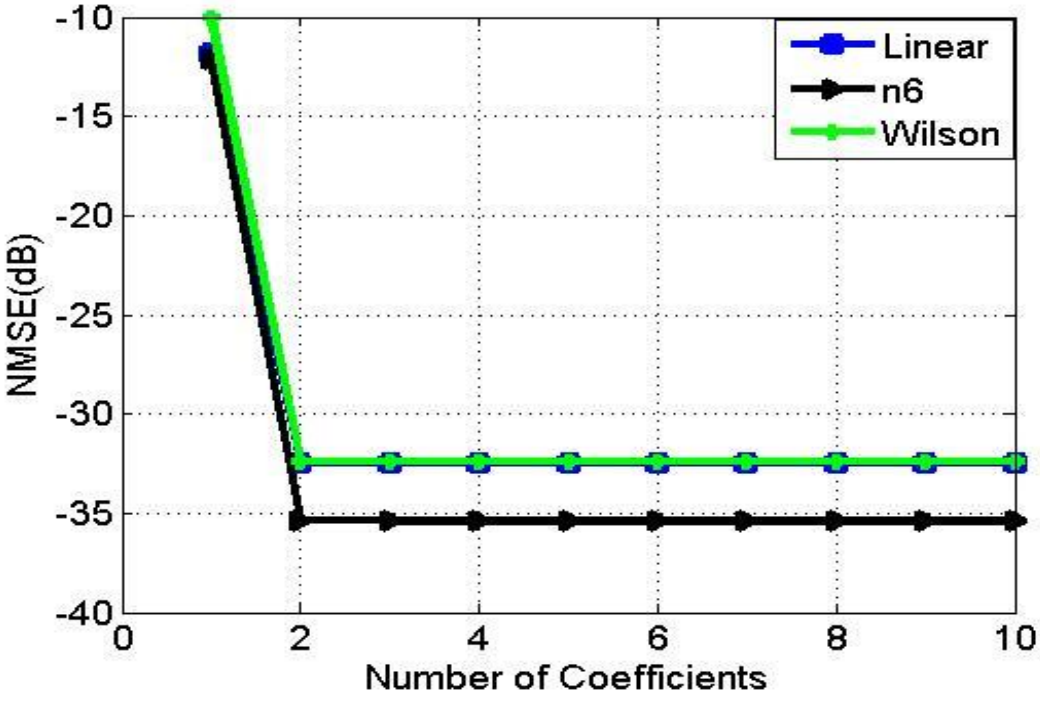

Figure 4.8 NMSE of the memoryless polynomial sub-model for phase of the polar MP model vs number of coefficients for the 20 MHz signal

In Figure 4.9, The best performance of the polar MP model for the three cases tested with the 20 MHz LTE signal is shown. One of the most important points from Figure 4.9 is that in this new model all cases converge after a low number of coefficients which is around 8 coefficients in Wilson and around 11 in n6 and linear cases.

It is obvious that n6 shaping function has the best performance, and then the linear case with slight performance degradation. Conversly, the Wilson function has the worst performance (almost -27.5 dB). Comparing with the performance of this model with the 5 MHz test signal, one can notice lower performance for the 20 MHz test signal for all cases and especially for Wilson case where there is up to 3 dB difference.

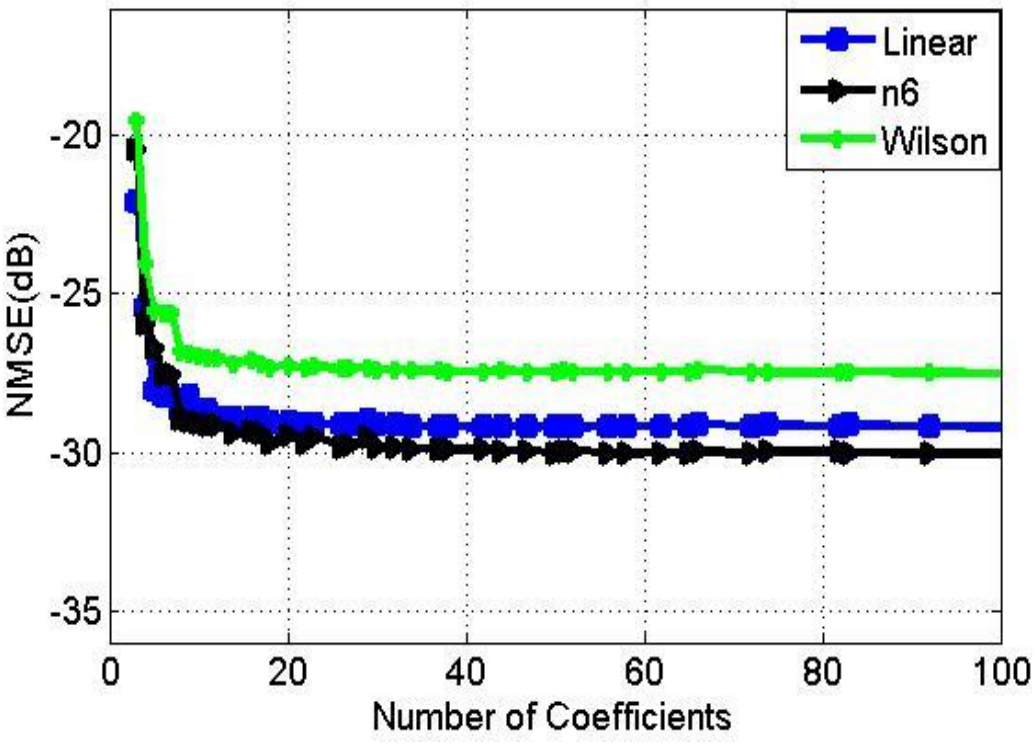

Figure 4.9 Best NMSE of the polar MP model vs number of coefficients for the 20 MHz signal

4.2 Polar Generalized Memory Polynomial Model

Based on the same way of splitting the model's input signal into its magnitude and phase, a second model is proposed. In this model, GMP sub-model is used for modelling the magnitude part, whereas a memoryless polynomial sub-model is applied for modelling the phase. Then, the outputs of both sub-models are combined to produce the estimated complex output signal of the polar GMP model.

4.2.1 Model Description

In Figure 4.10, the block diagram of the polar generalized memory polynomial model is shown. The coefficients in this model are real and the outputs of each sub-model are also real. In this figure, x(n) is the input complex signal which is decomposed to its magnitude and phase. The magnitude and phase components are applied to a GMP sub-model and a memoryless polynomial sub-model, respectively. After modelling each part, ($|\boldsymbol{y_{est}(n)}|$ and $\angle \boldsymbol{y_{est}(n)}$), these are combined to get the complex signal $\boldsymbol{y_{est}(n)}$.

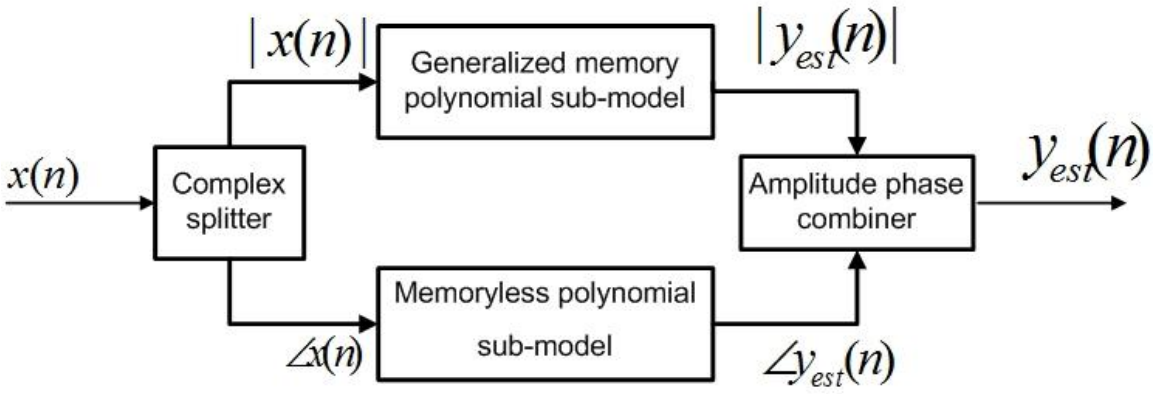

Figure 4.10 Block diagram of the polar generalized memory poltnomial model

From the upper sub-model, the estimated magnitude of the output signal can be calculated according to the following:

$$|y_{est}(n)| = \sum_{k=0}^{N_a-1}\sum_{m=0}^{M_a-1} a_{km}.|x(n-m)|^{k+1} + \sum_{k=1}^{N_b}\sum_{m=0}^{M_b-1}\sum_{l=1}^{L_b} b_{kml}|x(n-m)|.|x(n-m-l)|^{k} + \sum_{k=1}^{N_c}\sum_{m=0}^{M_c-1}\sum_{l=1}^{L_c} c_{kml}|x(n-m)|.|x(n-m+l)|^{k} \quad (4.5)$$

where, x(n) and y(n) are the input and the output of the GMP sub-model, respectively. a_{km} , b_{kml} and c_{kml} are the real coefficients of the time aligned, leading, and lagging branches, respectively. M_a and N_a are the memory depth and the nonlinear order of the time aligned branch, respectively. M_b, N_b and M_c, N_c are memory depths and nonlinearity orders of the lagging and leading branches, respectively. L_b and L_c are the lagging and leading tap lengths, respectively.

To construct the phase of this model, the following equation is used in the lower sub-model, which is the same as in polar MP model,

$$\angle y_{est}(n) = \sum_{i=1}^{Q} b_i.\angle x(n).|\angle x(n)|^{i-1} \quad (4.6)$$

where Q is the order of memoryless model, b_i are the coefficients of memoryless model, and $\angle y_{est}(n)$ is the estimated output phase of the model.

After that, the outputs of each sub-model are combined to produce the estimated complex output signal, as it is shown in Equation 4.7.

$$y_{est}(n) = \left(\sum_{k=0}^{N_a-1} \sum_{m=0}^{M_a-1} a_{km} |x(n-m)|^{k+1} + \sum_{k=1}^{N_b} \sum_{m=0}^{M_b-1} \sum_{l=1}^{L_b} b_{kml} |x(n-m)|.|x(n-m-l)|^{k} \right.$$
$$\left. + \sum_{k=1}^{N_c} \sum_{m=0}^{M_c-1} \sum_{l=1}^{L_c} c_{kml} |x(n-m)|.|x(n-m+l)|^{k} \right) e^{j \sum_{i=1}^{Q} b_i . \angle x(n) . |\angle x(n)|^{i-1}} \quad (4.7)$$

where $y_{est}(n)$ is the estimated complex output signal of the polar memory polynomial model after combining its magnitude and phase from sub-models.

The number of coefficients of this model, which affects its complexity, can be calculated by the following:

$$Number\ of\ Coefficients = M_a * N_a + M_b * N_b * L_b + M_c * N_c * L_c + Q \quad (4.8)$$

where $M_a, N_a, M_b, N_b, M_c, N_c, L_b, and\ L_c$ are the coefficients of the GMP sub-model of the magnitude part, and Q is the nonlinearity order of the memoryless polynomial sub-model of the phase part.

In the remainder of this section, the performance of polar GMP model is reported for the three shaping functions with the 5 MHz and the 20 MHz LTE test signals.

4.2.2 Model Performance with the 5 MHz LTE Test signal

The GMP sub-model was applied for the modeling of the amplitude part for the three ETPA shaping functions by sweeping the parameters as follows: ; M_a from 1 to 10, N_a from 1 to 10, M_b, N_b, M_c, and N_c from 1 to 5 and L_b and L_c were set to 1. According to that, the lowest total number of coefficients is 3, whereas the highest number of coefficients is 150 for the upper sub-model. Similarly, for the lower sub-model used to

model the phase part, the sweep of the memoryless polynomial parameters from 1 to 10, as was the case in the polar MP model.

In Figure 4.11, the NMSE performance versus number of coefficients of the GMP sub-model for the amplitude is shown for the linear, the n6, and the Wilson shaping functions with the 5 MHz LTE test signal. From these results, one can mention that the three cases converge after a low number of coefficients with an NMSE performance reaches up to -36 dB. The best NMSE performance versus the number of coefficients of the three cases is shown in Figure 4.12. It is noticeable that the linear case has the best performance with slight difference compared with the Wilson and the n6 cases.

For the phase part, the NMSE versus number of coefficients of the memoryless polynomial sub-model is shown in Figure 4.13, where Wilson case has the best performance with -40 dB and it is converges to this value after only four coefficients. For the linear and the n6 cases, they have almost the same performance and also converge after two coefficients but to around -35 dB.

After modelling the amplitude with the GMP sub-model and the phase with the memoryless polynomial sub-model independently, the output amplitude of each model size of GMP sub-model is combined with output phase of different model sizes of the memoryless polynomial sub-model. Then, the estimated complex output signal is compared with the measured output signal for each case.

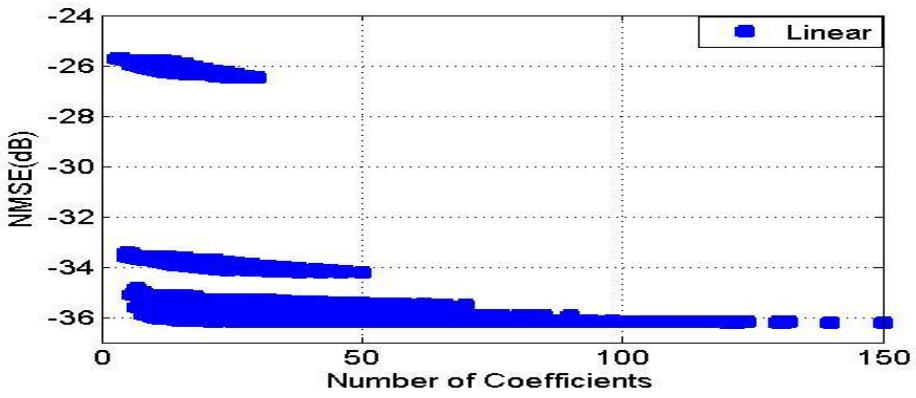

(a)

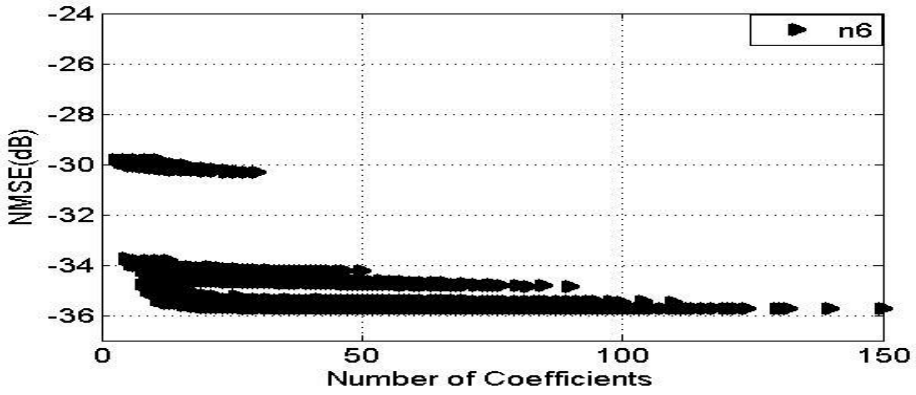

(b)

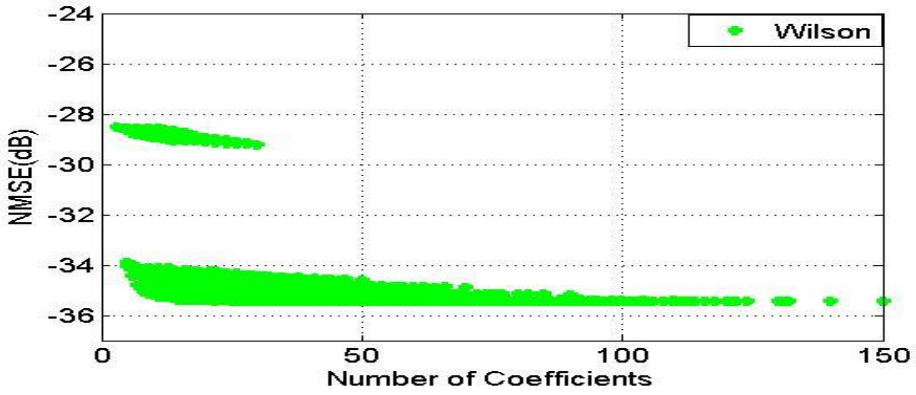

(c)

Figure 4.11 NMSE of the GMP sub-model for amplitude vs number of coefficients for (a) Linear (b) n6 (c) Wilson for the 5 MHz signal

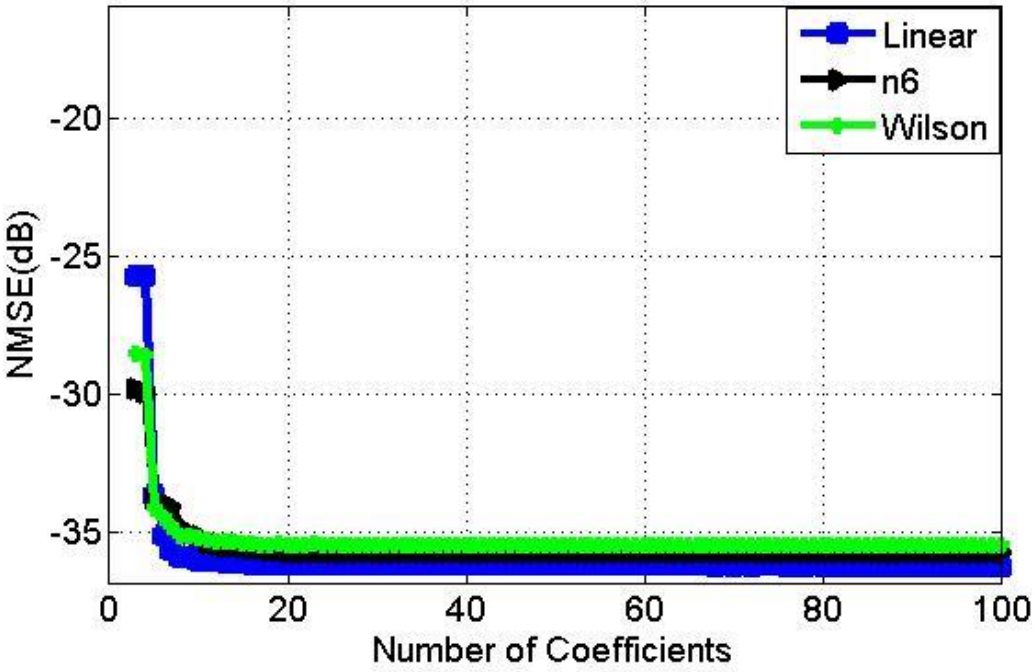

Figure 4.12 Best NMSE of the GMP sub-model of the polar GMP model vs number of coefficients for the 5 MHz signal

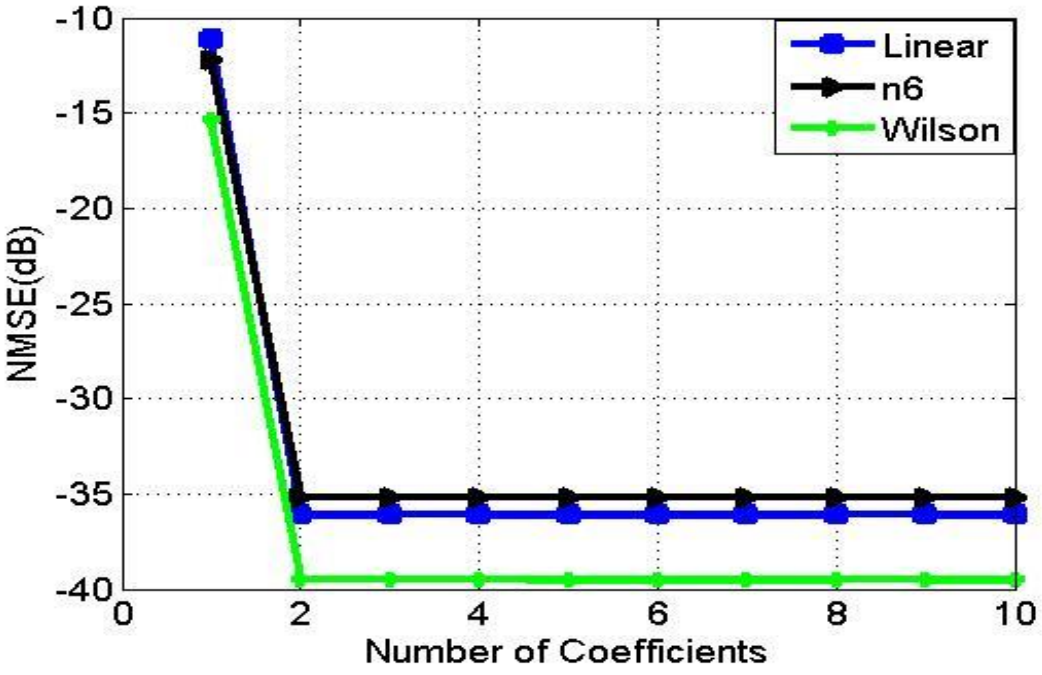

Figure 4.13 NMSE of the memoryless polynomial sub-model of the polar GMP model vs number of coefficients for the 5 MHz signal

The best NMSE performance as a function of the total number of coefficients for three cases of polar GMP model under the 5 MHz LTE test signal is shown in Figure 4.14. It is obvious that Wilson and linear cases have almost the same performance and they converge after 8 coefficients to almost -31 dB, and then n6 case converge to -30.7 dB but after 11 coefficients.

Another important observation one can get from Figure 4.14 is that this model has almost the same trend of GMP sub-model for amplitude part.

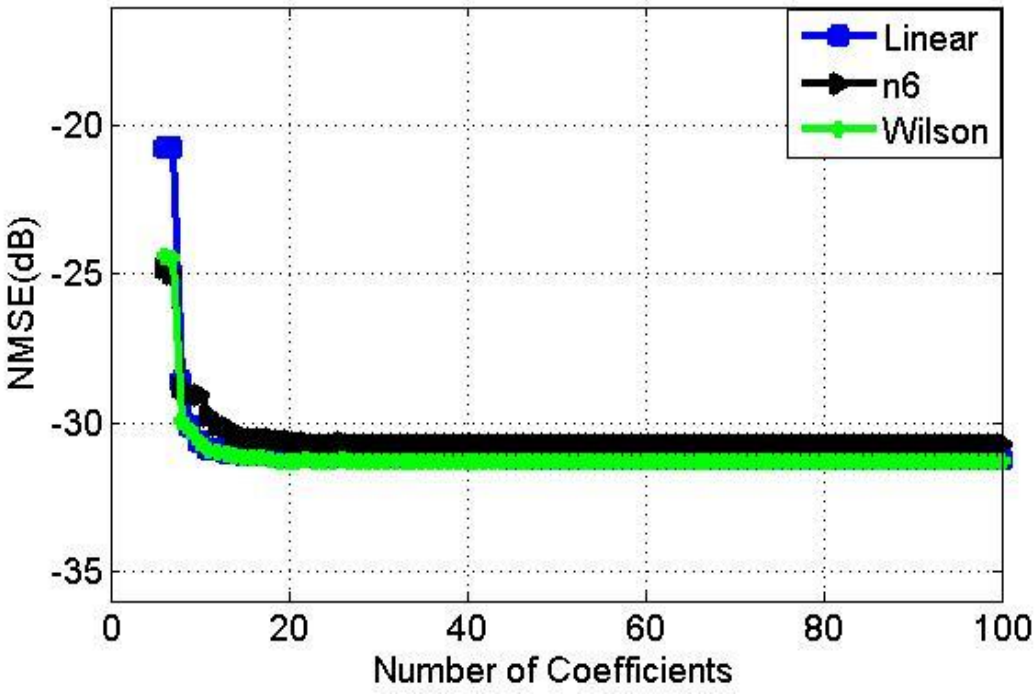

Figure 4.14 Best NMSE of the polar GMP model vs number of coefficients for the 5 MHz signal

4.2.3 Model Performance with the 20 MHz LTE Test Signal

In this sub-section, the use of the polar GMP with the 20 MHz LTE signal is described, beginning from GMP sub-model for the amplitude to the memoryless

polynomial sub-model for the phase part until the combination process to get the complex output signal.

The GMP sub-model is used with the following parameters: M_a from 1 to 10, N_a from 1 to 10 , $M_b, N_b, M_c,$ and N_c from 1 to 5 and L_b and L_c values were set to 1. Based on that, the lowest number of coefficients is 3, whereas the highest number of coefficients is 150 for the upper sub-model. Another maximum of 10 coefficients is used for the lower sub-model of the phase part, where Q is changed from 1 to 10. After the combination process, this sweep leads to 4 coefficients as a lowest model size and 160 coefficients as a largest size for this model. Results of using the GMP sub-model of the amplitude part for the linear, n6, and Wilson cases with the 20 MHz LTE signal are shown in Figure 4.15. From this figure, one can observe that the three cases have very good performance which is better than what was obtained with the MP sub-model for amplitude in the polar MP model. The best NMSE performance as a function of the number of coefficients for the three cases is shown in Figure 4.16. For the linear case, the NMSE converges after around 7 coefficients to approximately -35 dB, the Wilson case comes second with around -34 dB. For the n6 shaping function, it converges after more coefficients (approximately 10 coefficients) to -34.5 dB.

For the phase part, the results are shown in Figure 4.17 for the three cases. All cases have the same trend and their NMSE converges after four coefficients. The best performance with around -35 dB is for the n6 shaping function, then linear and Wilson with -32.5 dB which is exactly the same as in the polar MP model.

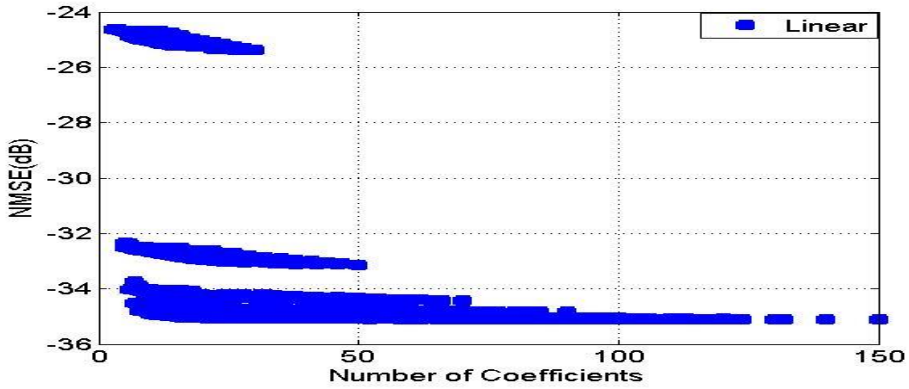

(a)

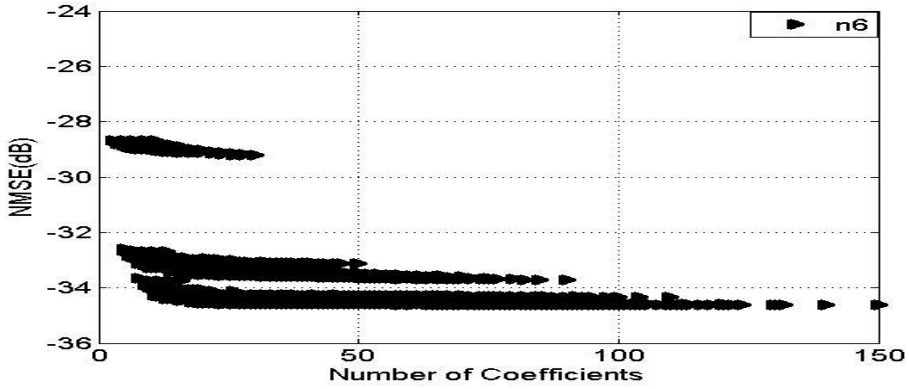

(b)

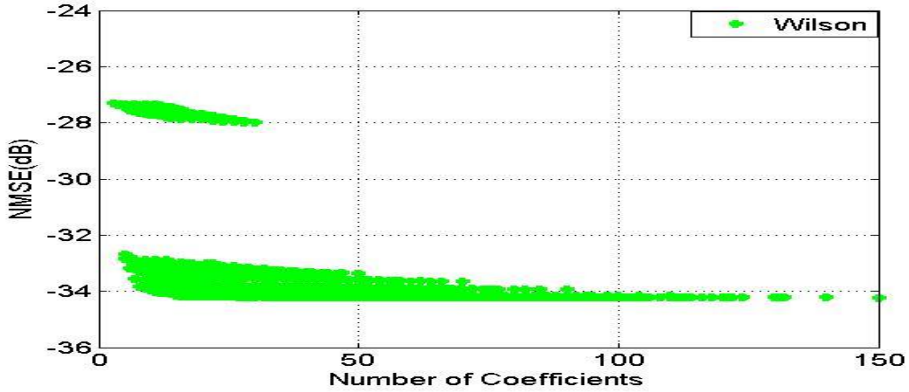

(c)

Figure 4.15 NMSE of the GMP sub-model vs number of coefficients for (a) Linear (b) n6 (c) Wilson for the 20 MHz signal

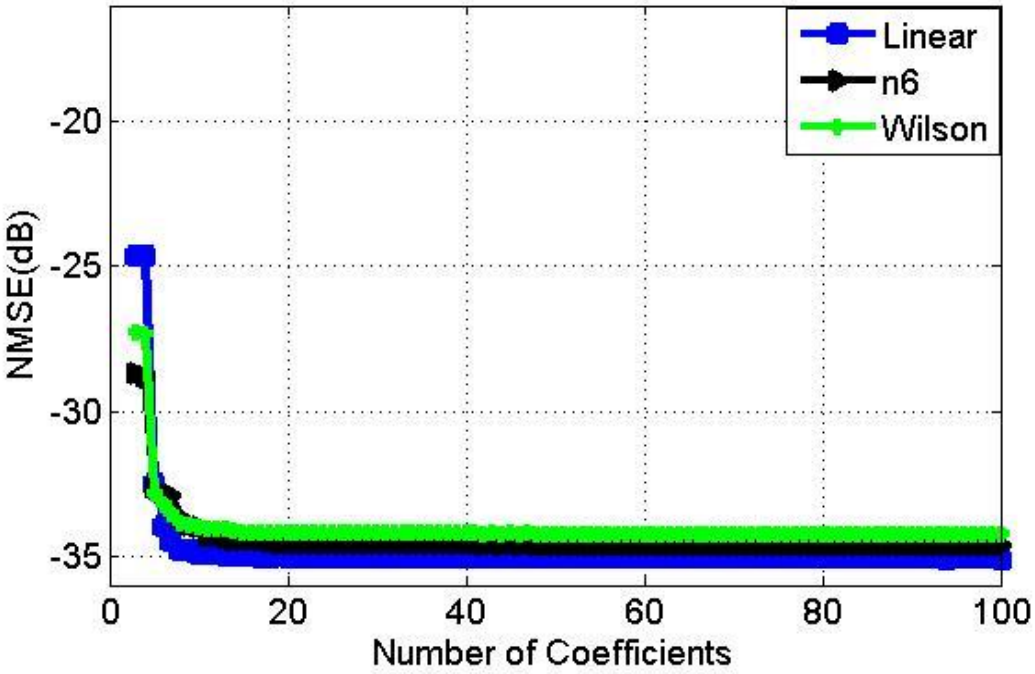

Figure 4.16 Best NMSE of the GMP sub-model of the polar GMP model vs number of coefficients for the 20 MHz signal

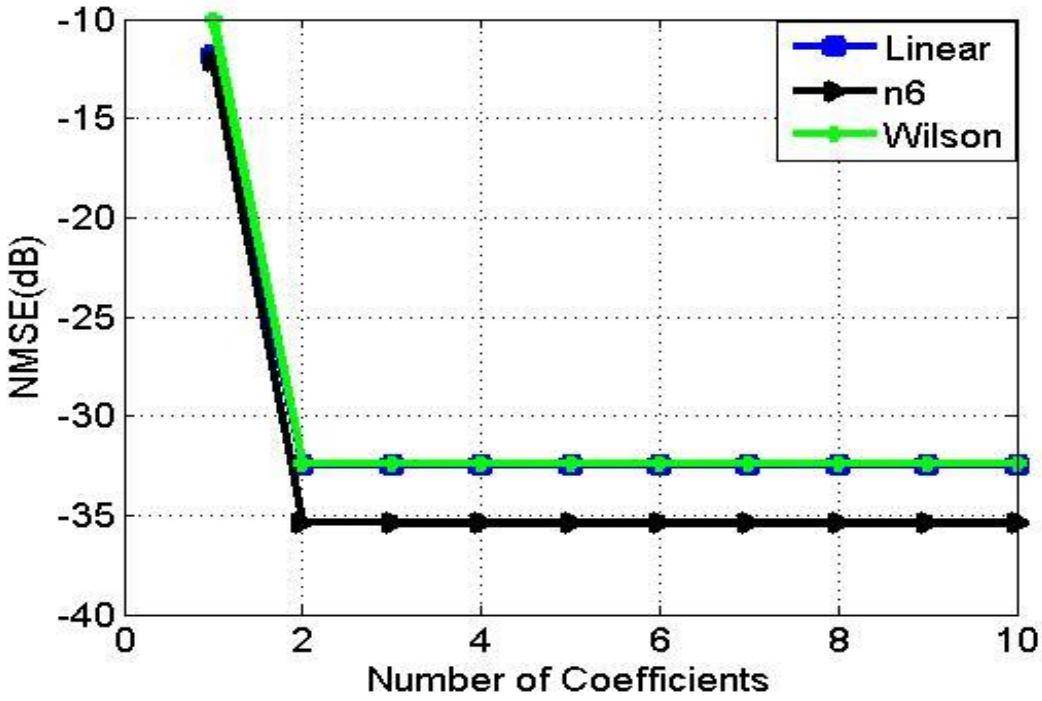

Figure 4.17 NMSE of the memoryless polynomial sub-model of the polar GMP model vs number of coefficients for the 20 MHz signal

After modelling the amplitude component with GMP sub-model and the phase component with the memoryless polynomial sub-model independently, the output from each model size of GMP sub-model are combined with the output of different model sizes of the memoryless polynomial sub-model, and then the estimated complex output signal is compared with the measured output signal for each case.

In Figure 4.18, The best NMSE performance of the polar GMP model for the various shaping functions tested with the 20 MHz LTE signal is shown. One of the main observations from Figure 4.18 is that in this model all cases converge after a low number of coefficients which is around 9 coefficients in the Wilson and linear cases, where it is around 11 for the n6 case. It is obvious that the n6 case has the best performance, and then the linear case with slightly lower performance. The wilson case has the worst NMSE performance with almost -28 dB.

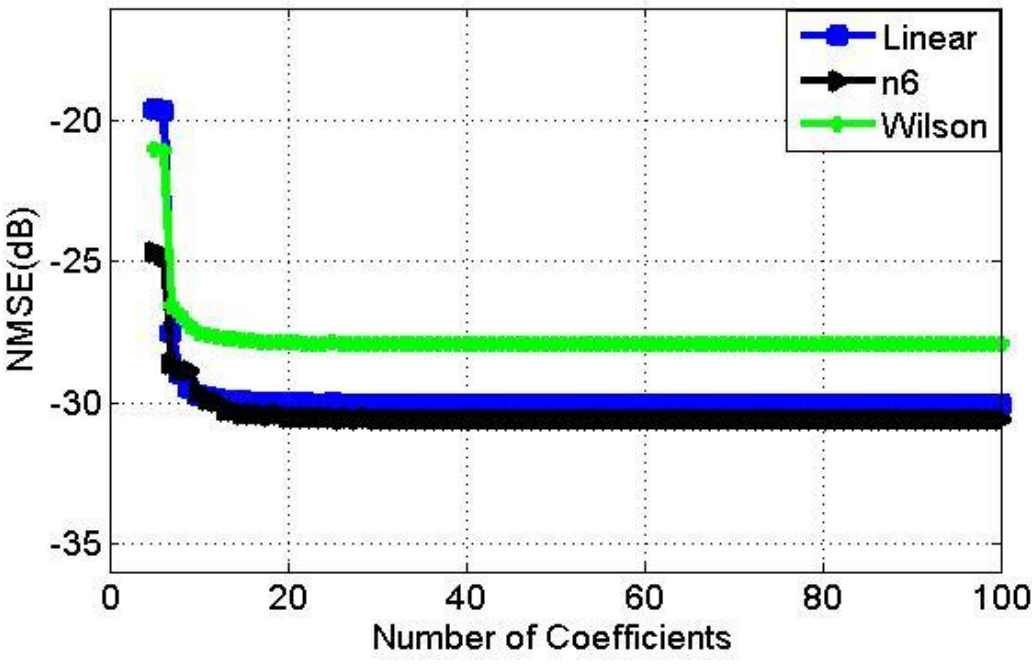

Figure 4.18 Best NMSE of the polar GMP model vs number of coefficients for the 20 MHz signal

4.3 Model Benchmarking

At this point, and after assessing the performance of the proposed models, it is necessary to compare the proposed models with conventional SISO models that were described in chapter 3. This comparison can be done by multiplying the total number of coefficients in the conventional models by two as they are complex coefficients and the coefficients of the proposed models are real valued.

4.3.1 Models Benchmarking for the 5 MHz LTE Signal

The comparison of performance between MP, GMP, FTNTB, polar MP, and polar GMP models for the three shaping functions with the 5 MHz LTE signal are reported in this sub-section.

In Figure 4.19 (a), the performance of the five models for the linear case is shown. Whereas the performance of MP and polar MP models are shown in Figure 4.19 (b). The comparison between GMP and polar GMP models is clear in Figure 4.19 (c). One can see that all models converge to almost same NMSE while the main difference is in the convergence speed and the minimum number of coefficients that each model needs to have the same performance as the other ones. For the linear case, it is obvious that polar MP model needs lower number of coefficients (around 9) to get the same performance of MP model having around 16 coefficients. When comparing the polar GMP with GMP model, only 9 coefficients are needed for the polar GMP to get the same performance that are obtained with 20 coefficients in the GMP model. This shows that the proposed model leads to around 55% of reduction. Similar comparisons are described in Figure 4.20 and Figure 4.21 for the n6 and the Wilson cases, respectively.

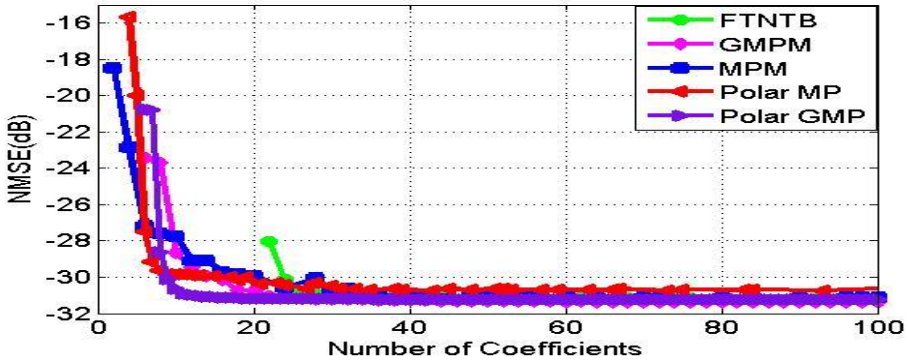

(a)

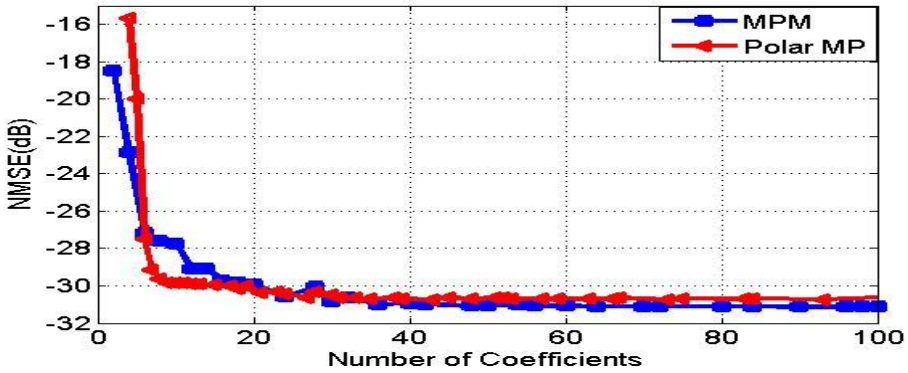

(b)

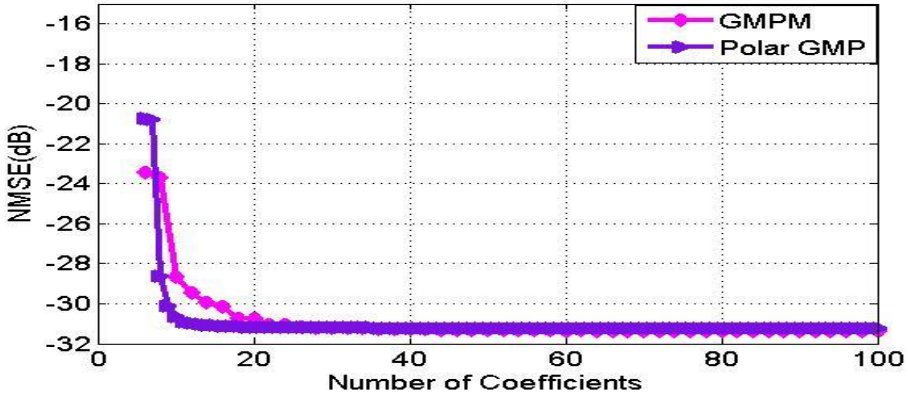

(c)

Figure 4.19 NMSE vs number of coefficients for the linear case (a) All models (b) MP vs Polar MP (c) GMP vs Polar GMP for the 5 MHz signal

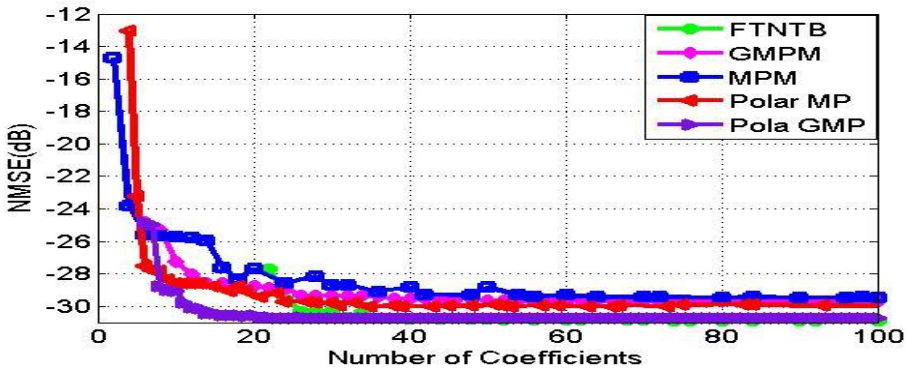

(a)

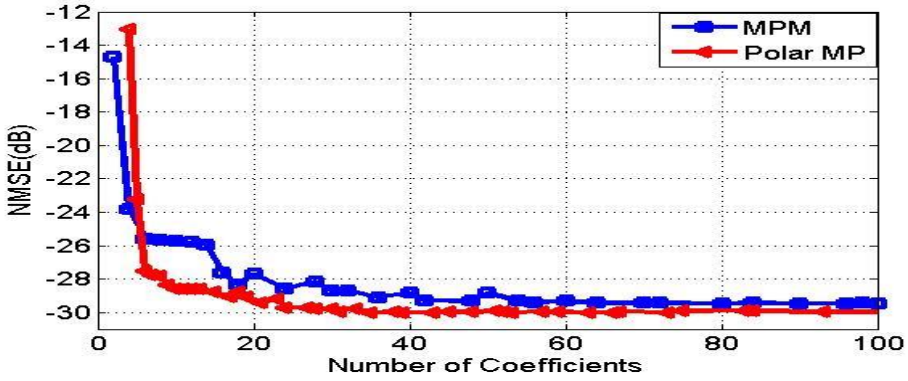

(b)

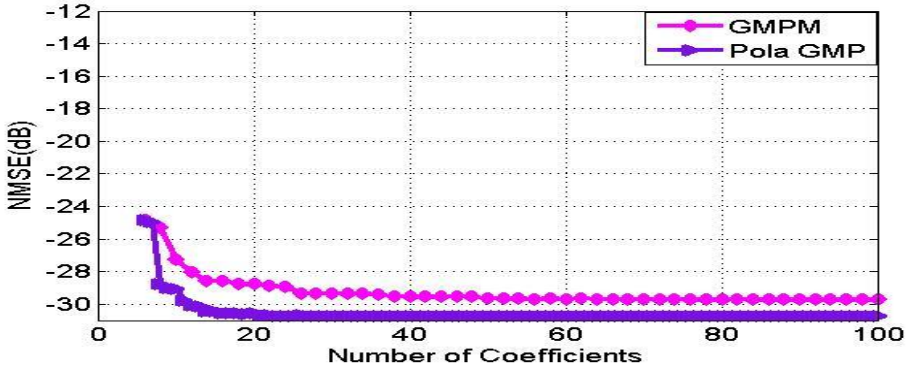

(c)

Figure 4.20 NMSE vs number of coefficients for the n6 case (a) All models (b) MP vs Polar MP (c) GMP vs Polar GMP for the 5 MHz signal

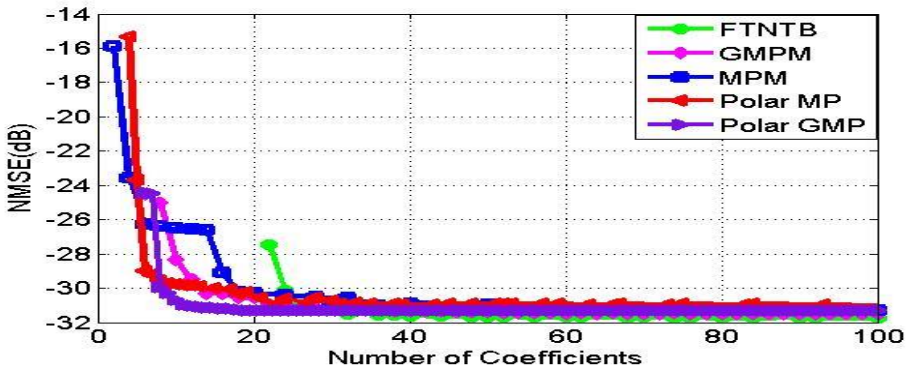

(a)

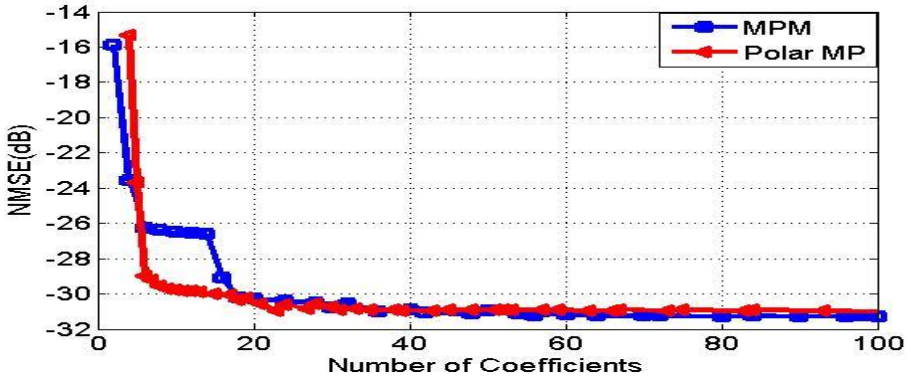

(b)

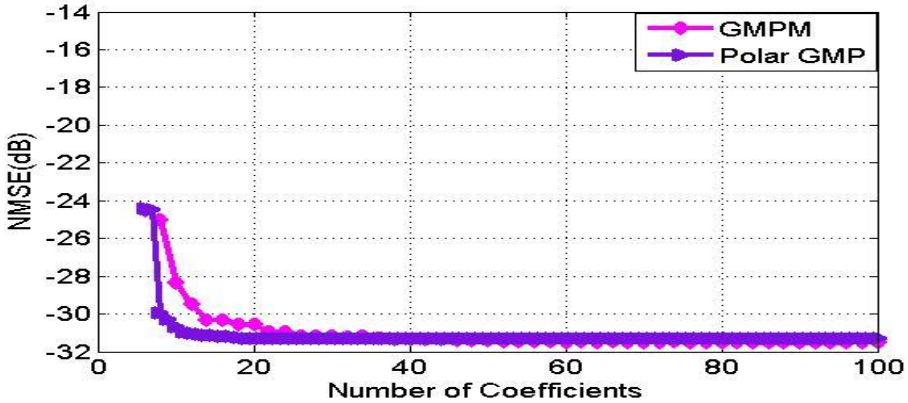

(c)

Figure 4.21 NMSE vs number of coefficients for the Wilson case (a) All models (b) MP vs Polar MP (c) GMP vs Polar GMP for the 5 MHz signal

Figure 4.20 (a) shows the performance of the five models of the n6 case. The performance of the MP and the polar MP models are shown in Figure 4.20 (b), and the comparison between the GMP and the polar GMP is depicted in Figure 4.20 (c). It is noticeable that all models converge to almost the same NMSE. It is obvious that polar MP model needs lower number of coefficients (around 8) to get the same performance as that of the MP model with around 18 coefficients. Also for a low number of coefficients, there is a difference of almost 3 dB between the NMSE obtained with the polar MP model and that of the MP model. Similarly, when comparing the polar GMP with the GMP model, one can notice that the polar GMP has better performance for same number of coefficients with considerable NMSE enhancement at low number of coefficients.

For the Wilson shaping function, the performance of all five models, the performance of the MP and the polar MP models, and the comparison between the GMP and the polar GMP models are shown in Figure 4.21 (a), (b), and (c), respectively. The conclusion is the same as in the linear and the n6 cases. All models converge to the same value of NMSE. To compare between the MP and the polar MP models, one must take into consideration that 18 coefficients are needed for MP model to reach the same performance that can be obtained with a polar MP model having only 11 coefficients. When the models size is between 8 and 16 coefficients, the polar MP model has better performance with almost 3 dB better NMSE. When comparing the polar GMP with the GMP models, to reach to -31 dB of NMSE, only 9 coefficients are needed for the polar GMP whereas at least 22 coefficients are needed in the GMP model. This represents around 59% of complexity reduction.

In the three shaping functions, one can see that according to the reduction of the number of coefficients, the proposed models have better performance than state of the art models.

4.3.2 Models Benchmarking for the 20 MHz LTE Signal

The comparison of performance between MP, GMP, FTNTB, polar MP, and polar GMP models for the linear, n6, and Wilson cases are described in this sub-section for 20 MHz signal.

The performance of the five models for the linear, n6, and Wilson cases are shown in Figure 4.22, Figure 4.23, and Figure 4.24, respectively. For each figure, the performance of the five models is shown in (a) while the performance of the MP and the polar MP models is shown in (b), where the comparison between the GMP and the polar GMP models is reported in (c).

For the linear shaping function, all models converge to -30 dB. Five coefficients are needed for the polar MP model to achieve -28 dB whereas at least 12 coefficients are needed for MP model. Comparing between the polar GMP and the GMP models, there is around 2 dB difference at low number of coefficients.

Refer to Figure 4.23, it is noticeable that all models converge to almost same NMSE for the n6 case. It is obvious that the polar MP model needs lower number of coefficients to get the same performance as its MP counterpart. When comparing the polar GMP with the GMP model, one can notice that the polar GMP has better performance for same number of coefficients with noticeable performance enhancement amount at low number of coefficients.

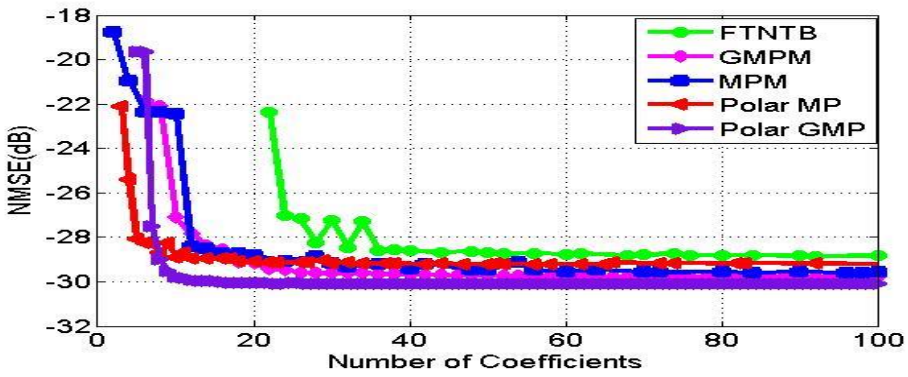

(a)

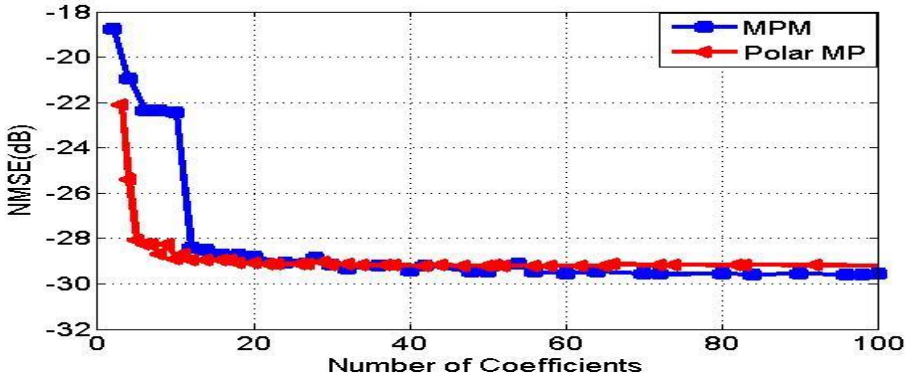

(b)

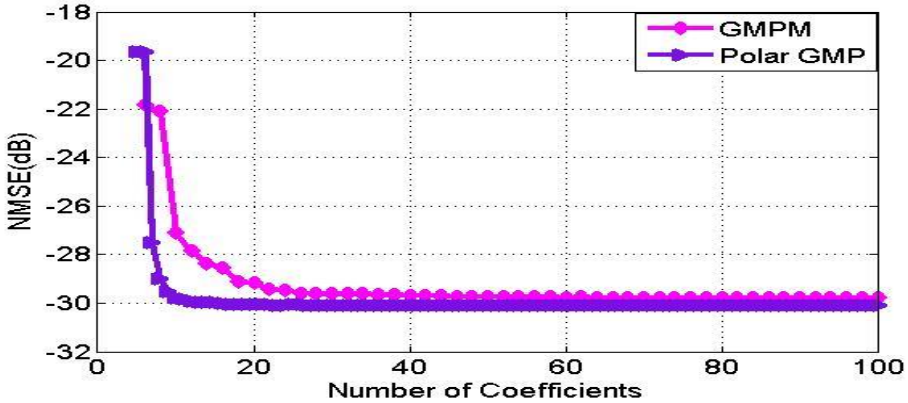

(c)

Figure 4.22 NMSE vs number of coefficients for the linear case (a) All models (b) MP vs Polar MP (c) GMP vs Polar GMP for the 20 MHz signal

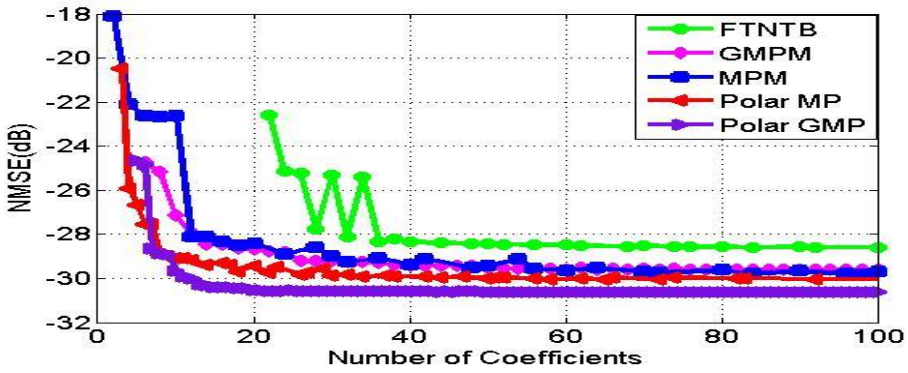

(a)

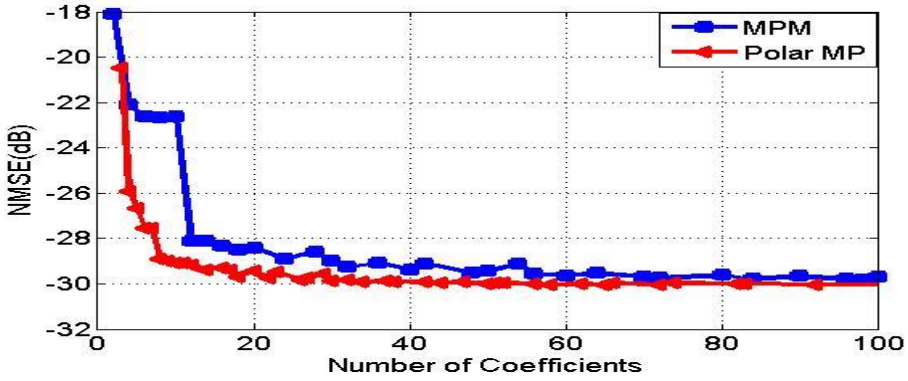

(b)

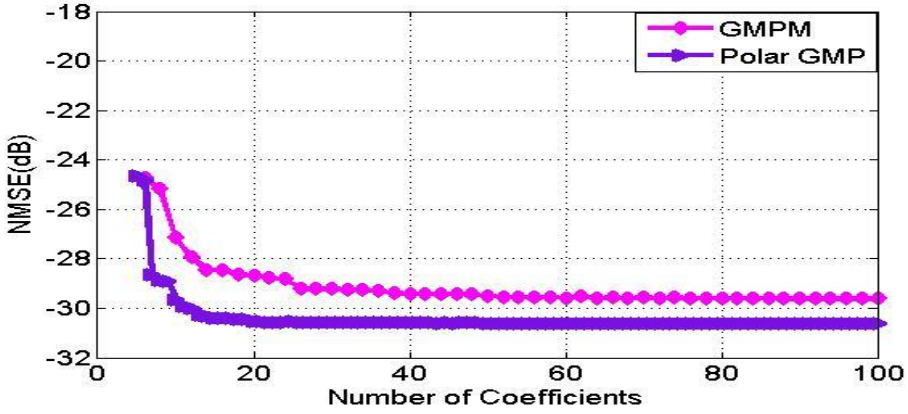

(c)

Figure 4.23 NMSE vs number of coefficients for the n6 case (a) All models (b) MP vs Polar MP (c) GMP vs Polar GMP for the 20 MHz signal

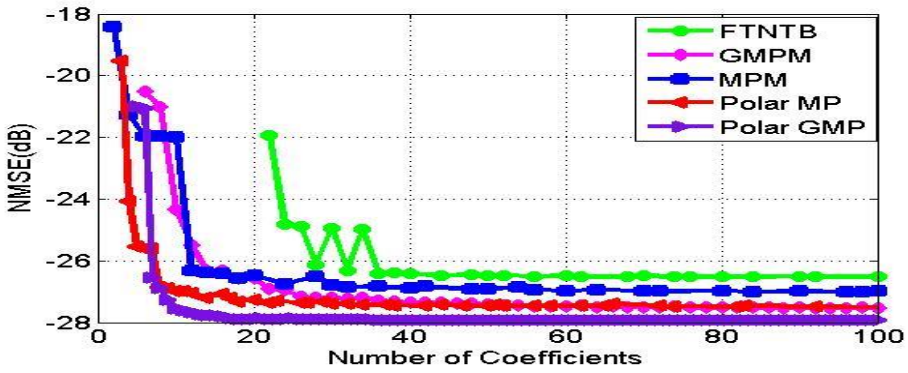

(a)

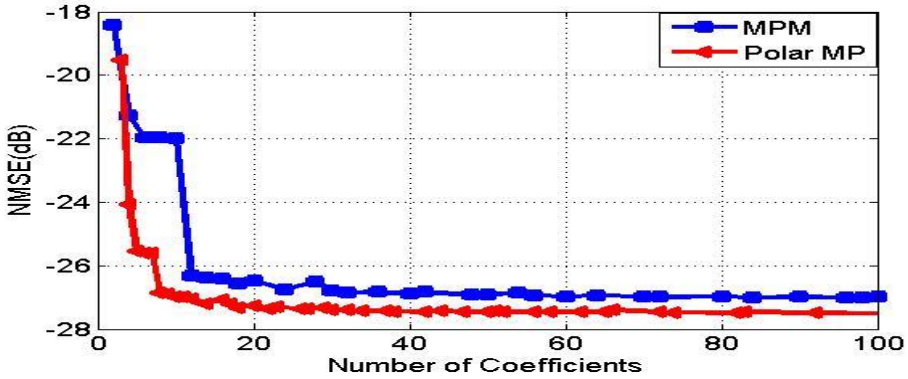

(b)

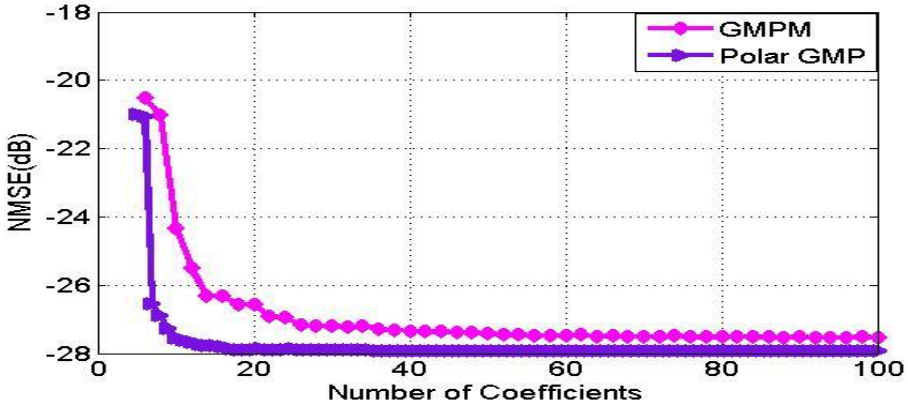

(c)

Figure 4.24 NMSE vs number of coefficients for the Wilson case (a) All models (b) MP vs Polar MP (c) GMP vs Polar GMP for the 20 MHz signal

For the Wilson case, the polar MP model has better performance than the MP model, and also the polar GMP model has better performance for the same number of coefficients. At low number of coefficients, considerable NMSE improvement is observed between the proposed models and the conventional models.

From models benchmarking for the 5 MHz and the 20 MHz test signals, one can clearly notice that the two proposed models have better performance than the MP model and the GMP model for all shaping functions. For NMSE after convergence, there is no significant difference in the linear and the Wilson cases between all models. For the n6 case, the polar GMP model outperforms all models with considerable NMSE enhancement for both the 5 MHz and also 20 MHz test signals.

CHAPTER 5

Conclusion and Future Work

5.1 Conclusions

Developing new behavioral models to accurately describe the performance of envelope tracking power amplifier was the main objective of this work.

Two new models were proposed. First, the polar memory polynomial model which is based on using the memory polynomial model for the magnitude part in parallel with a memoryless polynomial model for the phase part was proposed. The validation of this model was carried out using 5 MHz and 20 MHz LTE signals with three different shaping functions: linear, n6, and Wilson.

Secondly, the polar generalized memory polynomial model which is built using the generalized memory polynomial model for the magnitude part in parallel with a memoryless polynomial model for the phase part was introduced. The validation of this model was performed for three ET shaping functions: linear, n6, and Wilson, for the 5 MHz and the 20 MHz LTE signals.

The results of these two models were compared with three conventional SISO models namely the MP, GMP and FTNTB models. The proposed models showed considerably lower complexity than state of the art models as they converge faster with almost the same performance after convergence for the linear and the Wilson cases with both the 5 MHz and the 20 MHz test signals, where the percentage of coefficients reduction varies from 34% to 55% according to the shaping function and signal. The

same behavior is also observed for the n6 case but with noticeably better NMSE for polar GMP model.

5.2 Future Work

The future work of this research topic can focus on applying the proposed models for wider bandwidth signals for the three different shaping functions and monitor the effects of increasing the signal bandwidth on the performance of the different models. Another aspect of the future work can examine the proposed models in dual input single output configuration, in the main path or the envelope tracking path or even in both paths. Furthermore, the scope of this work can be extended to digital predistortion in order to compensate for the distortions of ET power amplifiers driven by LTE signals. Finally, use hybrid shaping functions in the envelope tracking path and see how this will affect the efficiency and linearity of ET PA.

References

[1] M. Marsan, L. Chiaraviglio, D. Ciullo, and M. Meo, "Optimal energy savings in cellular access networks," GreenComm'09 -First international workshop on green communications, Dresden, Germany, June 2009.

[2] C. Weitzel, "RF power amplifiers for wireless communications," in 24th Annual technical digest gallium arsenide integrated circuit (GaAs IC) Symposium, pp. 127–130, 2002.

[3] F. Ghannouchi and O. Hammi, "Behavioral modeling and predistortion," IEEE Microwave Magazine, vol. 10, no. 7, pp. 52–64, Dec. 2009.

[4] M. Saleh, D. Cox, "Improving the power-added efficiency of FET amplifiers operating with varying-envelope signals," IEEE transactions on microwave theory and techniques, vol.31, no.1, pp.51-56, Jan. 1983.

[5] B. Geller, F. Assal, R. Gupta, and P. Cline, "A technique for maintenance of FET power amplifier efficiency under backoff," IEEE 1989 MTT- Digest, Long beach, California, pp. 949-952, June 1989.

[6] T. Stauth, R. Sanders, "Dynamic power supply design for high-efficiency wireless transmitters", M.Sc. Thesis, University of California at Berkeley, 2006.

[7] B. Kim, J. Kim, D. Kim, J. Son, Y. Cho, J. Kim, and B. Park, "Push the Envelope", , IEEE microwave magazine special issue, May 2013.

[8] S. Baker, and A. Howard, Agilent Technologies, RF power amplifier design series, Part 5: Envelope-Tracking simulation and analysis, pp. 8, Dec. 2012.

[9] A. Cidronali, G. Manes, N. Giovannelli, T. Vlasits, and R. Hernaman, "Efficiency and linearity enhancements with envelope shaping control in dual-band envelope tracking GaAs PA," European microwave integrated circuit conference,, pp. 308-311, 2011.

[10] D. Kim, D. Kang, J. Choi, Y. Cho, and B. Kim, "Optimization for envelope shaped operation of envelope tracking power amplifier," IEEE Transaction on microwave theory and techniques, vol. 59, 2011.

[11] J. Moon, J. Son, J. Lee, and B. Kim, "A multimode/multiband envelope tracking transmitter with broadband saturated amplifier," IEEETrans. Microwave theory techniques, vol. 59, no. 12, pp. 3463‑3473, Dec. 2011.

[12] D. Kang, D. Kim, J. Choi, J. Kim, Y. Cho, and B. Kim, "Amultimode/multiband power amplifier with a boosted supply modulator," IEEE transaction microwave theory techniques, vol. 58, no. 10, pp. 2598-2608, Oct. 2010.

[13] F. Wang, A. Yang, D. Kimball, L. Larson, and P. Asbeck, "Design of wide-bandwidth envelope-tracking power amplifiers for OFDM applications," IEEE transaction microwave theory techniques, vol.53, no. 4, pp. 1244-1255, Apr. 2005.

[14] J. Jeong, D. Kimball, M. Kwak, C. Hsia, P. Draxler, and P. Asbeck, "Wideband envelope tracking power amplifier with reduced bandwidth power supply waveform," in IEEE MTT-S internatinal microwave Symposium Digital, Boston, MA, pp. 1381-1384, June 2009.

[15] M. Hassan, L. Larson, V. Leung, D. Kimball, and P. M.Asbeck, "A wideband CMOS/GaAs HBT envelope tracking power amplifier for 4G LTE mobile terminal applications," IEEE transaction microwave theory techniques., vol. 60, no. 5, pp. 1321-1330, May 2012.

[16] J. Choi, D. Kim, D. Kang, and B. Kim, "A polar transmitter with CMOS programmable hysteretic-controlled hybrid switching supply modulator for multistandard applications," IEEE Trans. MicrowaveTheory Tech., vol. 57, no. 7, pp. 1675-1686, July 2009.

[17] D. Kim, D. Kang, J. Choi, J. Kim, Y. Cho, and B. Kim, "Optimization for envelope shaped operation of envelope tracking power amplifier,"IEEE transaction microwave theory tecniques., vol. 59, no. 7, pp. 1787–1795, July 2011.

[18] B. Kim, J. Kim, D. Kim, J. Son, Y. Cho, J. Kim, and B. Park, "Push the envelope: Design concepts for the envelope-tracking power amplifiers,"IEEE Microwave Magazine, vol. 14, no. 3, pp. 68–81, Apr. 2013.

[19] D. Mirri, G. Luculano, F. Filicori, G. Pasini, G. Vannini, and G. P. Gabriella, "A modified Volterra series approach for nonlinear dynamic systems modeling," IEEE transaction circuits systems and theory Application, vol. 49, no. 8, pp. 1118–1128, Aug. 2002.

[20] A. Zhu and T. Brazil, "An Overview of Volterra series based behavioral modeling of RF/microwave power amplifiers," in 2006 IEEE annual wireless and microwave technology conference, pp. 1–5, 2006.

[21] J. Staudinger, "DDR Volterra series behavioral model with fading memory and dynamics for high power infrastructure amplifiers," in 2011 IEEE topical conference on power amplifiers for wireless and radio applications, pp. 61–64, 2011.

[22] A. Zhu, J. Dooley, and T. Brazil, "Simplified Volterra series based behavioral modeling of RF power amplifiers using deviation-reduction," in 2006 IEEE MTT-S international microwave symposium digest, pp. 1113–1116, 2006.

[23] J. Kim and K. Konstantinou, "Digital predistortion of wideband signals based on power amplifier model with memory," Electronics Letter, vol. 37, no. 23, p. 1417, 2001.

[24] O. Hammi, F. M. Ghannouchi, and B. Vassilakis, "A Compact envelope-memory polynomial for RF transmitters modeling with application to baseband and RF-digital predistortion," IEEE microwave wireless components letter, vol. 18, no. 5, pp. 359–361, May 2008.

[25] O. Hammi, M. Younes, and F. Ghannouchi, "Metrics and methods for benchmarking of RF transmitter behavioral models with application to the development of a hybrid memory polynomial model," IEEE Transaction Broadcast., vol. 56, no. 3, pp. 350–357, Sep. 2010.

[26] D. Morgan, Z. Ma, J. Kim, M. Zierdt, and J. Pastalan, "A Generalized memory polynomial model for digital predistortion of RF power amplifiers," IEEE transaction in signal processing, vol. 54, no. 10, pp. 3852–3860, Oct. 2006.

[27] O. Hammi, A. Kedir, and F. Ghannouchi, "Nonuniform memory polynomial behavioral model for wireless transmitters and power amplifiers," Asia pacific microwave conference proceedings, pp. 836–838, 2012.

[28] O. Hammi and F. Ghannouchi, "Twin nonlinear two-box models for power amplifiers and transmitters exhibiting memory effects with application to digital predistortion," IEEE Microwave Wireless. Components Letter, vol. 19, no. 8, pp. 530–532, Aug. 2009.

[29] J. Pedro and S. Maas, "A comparative overview of microwave and wireless power-amplifier behavioral modeling approaches," IEEE transaction microwave theory techniques, vol. 53, no. 4, pp. 1150–1163, Apr. 2005.

[30] M. Schetzen, "The Volterra and Wiener Theories of Nonlinear Systems", reprint ed. Melbourne, FL: Krieger, 1989.

[31] V. Mathews and G. Sicuranza, "Polynomial Signal Processing", New York: Wiley, 2000.

[32] V. Marmarelis, "Nonlinear Dynamic Modeling of Physiological Systems", New York: Wiley, 2004.

[33] A. Zhu, M. Wren, and T. Brazil, “An efficient Volterra-based behavioral model for wideband RF power amplifiers,” in IEEE MTT-S international microwave symposium digital, pp. 787–790, 2003.

[34] A. Zhu and T. J. Brazil, “Behavioral modeling of RF power amplifiers based on pruned Volterra series,” IEEE microwave wireless component letter, vol. 14, pp. 563–565, Dec. 2004.

[35] D. Mirri, G. Luculano, F. Filicori, G. Pasini, G. Vannini, and G. P. Gabriella, “A modified Volterra series approach for nonlinear dynamic systems modeling,” IEEE transactions circuits system in fundamental theory application, vol. 49, no. 8, pp. 1118–1128, Aug. 2002.

[36] A. Zhu, J. Dooley, and T. Brazil, “Simplified Volterra series based behavioral modeling of RF power amplifiers using deviation-reduction,” in 2006 IEEE MTT-S international microwave symposium digest, pp. 1113–1116, 2006.

[37] M. Isaksson, D. Wisell, and D. Ronnow, “Nonlinear behavioral modeling of power amplifiers using radial-basis function neural networks,” in IEEE MTT-S international microwave symposium digest, pp. 1967–1970,2005.

[38] D. Wisell, M. Isaksson, and N. Keskitalo, “A general evaluation criteria for behavioral power amplifier modeling,” in 2007 69th ARFTG conference, pp. 1–5, 2007.

[39] A. Cidronali, G. Manes, N. Giovannelli, T. Vlasits, R. Hernaman, "Efficiency and linearity enhancements with envelope shaping control in dual-band envelope tracking GaAs PA," European microwave integrated circuit conference,, pp. 308-311, 2011.

Vitae

Name	Saif Sameer Najmeddin
Nationality	Palestinian
Date of Birth	20/10/1988
Email	g201204340@kfupm.edu.sa; saif.najmeddin@gmail.com
Address	Ain Sarah Street, Hebron, Palestine
Academic Background	Bachelor in Communication and Electronics Engineering. Palestine Polytechnic University (PPU), 2011.

Work Experience

- **Network Engineer:** Home Plaza Company, Hebron, Palestine, from Jan. 2012 to Aug. 2012.
- **Research Assistant:** Deanship of scientific research in Palestine Polytechnic University (PPU), from Feb. 2012 to Aug.2012 (Part-Time).

Major Projects

- **Simulation of Green Communication concept for the Cellular networks 2 G and 3G**, including RF optimization and capacity planning.
- **Comparing between routing protocol in wireless local area network s (W LAN),** with Static routing and dynamic routing and interfacing routers and addressing PCs

- **Simulation local area network s (LAN) with different protocols (RIP, OSPF, EIGRP), by doing** Redistribution OSPF and EIGRP and interfacing routers and switches.
- Performed various duties related to the electrical engineering department in KFUPM.
- Grading and proctoring the examination of undergraduate students from time to time.